Performance Optima for Endoreversible Systems

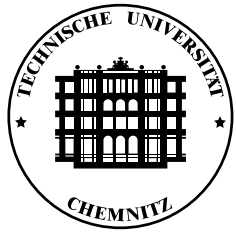

von der Fakultät für Naturwissenschaften
der Technischen Universität Chemnitz
genehmigte Dissertation
zur Erlangung des akademischen Grades
Doktor der Naturwissenschaften
(Doctor rerum naturalium)
(Dr. rer. nat.)

vorgelegt von

Dipl.-Phys. Josef Maximilian Burzler

geboren am 19. Juni 1969 in Regensburg

Gutachter	Prof. Dr. Karl Heinz Hoffmann Prof. Dr. Michael Schreiber Prof. Dr. Bjarne Andresen
Verteidigung	28. Januar 2002
Archivierung	http://archiv.tu-chemnitz.de/pub/2003/0001

Bibliographische Beschreibung und Referat

BURZLER, JOSEF MAXIMILIAN

Performance Optima for Endoreversible Systems

Technische Universität Chemnitz, Fakultät für Naturwissenschaften
Dissertation, 2001 (in englischer Sprache)
130 Seiten, 24 Abbildungen, 6 Tabellen, 5 Anhänge, 136 Literaturzitate

In dieser Arbeit werden theoretische Grenzen für verschiedene Leistungsmerkmale von thermodynamischen Systemen unter der Bedingung endlicher Zeiten und Prozessraten im Rahmen endoreversibler Modelle untersucht. Diese Modelle bestehen aus reversiblen Subsystemen, welche über allgemein irreversible Wechselwirkungen Energie austauschen. Analytische und nummerische Berechnungen quantifizieren diese Grenzen und liefern optimale Prozess- und Konstruktionsparameter für vier Modellsysteme:

Für eine auf maximale Ausgangsarbeit optimierte Wärmekraftmaschine, bei der die Wärme zwischen Arbeitsmedium und Wärmereservoirs während allgemeiner polytroper Zustandsänderungen des Arbeitsmediums übertragen wird, werden optimale Temperaturen und Zeiten für die Wärmeübertragungsprozesse sowie die thermischen Wirkungsgrade bestimmt.

Für ein wirkungsgrad-optimiertes Modell eines verallgemeinerten thermischen Umwandlungssytems, das sowohl Wärmekraftmaschinen, Kühler und Wärmepumpen beschreibt, wird die optimale Verteilung von Investitionskosten auf die Wärmetauscher ermittelt und die Anwendung der allgemeingültigen Ergebnisse anhand mehrerer Beispiele demonstriert.

Für eine Wärmekraftmaschine mit mehreren Wärmereservoirs wird bestimmt, welche der Wärmereservoirs wie lange kontaktiert werden müssen, um eine maximale Ausgangsarbeit zu erzielen.

Für einen Dieselmotor wird die Kolbenbewegung so optimiert, dass bei gegebener Treibstoffmenge eine maximale Ausgangsarbeit erzielt wird. Das endoreversible Modell des Dieselmotors berücksichtigt die Temperaturabhängigkeit der Wärmekapazität, Wärmeleitfähigkeit und Viskosität des Arbeitsfluids, die Zeitabhängigkeit des Verbrennungsprozesses sowie Reibungs- und Wärmeverluste.

Schlagworte

Thermodynamik endlicher Zeiten, Entropie, endoreversibles System, optimale Prozessführung, polytroper Prozess, Effizienzoptimierung, Kostenoptimierung, Pfadoptimierung, Wärmekraftmaschine, Wärmereservoir, Wärmetauscher, Dieselmotor

Contents

List of Figures

List of Tables

Introduction

First steps of thermodynamics as a science were taken in the 19th century, relatively early, when technology was mainly the domain of skilled inventors and constructors who designed their machinery by practical experience and empirical knowledge. It was the French engineer Sadi Carnot who undertook a systematic study on the physical processes occurring within steam engines and who discovered the basic limit on the performance of heat engines [1]. Carnot showed, that any engine which draws heat from a hot reservoir at temperature T_{H} to produce work, has to reject some of the heat to a reservoir at lower temperature T_{L}. The maximum fraction of heat which can be converted to work,

$$\eta_{\mathrm{C}} = 1 - T_{\mathrm{L}}/T_{\mathrm{H}} \ , \tag{1}$$

is now known as the Carnot efficiency.

The middle and the end of the 19th century saw major discoveries and a swift development in what we call the field of classical thermodynamics nowadays. This branch of natural science has been shaped by great researchers. The list of famous names includes Robert Mayer and James P. Joule, who found out that work and heat are equivalent with respect to energy. William Thomson (the later Lord Kelvin) and Rudolf Clausius layed out the theoretical principles of the classical theory. James P. Joule, Hermann von Helmholtz, and Josiah W. Gibbs introduced thermodynamic potentials, thus shifting away the focal point of the subject from process variables like work or efficiency towards new state variables like energy, entropy or availability. Ludwig Boltzmann augmented the scope of the equilibrium theory with a microscopic theory of the equilibrium states and statistical mechanics. The mathematician C. Carathéodory condensed the first and second law of thermodynamics into an axiomatic formulation.

Classical thermodynamics eventual became a common tool for studies in engineering, chemistry and physics; it even played an important role in the discovery of quantum mechanics, when Max Plank unfolded his idea of discrete states in conjunction with a thermodynamic formalism to explain the properties of black body radiation.

Despite the great achievements made with the classical version of equilibrium thermodynamics, this theory also shows serious drawbacks, because thermodynamic potentials traditionally were defined regardless of time. Irreversibilities due to finite time or process rates were neglected and processes were effectively treated as if they would proceed without loss and at infinite slow speed. Solely reversible processes picture a world virtually frozen in equilibrium states where macroscopic flows are vanishing. However, this contradicts the dynamics of the world we are used to live in. Although the performance limits of reversible processes are always upper bounds for real, irreversible processes, they may not be guides useful enough for the evaluation of real processes. Existing heat engines, for example, seldom attain more than a fraction of the reversible Carnot efficiency.

For this reason, engineers are often less concerned about the reversible limits, but rely on traditional techniques of empirical rules, experimental design or computer simulations to evaluate and improve their applications. Rapid technological advances in engineering nonetheless have drawn back the attention to in-principle limits of energy conversion and gives raise to questions like:

> *Are there theoretical bounds for the performance of thermodynamic processes under the constraints of finite process times or rates?*
>
> *If such bounds exist, what are the optimal operating conditions necessary to reach these bounds?*

This kind of questions is indeed important for the future development of technologies and have thus inspired researchers to conduct a wide range of scientific inquiries leading to a new branch of thermodynamics know as *finite-time thermodynamics*.

The origin of finite-time thermodynamics can be dated back to the late 50's of last century when the German H. Müser found mathematical expressions for the power output of solar cells under the condition of a finite, irreversible, radiative energy transfer [2]. Around the same time the Russians Novikov [3, 4] and Vukalovich [5] investigated the effect of finite heat transfer on the efficiency and maximum power output of nuclear power plants. Novikov and Vukalovich set up a simple model of power plants and discovered, that efficiency at the maximum power point,

$$\eta_{\mathrm{CA}} = 1 - \sqrt{T_{\mathrm{L}}/T_{\mathrm{H}}}\,, \tag{2}$$

is significantly lower than the corresponding Carnot efficiency $\eta_{\mathrm{C}} = 1 - T_{\mathrm{L}}/T_{\mathrm{H}}$. Although this results entered some textbooks [5–8] and appeared within a few other isolated publications [9, 10], the thermodynamics of finite-time processes has received little attention until 1975 when the oil crisis demonstrated the scarcity of natural resources in general and fossil fuel in particular. At this time Curzon and Ahlborn [11]

re-discovered the efficiency expression of Novikov and Vulkalovich and found it remarkably corresponding to the performance data of existing power plants.

The following years saw a flow of research activities, which have not faded until today. In pioneering works (see papers of Andresen, Berry, Nitzan, and Salamon [12–15], Rubin, Ondrechen and Band [16, 17], De Vos [18–20] and Gordon [21], for example) the theoretical framework of finite-time thermodynamics was established. The variety of novel theoretical techniques have subsequently been applied to model the performance of heat engines, refrigerators, heat pumps, chemical processes and solar cells, just to name a few examples.

Sensible modeling of processes or devices requires identification of the main features of a system in order to make a model simple and general. Another aim is to simplify the mathematical description and to reduce the computational effort needed to evaluate the thermodynamic system, but to reproduce still the major performance characteristics and to find realistic optima and bounds for the operation of a thermodynamic system in question. In finite-time thermodynamics one of the most important and useful concepts to create models with these qualities are *endoreversible systems* as formally introduced by Rubin [16, 17]. Endoreversible systems are certain kinds of thermodynamic models basically composed of internal reversible subsystems with generally irreversible interactions between these subsystems. The loss due to finite time or rates of processes is located in the interactions only. The hypothesis of *endoreversibility* has been successfully applied to many different thermodynamic systems with remarkable results and became the foundation of a new research field known as *endoreversible thermodynamics*.

This thesis follows the agenda of finding performance bounds and optimal operating conditions of thermodynamic systems under the constraint of finite process times and rates. The systems investigated within this thesis are all endoreversible. They range from general theoretical setups to the real world example of a Diesel engine.

Chapter 1 provides a brief introduction to endoreversible thermodynamics in general and to definitions, concepts, and techniques needed to construct, characterize, evaluate and optimize endoreversible systems.

Chapter 2 considers a model of an endoreversible engine with generalized heat transfer branches and a finite heat capacity of the working fluid. Optimal operating conditions to achieve a maximum of work output of the engine are determined. The influence of the types of heat transfer and design parameters on the performance of the engine is analyzed. In particular, the question whether or not the Curzon–Ahlborn efficiency of Carnot-engines is still valid for these more general heat transfer branches is resolved.

Chapter 3 investigates the problem of optimal allocation of a given investment capital to the heat exchangers of a generalized thermal system to optimize the performance of the system. The investigation takes into account that the dependency between the costs and the effectiveness of a heat exchangers can be non-linear and different for the hot and cold side of thermal system.

Chapter 4 optimizes the average power output of an endoreversible heat engine with several heat reservoirs. Systems with more than one heat reservoir are common for many real-world applications such as industrial heat-recovery systems and solar energy installations. A recipe of how to optimally allocate the contact times to the different heat reservoirs is developed.

Chapter 5 introduces a novel endoreversible model of a Diesel engine. It is investigated how the efficiency of the engine can be improved by optimizing the path of the engine's piston. The endoreversible model accounts for the time-dependence of the combustion process, the temperature dependence of the working fluid properties and the friction losses. The heat losses through the walls of the cylinder are modeled using a sophisticated, empiric description in order to derive realistic results,

Chapter 6 summarizes the new results obtained by this thesis.

Several appendices augment this thesis and for instance provide details on the classic Curzon-Ahlborn heat engine and an overview about commonly used heat transfer laws. Some of the auxiliary calculation, which already have been published elsewhere, are also included as appendices.

Chapter 1

Endoreversible systems

Endoreversible systems are models of thermodynamic systems made up of a number of *subsystems* interacting with one another and, possibly, with their surroundings. The subsystems are chosen such that each of them undergoes only reversible thermodynamic processes. Therefore simple balance equations are often sufficient to describe the operation of such subsystems. Dissipation or irreversibilities are solely located in the *interactions* between reversible subsystems and between the surroundings. Endoreversible systems are then fully defined by the properties of their subsystems and interactions. Processes of endoreversible systems are referred to as *endoreversible processes*.

The decomposition of a given thermodynamic system into a network of interacting reversible subsystems requires to identify the main sources of dissipation and the time-scales of relaxation processes in a thermodynamic system. One can assume that during an interaction the participating subsystems are always in a state of *internal quasi-equilibrium*, i. e. the time-scale for their internal relaxation processes is short compared to the duration of the interaction. Such a system is referred to as *quasi-static*. The restrictions imposed by endoreversibility may exclude certain distributed systems, non-equilibrium systems, or chemical systems where different substances are not in chemical equilibrium among each other (see [22] for example). Subsystems of endoreversible models do not need to be spatially uniform though. They also can be more aggregate objects, like reversible operating energy transforming devices, as long as the requirement of quasi-equilibrium is fulfilled for each *contact* where the subsystem interacts with another subsystem or the environment.

1.1 Thermodynamics of endoreversible systems

The following describes the key features of endoreversible systems in a formal way following [23].

1.1.1 Thermodynamics of equilibrium subsystems

The basic building block of endoreversible systems are thermal equilibrium subsystems which can be characterized by their state variables. As usual for equilibrium systems, one has some freedom in the choice of these state variables. As an example consider an ideal gas, which can be described for instance by its volume and pressure, or by its volume and entropy. Thermodynamic variables like volume, energy and entropy which scale with the size of a system are *extensive variables*; variables like pressure or temperature which do not scale with the size of the system are *intensive variables.*

To simplify the description of the theory a special choice of variables is taken, namely the energy picture where the energy E is considered to be a function of all the other extensive thermodynamic variables of a system. The property X_i^α refers to the extensive thermodynamic variables of subsystem i in the following, for instance the volume V_i, or particle number N_i, all of which are counted by α. The entropy S_i of subsystem i is a well defined state variable due to endoreversibility and belongs to the set of extensive variables. Thus the state of the subsystem is uniquely described by the set of its extensities $\{X_i^\alpha\}$. The energy E_i of a subsystem i,

$$E_i = E_i(X_i^\alpha) \,, \tag{1.1}$$

defines the properties of this subsystem, which means it specifies E_i as a function of the X_i^α and determines the (thermal) behavior of that subsystem. The energy E_i is not confined to be the internal energy, it can in addition include the translational kinetic energy, the rotational kinetic energy, or the potential energy in one or more external fields. In each case the proper extensive variables must be included in the set of extensities. Naturally the energy then becomes also a function of these variables.

Due to endoreversibility all the standard equilibrium relations hold within a subsystem. The respective conjugate intensive variables Y_i^α are obtained from (1.1) as

$$Y_i^\alpha = \frac{\partial E_i}{\partial X_i^\alpha} \,. \tag{1.2}$$

The Gibbs equation becomes

$$\mathrm{d}E_i = \sum_\alpha Y_i^\alpha \mathrm{d}X_i^\alpha \tag{1.3}$$

in each subsystem i. As a consequence of the Gibbs equation, each influx of an extensity $J_i^\alpha = \dot{X}_i^\alpha$ into the system carries an accompanying influx of energy I_i^α [24]:

$$I_i^\alpha = Y_i^\alpha J_i^\alpha \ . \tag{1.4}$$

For example, any heat flux q is carried by an entropy flux q/T, or any particle flux J^{particle} carries an energy flux $\mu J^{\mathrm{particle}}$ where μ is a chemical potential.

1.1.2 Subsystems and contact points

A given set of subsystems can be knotted as a network by characterizing each subsystem i by a number of contact points (or contacts) through which the subsystem receives or discards energy. Energy is not the only exchanged quantity. Through each contact the energy is transported by an extensity (a carrier) X_i^α, for instance entropy, momentum or a particle flux. The contacts for the same extensity in one subsystem are numbered by r.

Each contact has three (time-dependent) functions assigned to it $(Y_i^{\alpha,r}, J_i^{\alpha,r}, I_i^{\alpha,r})$. Here $I_i^{\alpha,r}$ is the energy flux into the system, $J_i^{\alpha,r}$ is the associated flux of the carrier X_i^α, and $Y_i^{\alpha,r}$ is the corresponding thermodynamic intensity for that contact.

To make the notation simpler the indices (i, α, r) are combined into a single one ν, which counts all different contacts in the composite network:

$$Y_\nu = Y_i^{\alpha,r} \quad , \quad \text{etc.} \tag{1.5}$$

Endoreversibility guarantees that the energy and extensity influx at each contact are always related by

$$I_\nu = Y_\nu J_\nu, \tag{1.6}$$

in other words, the intensity associates a value for the energy flux on the influx of an extensity.

1.1.3 Reservoirs

Reservoirs are special thermodynamic subsystems at equilibrium, characterized by either

a) given intensities Y_i^α. This is the case for infinite reservoirs where the influx or outflux of an extensity does not change the value of the intensity. An example of where heat reservoirs of this type occur is the Curzon–Ahlborn heat engine as described in appendix A.

b) its extensities X_i^α and its energy function $E_i(X_i^\alpha)$. Then the intensities are known $Y_i^\alpha = \partial E_i/\partial X_i^\alpha$, and due to its internal equilibrium they are uniform throughout the subsystem and thus the intensities at the contacts $Y_i^{\alpha,1} = Y_i^{\alpha,2} = \cdots \equiv Y_i^\alpha$ are equal for all r. If the extensities within the reservoir are neither destroyed or produced one finds balance equations for the extensities

$$\dot{X}_i^\alpha = \sum_r J_i^{\alpha,r} \tag{1.7}$$

and for the energy

$$\dot{E}_i = \sum_{\alpha,r} I_i^{\alpha,r} = \sum_{\alpha,r} Y_i^{\alpha,r} J_i^{\alpha,r} = \sum_\alpha Y_i^\alpha \sum_r J_i^{\alpha,r} \ . \tag{1.8}$$

1.1.4 Balance equations of subsystems

Balance equations for selected extensities and energy are very useful to describe the operations of thermodynamic subsystems as they relate the intensites at the contacts to one another. Balance equations can be set up without knowing the details of a subsystem like, for example, equations of state of a working fluid. In particular, balance equations are especially applicable to reversible subsystems operating in a closed cycle. This may be the case for refrigerating, thermoelectric, photo-electric or other energy converting subsystem. If an extensity is neither produced nor destroyed inside a subsystem i its influx and outflux has to cancel each other.

If this condition is fulfilled at every moment of time the balance equations can be written as

$$0 = \sum_{\alpha,r} I_i^{\alpha,r} = \sum_{\alpha,r} Y_i^{\alpha,r} J_i^{\alpha,r} \qquad \text{(energy balance)} \tag{1.9}$$

for the energy and

$$0 = \sum_r J_i^{\alpha,r} \qquad \text{(extensity balance)} \tag{1.10}$$

for a flow J^α of an extensity X^α.

In the case of a *cyclic operating* subsystem it is sufficient to have energy and all other extensities balanced at the end of every cycle. Balance equations are then obtained by integrating the sum of the fluxes over one cycle of duration τ_{tot} because fluxes may vary in time:

$$0 = \int_0^{\tau_{\mathrm{tot}}} \mathrm{d}t \sum_{\alpha,r} I_i^{\alpha,r} = \int_0^{\tau_{\mathrm{tot}}} \mathrm{d}t \sum_{\alpha,r} Y_i^{\alpha,r} J_i^{\alpha,r} \qquad \text{(energy balance)} \tag{1.11}$$

and

$$0 = \int_0^{\tau_{\rm tot}} \mathrm{d}t \sum_r J_i^{\alpha,r} \qquad \text{(extensity balance)} \,. \tag{1.12}$$

1.1.5 Interactions

Interactions describe how the contacts of the subsystems exchange energy. The contact points are connected by interactions such that each contact belongs to one specific interaction. An interaction Ω is characterized by the set of contacts which belong to it, and by the specific extensity X^α, through which the contacts exchange energy. If the interaction is reversible, only contacts for the exchanged extensity are needed. If the interaction is irreversible, entropy is produced, and then at least one additional contact is needed to deposit the produced entropy. Some of the extensities (like angular momentum) and energy are conserved quantities by nature, while others (like entropy) are not. In a complete interaction all the conserved quantities must balance to zero. A specific interaction Ω can be either reversible or irreversible and can belong to either one of the two following cases:

a) All the intensities of the contacts $\nu, \mu \in \Omega$ obey $Y_\nu = Y_\mu$.

b) The interaction is defined by a transport law which gives either the flux of the extensity

$$J_\nu = J_\nu(\{Y_\omega\}, \{X_i^\alpha\}, z_m) \tag{1.13}$$

or the corresponding flux of the energy

$$I_\nu = I_\nu(\{Y_\omega\}, \{X_i^\alpha\}, z_m) \tag{1.14}$$

at each of the involved contacts as functions of the intensities, the extensities (for reservoirs) and of additional external parameters z_m, which are counted by m. These parameters are mentioned here explicitly, as they will be used as *controls* to adjust the fluxes in optimizing the performance of endoreversible systems.

In principle, interactions act as constraint for the contact variables. A very common interaction is the exchange of heat between a subsystem 1 and a subsystem 2. The flow of thermal energy $q = q(T_1, T_2, z_m)$ often is a function of the temperatures T_1 and T_2 at the contact points of the respective subsystem and possibly some external parameters z_m like the area and conductivity of heat exchangers or geometry factors

of solar collectors. Some examples of commonly used heat transport laws are presented in appendix B. All the heat transfer laws used in this thesis satisfy common requirements for monotonicity in T_1 and T_2:

$$q_i(T_1, T_2, z_m) = \begin{cases} > 0, & \text{if} \quad T_1 > T_2 \\ = 0, & \text{if} \quad T_1 = T_2 \\ < 0, & \text{if} \quad T_1 < T_2 \end{cases} . \tag{1.15}$$

1.2 Characterization of endoreversible systems

By collecting the different elements introduced above, one finds that an endoreversible system is characterized by its contact variables, the extensities of the subsystems and the interactions. If, for example, a system does contain reservoirs with infinite capacities, like heat reservoirs with fixed temperatures, the extensities of these reservoirs can be excluded from the description. Usually some of the contact variables and extensities will be given while others remain undetermined yet still related by constraints due to

- the Gibbs relation at each contact
- the balance equations in the subsystems
- the interactions.

For some aggregated subsystems some additional equations might exist, which define and relate internal properties and contact variables, for instance a given time dependent heat production rate or temperature function of a heat source. Thus an endoreversible system is completely characterized by a set of algebraic and ordinary differential equations.

The characterization of an endoreversible system can often be simplified by excluding some of the contact variables from the description. Naturally it depends on the analysis intended which variables can be excluded. For example, if an engine subsystem delivers its power to a driving shaft one might not be interested in the dissipated energy and the angular momentum going into the bearing. Note that in this case of a *partial* interaction the equal intensities do not indicate a reversible contact, and that the energy is no longer conserved in such an interaction. This implies that some of the balance equations for carriers X_i^α in the subsystems might be safely ignored. The reason is that without an effect on the energy balance, contacts for carriers with zero intensities can be added to correct the balance equations.

In most of the publications on endoreversible systems the only carrier taken into account is entropy, and thus only entropy contacts and so-called *work contacts* are considered, the latter implying that there is no entropy transported through that contact and that the carrier can be neglected. Many endoreversible systems are using another common simplification: some interactions are exchanging energy with the outside of the system and are not explicitly connected to a subsystem. Many models of engines or refrigerators, for example, do not have a *work reservoir*: the power just leaves or enters the endoreversible system.

1.3 Analysis and optimization of endoreversible systems

The analysis and optimization of endoreversible systems requires the use of appropriated schemes and mathematical tools to for instance determine the performance of the system with respect to some parameters.

1.3.1 Performance measures and performance characteristics

Depending on what type of energy transformation device is studied common performance measures include power or work output or efficiency of engines, coefficients of performance of coolers and heat pumps, loss of availability, ecological criteria, and entropy production.

From a geometric point of view an endoreversible system is characterized by a hypersurface of all possible operating points in the multidimensional space spanned by all the contact variables and, possibly, external controls and derived parameters describing the system. Optimizing the system with respect to a performance measure effectively creates a lower-dimensional projection of the complicated, higher-dimensional hyper-surface. Here, such projections are called performance characteristics, and are usually depicted as two or three-dimensional diagrams where the performance measure is plotted versus some interesting parameters of a system. Typical examples are power versus efficiency characteristics or coefficients of performance versus cooling load characteristics. Optimizing the performance of a system for all degrees of freedom leads to one single point on the hyper-surface, if the solution is non-degenerate.

1.3.2 Temporal evolution of systems

The level of mathematical sophistication needed for the analysis and optimization of a system significantly depends on how the process variables and parameters of the system depend on time. Here, three types of temporal evolutions of thermodynamic systems are distinguished.

Stationary conditions

Among the simplest systems are those where all fluxes and intensities are required to be constant in time. If some of the fluxes are non-zero these systems are not in equilibrium among each other, but, figuratively spoken, seem to run at a never changing pace. The contact variables of such systems are time-independent. Some of the contact variables may have externally assigned fixed values, like the temperatures of some heat reservoir, while others remain undetermined, but still restricted by the constraints of the system. The system can be characterized by a set of rate equations for extensities alone. This simple structure often allows to calculate the performance characteristics and working point of optimal performance analytically. Within this thesis, a system with such properties is referred as to be operating under *stationary conditions*. Note that in some publications systems of this kind are refereed to as *steady-state systems*. An example for a system operating under stationary conditions is an endoreversible heat engine where a reversible, energy converting subsystem uses different contact points at different temperatures to connect to two or more heat reservoirs simultaneously.

Cyclic conditions

A more complicated type of time dependence occurs in systems where contact variables are allowed to switch between several processes with temporally constant contact variables. Many of these systems additionally operate in a cyclic fashion. Then τ_{tot} is defined as cycle time after which the system has regained its initial state (apart from the changes in the reservoirs). In terms of contacts, the switching is accounted for by assigning each contact b tuples of contact variables $(Y_{\nu,b}, \Delta X_{\nu,b} = \tau_b J_{\nu,b}, \Delta E_{\nu,b} = \tau_b I_{\nu,b})$, each obeying $\Delta E_{\nu,b} = Y_{\nu,b} \Delta X_{\nu,b}$. Then the balance equations for an cyclic operating, reversible subsystem become

$$0 = \sum_b \sum_{\alpha,r} \Delta E_{i,b}^{\alpha,r} \qquad \text{(energy balance)} \tag{1.16}$$

$$0 = \sum_b \sum_{r} \Delta X_{i,b}^{\alpha,r} \qquad \text{(extensity balance)} , \tag{1.17}$$

where in endoreversible systems one of the most important extensity changes ΔX^α is the entropy change ΔS.

If a total time τ_{tot} of the process is a given constant, the process can be divided into several branches i of duration τ_i such that

$$\tau_{\mathrm{tot}} = \sum_i \tau_i \ . \tag{1.18}$$

Sometimes one only wants to know the total time spent in a branch and the branches do not need to be taken in any particular order. The system even could arbitrarily jump between the different branches as long as at the end of the process the total time spent in each branch is equal to the respective τ_i. For such systems one can define dimensionless fractions $\gamma_i = \tau_i/\tau_{\mathrm{tot}}$ of the total cycle time τ_{tot} with $\gamma_i \geq 0$, $\sum_i \gamma_i = 1$. These fractions are referred to as *parts* of the total time. They describe the relative amount of time spent within a branch i.

The switching parameters, for example the time during which a subsystem connects to a heat reservoir, are usually externally controllable and can be optimized with respect to a certain objective, such as the power output of the heat engine. Typically most of the fluxes will vanish, as the interaction – for instance the heat conduction from a reservoir to the engine – is active only during some of the branches.

Dynamic conditions

A very general way to treat the time dependence of a system is to allow the system to evolve along a path and consider the full dynamics of the processes. In this case, the process evolves along a path which is not fixed (except for some constraints and bounds such as initial and final conditions) but can be influenced by some external controls. The optimization problem is on how to control the system such that a certain performance measure is extremalized. Take, for example, the problem of optimizing the piston movement for an internal combustion Diesel engine such that the power output is maximized. The only controllable variable of the system is the volume of the cylinder which can be adjusted by moving the piston. Solving this optimization problem should give the optimal piston movement, the resulting optimal work and possibly some other process variables such as temperature and pressure.

The so-called *path optimization* of a thermodynamic system is much more complicated and costly than the analysis of a parameterized system operating under stationary or switching conditions. However, there are well-established mathematical methods for path optimization like *optimal control theory* (see [25–27] for example).

Chapter 2

Heat engines with polytropic cycles

Endoreversible models of heat engines with isothermal heat transfer branches and heat reservoirs at constant temperature have been extensively studied in the literature, for example in [11, 14–16, 28–33]. There are much less publications in the field of finite-time thermodynamics where other types of engines like, for example, those with heat reservoirs at variable temperatures [34], with finite heat capacities of the heat reservoirs [17, 34–38], or non-isothermal heat transfer branches [39, 40] have been analyzed.

However, engine cycles with non-isothermal branches and finite heat capacities of the working fluids are very often discussed in standard textbooks of classical thermodynamics, for example in [41–46]. These textbooks commonly refer to *polytropic processes* to describe the state change of the working fluid during a heat transfer in a generalized way. Polytropic processes include common standard branches, such as isotherms, isochors, and isobars, as special cases. A polytropic process of a working fluid is characterized by a constant product pV^n where p is the pressure and V is the volume of the working fluid. The constant exponent n refers to the *polytropic degree* of the heat transfer process.

This chapter takes the concept of polytropic processes into the realm of finite-time thermodynamics. A first step in this direction was taken by Pathria, Nulton and Salamon [115]. One of the open questions in this field is, for instance, whether the Curzon–Ahlborn efficiency is still applicable for cycles of a general, polytropic character.

2.1 Heat transfer in polytropic processes

Consider a thermodynamic system where heat is transferred between a heat reservoir at constant temperature T_0 and a working fluid at variable temperature $T(t)$. In case of a linear heat-transfer law, the rate of heat flowing into the working fluid is given by a linear expression

$$q(T_0, T) = K(T_0 - T) \tag{2.1}$$

where K is the thermal conductance. A negative q indicates a heat flow from the working fluid to the heat reservoir. The working fluid is assumed to have a constant heat capacity and to undergo a polytropic process where pV^n=const. with a known degree n during the heat transfer. The polytropic degree n can in principle take any value between $-\infty$ and ∞. Common standard processes correspond to $n = 1$ for isothermal, $n = 0$ for isobaric, $n = \pm\infty$ for isochor, and $n = \gamma$ for adiabatic processes. The property $\gamma = C_p/C_V$ is the ratio of the heat capacities C_p and C_V of the working fluid at constant pressure and constant volume, respectively. In practice, a desired polytropic process can be achieved by controlling some of the state variables, for instance the volume or the pressure of the working fluid. The polytropic degree n is directly related to the polytropic heat capacity which is defined as

$$C_n = C_v \frac{n - \gamma}{n - 1} \tag{2.2}$$

The polytropic heat capacity C_n is not a material parameter but a *process parameter* and may in principle take any value between $-\infty$ and ∞, if no restrictions on n are imposed. A negative polytropic heat capacity C_n is not unrealistic. It could for example occur in a system where the working fluid receives heat and at the same time is very rapidly expanded such that the temperature $T(t)$ of the working fluid decreases with time. The polytropic heat capacity C_n becomes negative even though the heat capacity of the working fluid has a finite positive value.

If the working fluid is an ideal gas, the equations of state for the temperature can be used to derive a relation between the heat flow q and the temperature change $\mathrm{d}T$ of the working fluid. This calculation is a standard textbook example (e.g. [47]) and leads to the expression

$$\frac{\mathrm{d}T(t)}{\mathrm{d}t} = \frac{1}{C_n} q(T_0, T(t)) \ . \tag{2.3}$$

The fluid temperature $T(t)$ is determined by substituting the heat transfer law (2.1) into equation (2.3). The resulting differential equation is integrated with respect to the time t. With initial condition $T_1 := T(0)$ the fluid temperature is obtained as

$$T(t) = T_0 - [T_0 - T_1] \exp\left(-\frac{tK}{C_n}\right) \ . \tag{2.4}$$

The fluid temperature $T(t)$ is monotonically approaching the temperature T_0 of the heat reservoir but never reaches T_0. This implies that the sign of the temperature difference $T_0 - T$ is always the same and the heat flow q is directed either to or from the reservoir all the time.

The total amount of heat Q exchanged during a polytropic process of duration τ is obtained by substituting equation (2.4) into the heat transfer law (2.1) and integrating with respect to time t from 0 to τ:

$$Q(\tau) = C_n \left[1 - \exp\left(\frac{-\tau K}{C_n}\right)\right] [T_0 - T_1] \ . \tag{2.5}$$

By using equation (2.4) it is easily verified that the above expression coincides with the formula $Q = C_n(T_2 - T_1)$ for the heat transferred in a reversible, polytropic process where Q only depends on the initial temperature T_1 and the final temperature $T_2 := T(\tau)$ of the fluid [47, 48].

An important process variable is the change of the fluid entropy during the polytropic process. After substituting equation (2.4) into the expression for the rate of change of the fluid's entropy,

$$s(t) = \frac{q(T_0, T(t))}{T(t)} = K\left(\frac{T_0}{T(t)} - 1\right) \ , \tag{2.6}$$

the total entropy change $\Delta S(\tau)$ of the working fluid during a process of duration τ is calculated by integrating equation (2.6):

$$\Delta S(\tau) = C_n \ln\left(\frac{T_0 - (T_0 - T_1)\exp(-\tau K/C_n)}{T_1}\right) \ . \tag{2.7}$$

In the same way as for the exchanged heat one can show that the above formula is equivalent to the expression $\Delta S = C_n \ln(T_2/T_1)$ for the entropy change of an ideal gas in a reversible, polytropic process [47, 48].

Figure 2.1 depicts the temperature and entropy change of the working fluid versus the process time for different polytropic processes corresponding to different polytropic heat capacities C_n of the working fluid. The reservoir acts as a heat source here, since the initial temperature T_1 of the working fluid is lower than the temperature T_0 of the reservoir. The temperature and the entropy of the working fluid are monotonically increasing in time. The special case of an isothermal process is also depicted in figure 2.1 and obtained in the limit of $C_n \to \infty$ where the equations for the heat and entropy change, (2.5) and (2.7), become

$$Q_{\text{it}}(\tau) = \tau K(T_0 - T_1) \quad \text{and} \tag{2.8}$$

$$\Delta S_{\text{it}}(\tau) = \frac{\tau K(T_0 - T_1)}{T_1} \ . \tag{2.9}$$

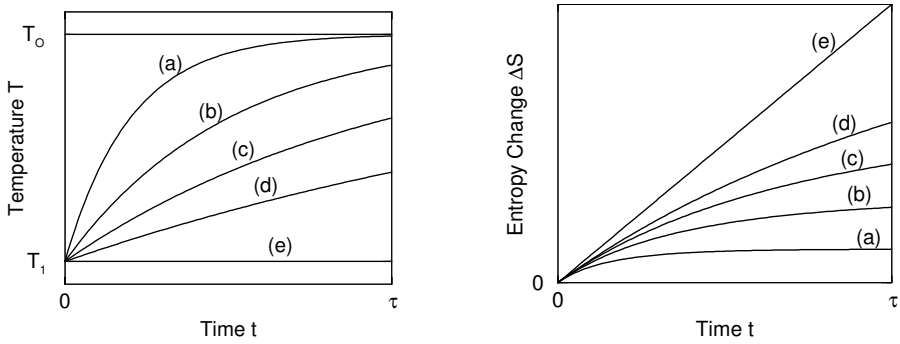

Figure 2.1: Time evolution of the temperature T and entropy change ΔS of a working fluid for a polytropic process of duration τ with scaled, dimensionless polytropic heat capacities $C_n/(\tau K)$ of (a) 0.2, (b) 0.5, (c) 1, (d) 2 and (e) ∞. The working fluid is an ideal gas at initial temperature T_1 and receives heat from a heat reservoir at constant temperature T_0.

Adiabatic processes, where $C_n \to 0$, are not considered here since no heat is transferred during such a process.

2.2 Work characteristic of the engine

The thermodynamic cycle of the endoreversible engine investigated in the following is made up of two polytropic and two adiabatic branches, like the example depicted in figure 2.2. The goal of this section is to derive the performance characteristic of this engine, i. e. its work output as a function of independent control parameters.

2.2.1 Assumptions and basic relations

The engine operates between heat reservoirs at constant high and low temperatures, $T_{0\mathrm{H}}$ and $T_{0\mathrm{L}}$, respectively. The suffixes H and L indicate if a quantity belongs to the upper or the lower polytropic heat transfer process. During the upper heat transfer process the entire working fluid is in thermal contact with the hot reservoir and receives the heat Q_{H}. During the lower transfer process the working fluid contacts the cold reservoir and rejects the heat Q_{L}. The heat Q_{L} is negative since it flows out of the working fluid. The respective durations of the heat transfer processes are τ_{H} and τ_{L}.

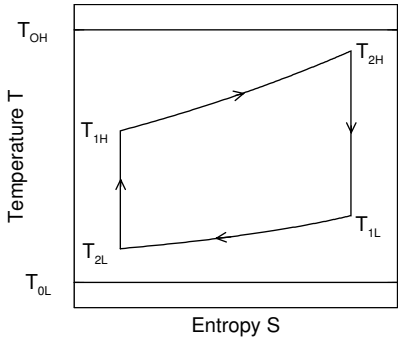

Figure 2.2: TS-diagram of an engine cycle with two polytropic and two adiabatic branches. The working fluid receives heat from a heat reservoir at constant temperature $T_{0\mathrm{H}}$ during the upper polytrop and changes its temperature from $T_{1\mathrm{H}}$ to $T_{2\mathrm{H}}$. The working fluid releases heat during the lower polytrop to a reservoir at constant temperature $T_{0\mathrm{L}}$ and changes its temperature from $T_{1\mathrm{L}}$ to $T_{2\mathrm{L}}$.

The endoreversibility hypothesis allows to apply the balance equation (1.9) for the work W delivered during one cycle

$$W = Q_{\mathrm{H}} + Q_{\mathrm{L}} \ . \tag{2.10}$$

The transferred heats are provided by section 2.1, equation (2.5), as

$$\begin{aligned} Q_{\mathrm{H}} &= C_{\mathrm{H}}(1-e_{\mathrm{H}})(T_{0\mathrm{H}} - T_{1\mathrm{H}}) && (2.11)\\ Q_{\mathrm{L}} &= C_{\mathrm{L}}(1-e_{\mathrm{L}})(T_{0\mathrm{L}} - T_{1\mathrm{L}}) \ , && (2.12) \end{aligned}$$

and the final temperatures of the working fluid in each of the polytropes is given by equation (2.4) as

$$\begin{aligned} T_{2\mathrm{H}} &= T_{0\mathrm{H}} - (T_{0\mathrm{H}} - T_{1\mathrm{H}})e_{\mathrm{H}} && (2.13)\\ T_{2\mathrm{L}} &= T_{0\mathrm{L}} - (T_{0\mathrm{L}} - T_{1\mathrm{L}})e_{\mathrm{L}} \ . && (2.14) \end{aligned}$$

Convenient abbreviations,

$$\begin{aligned} e_{\mathrm{H}} &= \exp(-\tau_{\mathrm{H}} K_{\mathrm{H}}/C_{\mathrm{H}}) \quad \text{and} && (2.15)\\ e_{\mathrm{L}} &= \exp(-\tau_{\mathrm{L}} K_{\mathrm{L}}/C_{\mathrm{L}}) \ , && (2.16) \end{aligned}$$

for the exponential functions are used to shorten the notation. Note that C_{H} and C_{L} are the *polytropic* heat capacities during the respective branches.

The heat transfer processes between the reservoirs and the working fluid are irreversible while the working fluid itself undergoes reversible processes, i.e. the total entropy change of the working fluid during a cycle is zero. Since the entropy of the

working fluid remains constant during the adiabatic branches, one only needs to consider the entropy changes ΔS_{H} and ΔS_{L} during the polytropes. Then the balance equation (1.10) takes the form

$$0 = \Delta S_{\mathrm{H}} + \Delta S_{\mathrm{L}} \; . \tag{2.17}$$

Substituting the entropy expression (2.7) for the appropriate branches into equation (2.17) and applying the exponential function on both sides of the resulting equation yields

$$1 = \left[\frac{T_{0\mathrm{H}} - e_{\mathrm{H}}(T_{0\mathrm{H}} - T_{1\mathrm{H}})}{T_{1\mathrm{H}}}\right]^{C_{\mathrm{H}}} \left[\frac{T_{0\mathrm{L}} - e_{\mathrm{L}}(T_{0\mathrm{L}} - T_{1\mathrm{L}})}{T_{1\mathrm{L}}}\right]^{C_{\mathrm{L}}} \; . \tag{2.18}$$

2.2.2 Equal polytropic heat capacities

Equation (2.18) cannot easily be treated analytically if C_{H} and C_{L} are different.

In order to continue the analytical calculations this section assumes an identical polytropic heat capacity in both heat transfer branches,

$$C = C_{\mathrm{H}} \stackrel{!}{=} C_{\mathrm{L}} \; . \tag{2.19}$$

With this assumption equation (2.18) simplifies to

$$1 = \frac{[T_{0\mathrm{H}} - e_{\mathrm{H}}(T_{0\mathrm{H}} - T_{1\mathrm{H}})][T_{0\mathrm{L}} - e_{\mathrm{L}}(T_{0\mathrm{L}} - T_{1\mathrm{L}})]}{T_{1\mathrm{H}} T_{1\mathrm{L}}} \; . \tag{2.20}$$

An important property of an heat engine is its efficiency,

$$\eta = \frac{W}{Q_{\mathrm{H}}} \; , \tag{2.21}$$

for which physically sensible values are between zero and the Carnot efficiency $\eta_{\mathrm{C}} = 1 - T_{0\mathrm{L}}/T_{0\mathrm{H}}$.

Altogether there are 5 independent equations, (2.10), (2.11), (2.12), (2.20), and (2.21), to eliminate the heats Q_{H} and Q_{L} and the initial temperatures $T_{1\mathrm{H}}$ and $T_{1\mathrm{L}}$ and to derive the work characteristic as a function of the three control parameters η, e_{H}, and e_{L}.

The initial temperature is calculated from equation (2.11) as

$$T_{1\mathrm{H}} = T_{0\mathrm{H}} - \frac{Q_{\mathrm{H}}}{C(1 - e_{\mathrm{H}})} \; . \tag{2.22}$$

Equation (2.12) is used to obtain an analogous expression for $T_{1\mathrm{L}}$. By substituting these expressions into equation (2.20), $T_{1\mathrm{H}}$ and $T_{1\mathrm{L}}$ are eliminated, and one obtains

$$1 = \frac{\left(T_{0\mathrm{H}} - \frac{e_{\mathrm{H}} Q_{\mathrm{H}}}{C(1-e_{\mathrm{H}})}\right)\left(T_{0\mathrm{L}} - \frac{e_{\mathrm{L}} Q_{\mathrm{L}}}{C(1-e_{\mathrm{L}})}\right)}{\left(T_{0\mathrm{H}} - \frac{Q_{\mathrm{H}}}{C(1-e_{\mathrm{H}})}\right)\left(T_{0\mathrm{L}} - \frac{Q_{\mathrm{L}}}{C(1-e_{\mathrm{L}})}\right)} , \tag{2.23}$$

which can be further simplified to

$$T_{0\mathrm{L}} Q_{\mathrm{H}} + T_{0\mathrm{H}} Q_{\mathrm{L}} - \frac{Q_{\mathrm{H}} Q_{\mathrm{L}} (1 - e_{\mathrm{H}} e_{\mathrm{L}})}{C(1-e_{\mathrm{H}})(1-e_{\mathrm{L}})} = 0 . \tag{2.24}$$

Combining equations (2.10) and (2.21) yields expressions for the heats,

$$Q_{\mathrm{H}} = W/\eta \quad \text{and} \tag{2.25}$$

$$Q_{\mathrm{L}} = W(\eta - 1)/\eta , \tag{2.26}$$

which are inserted into equation (2.24) to obtain a quadratic equation in W:

$$T_{0\mathrm{L}} \frac{W}{\eta} + T_{0\mathrm{H}} \frac{W(\eta-1)}{\eta} - \frac{W^2(\eta-1)(1-e_{\mathrm{H}}e_{\mathrm{L}})}{\eta^2 C(1-e_{\mathrm{H}})(1-e_{\mathrm{L}})} = 0 . \tag{2.27}$$

The first solution of this equation is a trivial one, $W = 0$, while the second solution is the desired work characteristic

$$W(\eta, e_{\mathrm{H}}, e_{\mathrm{L}}) = C \frac{\eta[(1-\eta)T_{0\mathrm{H}} - T_{0\mathrm{L}}]}{1-\eta} \times \frac{(1-e_{\mathrm{H}})(1-e_{\mathrm{L}})}{1-e_{\mathrm{H}}e_{\mathrm{L}}} . \tag{2.28}$$

This fundamental relation is a function of three independent control parameters: the efficiency η, the parameter e_{H}, and the parameter e_{L}. These parameters are sufficient to describe all possible modes of operation of the investigated endoreversible engine. The values of e_{H} and e_{L} are, according to equations (2.15) and (2.16), functions of the heat conductances K_{H} and K_{L} of the heat exchangers, and the branch times τ_{H} and τ_{L} and therefore referred to as design parameters in the following.

2.3 Optimization for maximum work at equal polytropic heat capacities

The necessary optimality conditions for maximum work output are derived by taking the derivatives of the work characteristic (2.28) with respect to the control parameters. As a consequence of an appropriate choice of independent control parameters, the

work characteristic (2.28) nicely separates into a term with the efficiency η and a term with the design parameters e_{L} and e_{H}. A similar factorization of the work characteristic has also been found for the optimal endoreversible Carnot heat engine [49]. The factorization immediately implies that the efficiency of the optimized heat engine is independent of the design parameters e_{L} and e_{H}.

2.3.1 Efficiency at maximum work output

The work W in equation (2.28) is zero for $\eta = 0$ and $\eta = 1 - T_{0\mathrm{L}}/T_{0\mathrm{H}}$ and positive for intermediate values of η. The optimality condition $\partial W/\partial \eta = 0$ for the efficiency η yields a quadratic equation,

$$(1-\eta)^2 \frac{T_{0\mathrm{H}}}{T_{0\mathrm{L}}} - 1 = 0 \,, \tag{2.29}$$

which has two solutions of which one solution is unrealistic because of the restriction $\eta \leq \eta_{\mathrm{C}}$. The second optimal solution

$$\eta^* = 1 - \sqrt{\frac{T_{0\mathrm{L}}}{T_{0\mathrm{H}}}} \tag{2.30}$$

is equal to the well-known Curzon-Ahlborn efficiency which originally was obtained for endoreversible Carnot engines [3, 11]. It is quite remarkable that the efficiency η^* at maximum work is a function of the reservoir temperatures only and does not depend on the details of the finite-rate heat transfers, like for example depend on the branch times or the conductances. Most important, η^* does not depend on the polytropic heat capacity. This means that it does not matter whether both heat transfer processes are isotherms, isochors, isobars, or something in between: as long as the polytropic heat capacities are equal in both branches, the efficiency at the maximum work point is always equal to the Curzon-Ahlborn efficiency.

2.3.2 Optimal allocation of branch times

This section analyses the influence of the second factor in equation (2.28). The goal is to find optimal branch times τ_{H}^* and τ_{L}^* which yield maximum work output of the engine in case of a given total duration

$$\tau_{\mathrm{tot}} = \tau_{\mathrm{H}} + \tau_{\mathrm{L}} \tag{2.31}$$

of the two heat transfer branches.

Note that the total duration τ_a of the adiabatic branches has no influence on the work output per cycle but only on the average power output of the engine $\bar{P} = W/(\tau_\mathrm{tot} + \tau_\mathrm{a})$. The average power $\bar{P}$ is improved if τ_a is as short as possible. Note that for a given τ_a the optimization of the work output per cycle also maximizes the average power output $\bar{P}$ of the engine.

The necessary optimality condition with respect to τ_H, $\partial W/\partial\tau_\mathrm{H} = 0$, yields

$$(1-e_\mathrm{H}e_\mathrm{L})\left[e'_\mathrm{H}(1-e_\mathrm{L})+(1-e_\mathrm{H})e'_\mathrm{L}\right]-(1-e_\mathrm{H})(1-e_\mathrm{L})(e'_\mathrm{H}e_\mathrm{L}+e_\mathrm{H}e'_\mathrm{L}) = 0 \quad (2.32)$$

where $e'_\mathrm{H} = \partial e_\mathrm{H}/\partial\tau_\mathrm{H}$ and $e'_\mathrm{L} = \partial e_\mathrm{L}/\partial\tau_\mathrm{H}$. The derivatives are calculated from equations (2.15) and (2.16) as

$$e'_\mathrm{H} = -e_\mathrm{H}\frac{K_\mathrm{H}}{C} \quad \text{and} \quad e'_\mathrm{L} = -e_\mathrm{L}\frac{K_\mathrm{L}}{C}\ , \tag{2.33}$$

and substituted into (2.32) which is further simplified to

$$\frac{(1-e_\mathrm{H})^2}{K_\mathrm{H}e_\mathrm{H}} = \frac{(1-e_\mathrm{L})^2}{K_\mathrm{L}e_\mathrm{L}}\ . \tag{2.34}$$

The denominators and squared terms on both sides of this equation are positive; the terms under the squares have equal signs. By taking the square root and using the algebraic relationship

$$\sinh(x/2) = [\exp^{1/2}(x) - \exp^{-1/2}(x)]/2 \tag{2.35}$$

for the sine hyperbolicus, the optimality condition finally transforms to

$$\frac{\sinh(x_\mathrm{H})}{\sqrt{K_\mathrm{H}}} = \frac{\sinh(x_\mathrm{L})}{\sqrt{K_\mathrm{L}}}\ , \tag{2.36}$$

where

$$x_\mathrm{H} = \frac{1}{2C}\tau_\mathrm{H}K_\mathrm{H} \quad \text{and} \tag{2.37}$$

$$x_\mathrm{L} = \frac{1}{2C}(\tau_\mathrm{tot}-\tau_\mathrm{H})K_\mathrm{L}\ . \tag{2.38}$$

Since the optimality condition (2.36) is a transcendental equation solutions for an optimal τ^*_H at given K_H and K_L generally have to be obtained numerically. The solutions are apparently independent of the sign of C because $\sinh$ is an odd function on both sides of the equation.

In the following two limiting cases are discussed. Isothermal branches are retrieved in the limit of $C \to \infty$ where the arguments x_L and x_H vanish. This allows to

approximate the $\sinh$ in equation (2.36) by the first term of its power series expansion, $x + \frac{x^3}{6} + \mathcal{O}(x)^5$, and to obtain a relation

$$\frac{\tau_{\mathrm{L}}}{\tau_{\mathrm{H}}} = \sqrt{\frac{K_{\mathrm{H}}}{K_{\mathrm{L}}}} \tag{2.39}$$

which is well known for Carnot cycles [11]. Solving for τ_{H} yields

$$\frac{\tau_{\mathrm{H}}}{\tau_{\mathrm{tot}}} = \frac{\sqrt{K_{\mathrm{L}}}}{\sqrt{K_{\mathrm{L}}} + \sqrt{K_{\mathrm{H}}}} = \frac{\sqrt{K_{\mathrm{tot}} - K_{\mathrm{H}}}}{\sqrt{K_{\mathrm{tot}} - K_{\mathrm{H}}} + \sqrt{K_{\mathrm{H}}}} \tag{2.40}$$

where $K_{\mathrm{tot}} := K_{\mathrm{H}} + K_{\mathrm{L}}$.

The limit of what might be referred to as *adiabatic heat transfer branches* is reached for $C \to 0$. These kind of branches are indeed not physical since no heat is transferred at all; the calculations are just performed to see what happens close to this limiting case. If the polytropic heat capacity C approaches zero both arguments x_{L} and x_{H} diverge. This means that $\sinh$ in equation (2.36) can be approximated by $\exp^{1/2}(x)$. Then equation (2.36) simplifies to

$$K_{\mathrm{L}} \exp(x_{\mathrm{H}}) = K_{\mathrm{H}} \exp(x_{\mathrm{L}}) \tag{2.41}$$

and, after taking the logarithm, further to

$$\log(K_{\mathrm{L}}) + x_{\mathrm{H}} = \log(K_{\mathrm{H}}) + x_{\mathrm{L}} \ . \tag{2.42}$$

The logarithmic terms can be neglected because here they are small compared to the diverging x_{H} and x_{L}. Then x_{H} and x_{L} must be equal. This leads to a simple linear relation

$$\frac{\tau_{\mathrm{H}}}{\tau_{\mathrm{L}}} = \frac{K_{\mathrm{L}}}{K_{\mathrm{H}}} \ , \tag{2.43}$$

between the branch times and conductances which alternatively can be written as

$$\frac{\tau_{\mathrm{H}}}{\tau_{\mathrm{tot}}} = \left(1 - \frac{K_{\mathrm{H}}}{K_{\mathrm{tot}}}\right) \ . \tag{2.44}$$

Figure 2.3 depicts the optimal branch time τ_{H} for given conductance K_{L}. The curves have been obtained by numerically solving equation (2.36) for different values of the polytropic heat capacity C. The result confirms the intuitive idea that a small heat conductance has to be compensated by a large branch time and vice versa. The curves are strictly monotonic and become linear in the unphysical limit of adiabatic heat transfer branches.

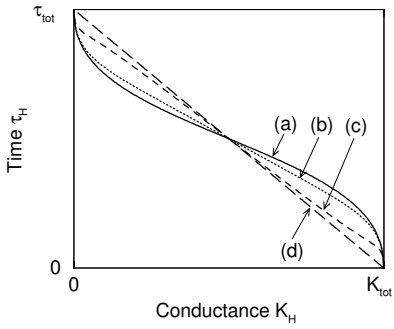

Figure 2.3: Graphs of the optimal time τ_{H} spent in an upper polytropic branch for given conductances K_{L} of the lower polytrop and different polytropic heat capacities where $C/(\tau_{\mathrm{tot}}K_{\mathrm{tot}})$ is (a) ∞ (isothermal limit), (b) 0.1, (c) 0.02 and (d) 0 (adiabatic limit).

2.3.3 Optimal allocation of the conductances

A further constraint could be introduced on the heat conductances which in real engines certainly cannot be made infinitely large. Here the total heat conductance is assumed to be restricted by

$$K_{\mathrm{tot}} = K_{\mathrm{H}} + K_{\mathrm{L}}\,. \tag{2.45}$$

In the following the problem of allocating the total heat conductance K_{tot} to the two heat transfer processes is solved. This kind of problem has been studied in the literature [37, 50–52] for a number of systems of less generality compared to system investigated in this chapter; These publications assume that the heat conductances are not controllable directly but depend on parameters like material and construction choices, areas, cost etc. which are available as controls instead. In some papers, for example in [53, 54], the thermal conductances K_{H} and K_{L} are defined as a product of variable heat transfer areas A_{H} and A_{L}, respectively, and an overall heat transfer coefficient U which is assumed to be the same for both heat exchangers.

Using the formulae developed above the task of determining the optimal allocation of the conductances is almost a trivial one. Equations (2.15) and (2.16) of e_{H} and e_{L} and the work characteristic (2.28) are symmetric with respect to branch times and conductances. Consequently, calculations of the optimal allocation of the conductances are done in the same manner as for the optimal allocation of the branch times in section 2.3.2. and yield an optimality condition

$$\frac{\sinh(x_{\mathrm{H}})}{\sqrt{\tau_{\mathrm{H}}}} = \frac{\sinh(x_{\mathrm{L}})}{\sqrt{\tau_{\mathrm{L}}}}\,. \tag{2.46}$$

This condition is analogous to the condition (2.36). The optimal K_{H} versus τ_{H} dependencies look like a copy of the curves in figure 2.3 with swapped labels for the abscissa and ordinate.

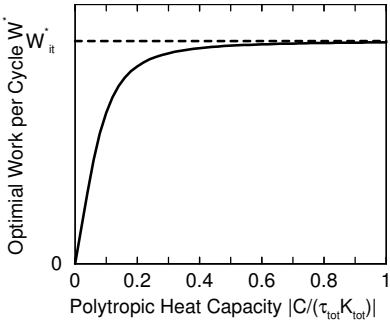

Figure 2.4: The optimal work output W^* is a monotonic increasing function of the scaled polytropic heat capacity $C/(\tau_{\rm tot}K_{\rm tot})$. The dashed line corresponds to the limit of isothermal branches where $C \to \infty$.

2.3.4 Fully optimized engine

A *fully optimized engine* refers to an engine whose work output has been maximized with respect to both, heat conductances and branch times. This requires that the conditions (2.36) and (2.46) are simultaneously fulfilled. This is only possible if the branch times and conductances of both branches are equal:

$$\tau_{\rm H}^* = \tau_{\rm L}^* = \frac{1}{2}\tau_{\rm tot} \qquad \text{and} \qquad K_{\rm H}^* = K_{\rm L}^* = \frac{1}{2}K_{\rm tot}\ . \tag{2.47}$$

Inserting the optimal solution into equations (2.15) and (2.16) results in

$$e^* := e_{\rm H}^* = e_{\rm L}^* = \exp\left(\frac{-\tau_{\rm tot}K_{\rm tot}}{4C}\right)\ . \tag{2.48}$$

Here e^* is still a functions of the polytropic heat capacity C.

2.3.5 Optimal work versus polytropic heat capacity

The maximum possible work output of a fully optimized engine is obtained by substituting the optimal values $\eta^* = 1-\sqrt{T_{0\rm L}/T_{0\rm H}}$, $e_{\rm H}^*$, and $e_{\rm L}^*$ into the work characteristic (2.28) to obtain

$$W^* = C\left(\sqrt{T_{0\rm H}} - \sqrt{T_{0\rm L}}\right)^2 \frac{1-e^*}{1+e^*}\ . \tag{2.49}$$

Figure 2.4 shows a plot of the optimal work W^* versus a scaled polytropic heat capacity. The scaling of C makes the graphs independent of the actual values of $\tau_{\rm H}$, $\tau_{\rm L}$, $K_{\rm H}$, and $K_{\rm L}$. The optimal work W^* is a monotonically increasing function of the absolute value $|C|$ of the polytropic heat capacity. The work output W^* vanishes in the

limit of adiabatic branches ($C \to 0$) where the heat transfer ceases. Maximum work output is achieved for $|C| \to \infty$ where the heat transfer approaches isotherms and corresponds to horizontal lines in the TS-diagram. This findings are consistent with results obtained elsewhere [14, 16, 39, 55], where isothermal heat transfer branches were found to yield an optimal performance of endoreversible heat engines. At the limit of isothermal heat transfer the exponential function in e^* can be replaced by a power series expansion, $e^* = 1 - \tau_{\rm tot} K_{\rm tot}/(4C) + \mathcal{O}(1/C)^2$, and the maximized work output transforms to

$$W^*_{\rm it} = \frac{1}{8}\tau_{\rm tot} K_{\rm tot} \left(\sqrt{T_{0\rm H}} - \sqrt{T_{0\rm L}}\right)^2 \ . \tag{2.50}$$

2.3.6 Optimal temperatures of the working fluid

For the actual design of a heat engine it is quite important to know the temperatures of the working fluid during the cycle. To calculate the optimal temperatures, equations (2.25) and (2.26) are substituted into equations (2.11) and (2.12), to eliminate the heats $Q_{\rm H}$ and $Q_{\rm L}$ and obtain

$$T_{1\rm H} = T_{0\rm H} - \frac{W}{\eta C(1-e_{\rm H})} \tag{2.51}$$

$$T_{1\rm L} = T_{0\rm L} - \frac{W(\eta-1)}{\eta C(1-e_{\rm L})} \ . \tag{2.52}$$

By inserting expression (2.28) for the work W, the initial temperatures are derived with respect to η, $e_{\rm H}$ and $e_{\rm L}$ as

$$T_{1\rm H} = T_{0\rm H} - \Delta_{\rm H}(\eta, e_{\rm H}, e_{\rm L}) \tag{2.53}$$

$$T_{1\rm L} = T_{0\rm L} + \Delta_{\rm L}(\eta, e_{\rm H}, e_{\rm L}) \tag{2.54}$$

where

$$\Delta_{\rm H}(\eta, e_{\rm H}, e_{\rm L}) = \frac{[(1-\eta)T_{0\rm H} - T_{0\rm L}](1-e_{\rm L})}{(1-\eta)(1-e_{\rm H}e_{\rm L})} \tag{2.55}$$

$$\Delta_{\rm L}(\eta, e_{\rm H}, e_{\rm L}) = \frac{[(1-\eta)T_{0\rm H} - T_{0\rm L}](1-e_{\rm H})}{1-e_{\rm H}e_{\rm L}} \ . \tag{2.56}$$

These expressions are subsequently substituted into equations (2.13) and (2.14) to yield equations for the final temperatures

$$T_{2\rm H} = T_{0\rm H} - e_{\rm H}\Delta_{\rm H}(\eta, e_{\rm H}, e_{\rm L}) \quad \text{and} \tag{2.57}$$

$$T_{2\rm L} = T_{0\rm L} + e_{\rm L}\Delta_{\rm L}(\eta, e_{\rm H}, e_{\rm L}) \tag{2.58}$$

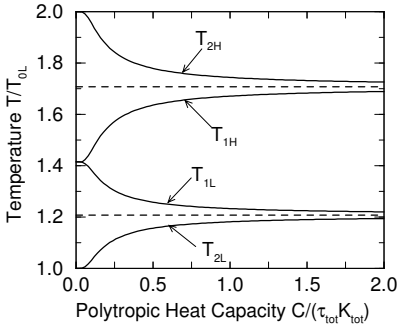

Figure 2.5: Optimal initial and final temperatures $T_{1\mathrm{H}}$ and $T_{2\mathrm{H}}$ on the upper polytrop and $T_{1\mathrm{L}}$ and $T_{2\mathrm{L}}$ on the lower polytrop versus the scaled polytropic heat capacity $C/(\tau_{\mathrm{tot}}K_{\mathrm{tot}})$. The dashed lines correspond to the limit of isothermal branches. The reservoir temperatures are chosen such that $T_{0\mathrm{H}} = 2T_{0\mathrm{L}}$.

of the upper and lower heat transfer branch, respectively. Note that these equations are valid for both, optimal and non-optimal cycles. The initial and final temperatures of the optimized engines are calculated by substituting the optimized control parameters η^*, e^*_{H}, and e^*_{L} into equations (2.55) and (2.56).

If the engine is fully optimized, the respective initial and final temperatures of the working fluid are

$$T_{1\mathrm{H}} = T_{0\mathrm{H}} - \frac{T_{0\mathrm{H}} - \sqrt{T_{0\mathrm{H}}T_{0\mathrm{L}}}}{1+e^*} \tag{2.59}$$

$$T_{2\mathrm{H}} = T_{0\mathrm{H}} - \frac{(T_{0\mathrm{H}} - \sqrt{T_{0\mathrm{H}}T_{0\mathrm{L}}})e^*}{1+e^*} \tag{2.60}$$

for the upper polytrop and

$$T_{1\mathrm{L}} = T_{0\mathrm{L}} + \frac{\sqrt{T_{0\mathrm{H}}T_{0\mathrm{L}}} - T_{0\mathrm{L}}}{1+e^*} \tag{2.61}$$

$$T_{2\mathrm{L}} = T_{0\mathrm{L}} + \frac{(\sqrt{T_{0\mathrm{H}}T_{0\mathrm{L}}} - T_{0\mathrm{L}})e^*}{1+e^*} \tag{2.62}$$

for the lower polytrop. The temporal evolution of the temperatures during the polytropic processes is calculated using equation (2.4) of section 2.1. The temperatures of the fully optimized engine are still functions of the polytropic heat capacity C since $e^* = \exp[-\tau_{\mathrm{tot}}K_{\mathrm{tot}}/(4C)]$. Figure 2.5 shows the optimal temperatures versus the scaled heat capacity $C/(\tau_{\mathrm{tot}}K_{\mathrm{tot}})$. The difference between the initial and final temperatures is decreasing for increasing $C/(\tau_{\mathrm{tot}}K_{\mathrm{tot}})$. In the limit of isothermal heat transfer, where $C \to \infty$ and $e^* = \exp[-\tau_{\mathrm{tot}}K_{\mathrm{tot}}/(4C)] \to 1$, the initial and final

temperatures become equal:

$$T^*_{1\mathrm{H}} = T^*_{2\mathrm{H}} = \frac{1}{2}\sqrt{T_{0\mathrm{H}}}(\sqrt{T_{0\mathrm{H}}} + \sqrt{T_{0\mathrm{L}}}) \tag{2.63}$$

$$T^*_{1\mathrm{L}} = T^*_{2\mathrm{L}} = \frac{1}{2}\sqrt{T_{0\mathrm{L}}}(\sqrt{T_{0\mathrm{H}}} + \sqrt{T_{0\mathrm{L}}})\,. \tag{2.64}$$

These temperatures are drawn as dashed lines into figure 2.5.

2.4 Optimization for maximum work at arbitrary polytropic heat capacities

Engine cycles with arbitrary, non-equal polytropic heat capacities C_H and C_L are not easily treated analytically. The analytical calculations of the previous section 2.3 have been restricted to cases where $C_\mathrm{H} = C_\mathrm{L}$ because of the form of the entropy balance equation (2.18) in section 2.2. This equation generally contains non-rational exponents, which makes closed analytical solutions infeasible and require the use of a numerical scheme.

2.4.1 Numerical optimization scheme

The numerical optimization scheme introduced here uses scaled quantities of some properties. This helps to improve the stability of the numerical scheme and leads to more general results. Scaled quantities are defined for the work output W, the polytropic heat capacities C_H and C_L, the branch times τ_H and τ_L, and the conductances K_H and K_L as

$$\widehat{W} = \frac{W}{\tau_\mathrm{tot} K_\mathrm{tot}}\,, \tag{2.65}$$

$$\widehat{C}_\mathrm{H} = \frac{C_\mathrm{H}}{\tau_\mathrm{tot} K_\mathrm{tot}} \quad \text{and} \quad \widehat{C}_\mathrm{L} = \frac{C_\mathrm{L}}{\tau_\mathrm{tot} K_\mathrm{tot}}\,, \tag{2.66}$$

$$\widehat{\tau}_\mathrm{H} = \frac{\tau_\mathrm{H}}{\tau_\mathrm{tot}} \quad \text{and} \quad \widehat{\tau}_\mathrm{L} = \frac{\tau_\mathrm{L}}{\tau_\mathrm{tot}}\,, \tag{2.67}$$

$$\widehat{K}_\mathrm{H} = \frac{K_\mathrm{H}}{K_\mathrm{tot}} \quad \text{and} \quad \widehat{K}_\mathrm{L} = \frac{K_\mathrm{L}}{K_\mathrm{tot}}\,, \tag{2.68}$$

respectively. Note that the definitions of $\widehat{\tau}_\mathrm{H}$ and $\widehat{\tau}_\mathrm{L}$ are equivalent to the fractions γ_H and γ_L of the total cycle time introduced in section 1.3.2.

The numerical optimization scheme is based on a scaled version of the energy balance equation (2.10)

$$\widehat{W} = \widehat{C}_{\mathrm{H}}(1-e_{\mathrm{H}})(T_{0\mathrm{H}}-T_{1\mathrm{H}}) + \widehat{C}_{\mathrm{L}}(1-e_{\mathrm{L}})(T_{0\mathrm{L}}-T_{1\mathrm{L}}) \tag{2.69}$$

where the abbreviations (2.15) and (2.16) are transformed to

$$e_{\mathrm{H}} = \exp\left(-\frac{\widehat{\tau}_{\mathrm{H}}\widehat{K}_{\mathrm{H}}}{\widehat{C}_{\mathrm{H}}}\right) \tag{2.70}$$

$$e_{\mathrm{L}} = \exp\left(-\frac{(1-\widehat{\tau}_{\mathrm{H}})(1-\widehat{K}_{\mathrm{H}})}{\widehat{C}_{\mathrm{L}}}\right) . \tag{2.71}$$

The numerical optimization scheme also employs a scaled version of the logarithm of the entropy balance equation (2.18):

$$0 = \widehat{C}_{\mathrm{H}} \log\left[\frac{T_{0\mathrm{H}} - e_{\mathrm{H}}(T_{0\mathrm{H}}-T_{1\mathrm{H}})}{T_{1\mathrm{H}}}\right] + \widehat{C}_{\mathrm{L}} \log\left[\frac{T_{0\mathrm{L}} - e_{\mathrm{L}}(T_{0\mathrm{L}}-T_{1\mathrm{L}})}{T_{1\mathrm{L}}}\right] . \tag{2.72}$$

The initial parameters of the optimization problem are the temperatures of the heat reservoirs $T_{0\mathrm{H}}$ and $T_{0\mathrm{L}}$, the sum of the branch times τ_{tot}, the sum of the heat conductances K_{tot}, and the scaled polytropic heat capacities $\widehat{C}_{\mathrm{H}}$ and $\widehat{C}_{\mathrm{L}}$. The control parameters are the temperatures at the beginning of the upper polytropic branch $T_{1\mathrm{H}}$, the scaled upper branch time $\widehat{\tau}_{\mathrm{H}}$ and the scaled heat conductance $\widehat{K}_{\mathrm{H}}$. The objective of the optimization is to adjust the controls such that both the physical constraints (namely entropy and energy balance) are fulfilled and the work output of the engine is maximized.

A downhill simplex method for multi-dimensions ([56], pp. 408-412) and a root finding bisection method ([56], pp. 350-354) are employed to solve the optimization problem. The simplex method has been augmented to ensure that the physically sensible range of $0 < \widehat{K}_{\mathrm{H}}, \widehat{K}_{\mathrm{L}}, \widehat{\tau}_{\mathrm{H}}, \widehat{\tau}_{\mathrm{L}} < 1$ is kept.

The optimization algorithm works as follows:

1. choose values for the parameters $T_{0\mathrm{H}}$ and $T_{0\mathrm{L}}$, $\widehat{C}_{\mathrm{H}}$, and $\widehat{C}_{\mathrm{L}}$ for which the optimization problem should be solved;
2. for the start of the simplex method, choose three arbitrary, linear independent vectors $\vec{v}_1$, $\vec{v}_2$ and $\vec{v}_3$ of the triple $(\widehat{\tau}_{\mathrm{H}}, \widehat{K}_{\mathrm{H}}, T_{1\mathrm{H}})$;
3. perform a simplex step which returns a new vector $\vec{v}_*$
   (a) by inserting the elements of $\vec{v}_*$ into equation (2.72) calculate the temperature $T_{1\mathrm{L}}$ using a root finding bisection method;

(b) calculate the work output W by inserting $T_{1\mathrm{L}}$ and $\vec{v}_*$ into equation (2.69);

(c) feed the (negative) work output back to simplex method which subsequently returns a new vector $\vec{v}_*$;

4. systematically repeat the simplex step 3 until the maximum work output is found within a given accuracy;

5. finally print out the work output, the optimal temperatures, the branch times, the cycle diagram, and the efficiency η of the numerically optimized engine.

2.4.2 Numerical results

Numerical optimizations of the heat engine have been performed for a temperature of the heat reservoirs of $T_{0\mathrm{L}} = 300\,\mathrm{K}$ and $T_{0\mathrm{H}} = 1200\,\mathrm{K}$. Detailed numerical results are compiled in tables printed in appendix C.

Some cycles of optimized engines are depicted in figure 2.6. The cycles (a) and (b) in the upper row of figure 2.6 are for symmetric cases where the polytropic heat capacities are identical, i. e. $\widehat{C}_{\mathrm{H}} = \widehat{C}_{\mathrm{L}}$. All other cycles are for cases of unequal $\widehat{C}_{\mathrm{H}}$ and $\widehat{C}_{\mathrm{L}}$. Both heat transfer branches of cycle (a), the upper heat transfer branch of cycles (c) and (e), and the lower heat transfer branch of cycles (b) and (f) are close to isotherms. The temperature of the working fluid in branches with relatively low values of the polytropic heat capacity can get very close to the temperatures of one of the reservoir. Cycles of this kind also have a poor work output although they are fully optimized.

Maximum work output versus polytropic heat capacities

The work output of the optimized cycles is a monotonically increasing function of the (positive) value of both polytropic heat capacities as can be seen from figure 2.7. The work output reaches its maximum value of $W^* \approx 37.5\tau_{\mathrm{tot}}K_{\mathrm{tot}}$ in the limit of two isothermal branches where $C_{\mathrm{H}}, C_{\mathrm{L}} \to \infty$. It remains at a high level for $C_{\mathrm{H}}, C_{\mathrm{L}} > 0.1\tau_{\mathrm{tot}}K_{\mathrm{tot}}$ and rapidly decreases if one of the polytropic heat capacities is below $0.1\tau_{\mathrm{tot}}K_{\mathrm{tot}}$. The more isothermal the heat transfer branches are the better becomes the optimized work output.

A plot of the efficiency versus the polytropic heat capacities is shown in figure 2.8. The efficiency η^* of the optimized is equal to the Curzon-Ahlborn efficiency $\eta_{\mathrm{CA}} = 1 - \sqrt{T_{0\mathrm{L}}/T_{0\mathrm{H}}}$ only if both polytropic heat capacities are equal. For all other cases the efficiency deviates up to about 8% from the Curzon-Ahlborn efficiency, especially if one or both of the polytropic heat capacities are below $0.1\tau_{\mathrm{tot}}K_{\mathrm{tot}}$.

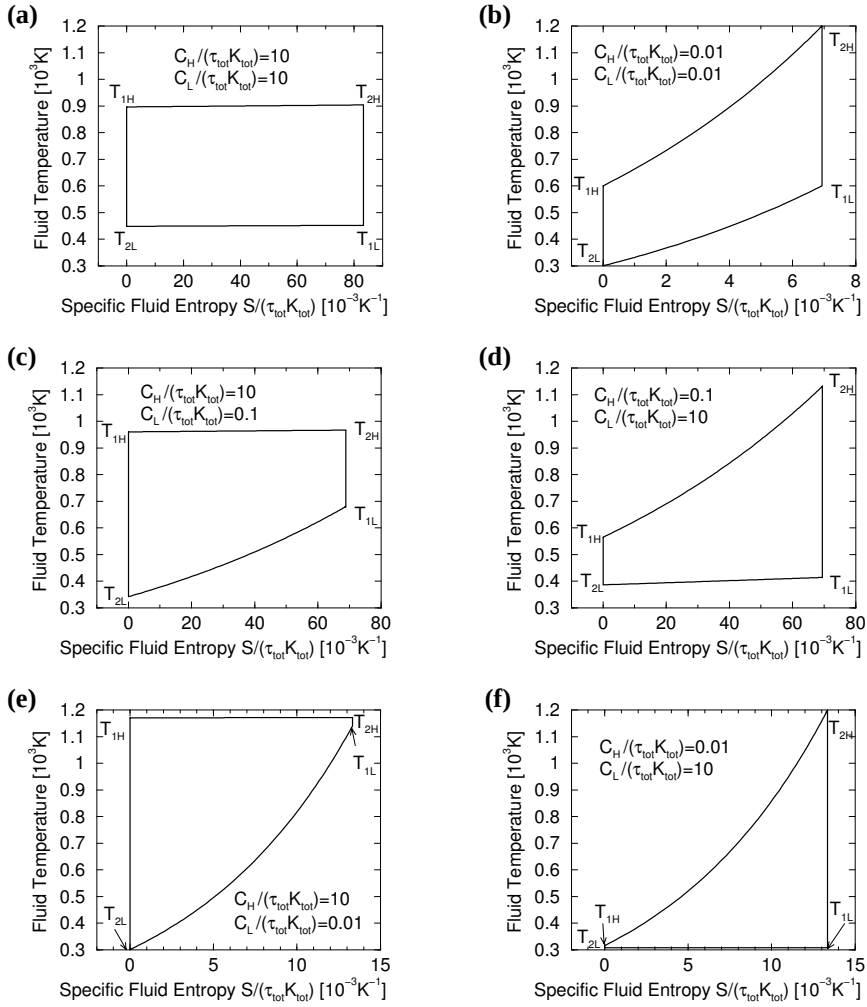

Figure 2.6: Examples for fully optimized polytropic engine cycles.

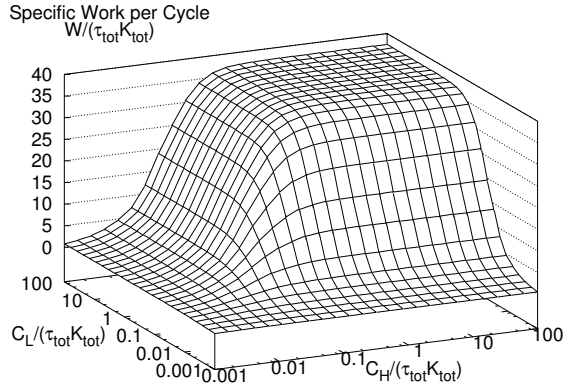

Figure 2.7: Optimal work output and efficiency versus polytropic heat capacities.

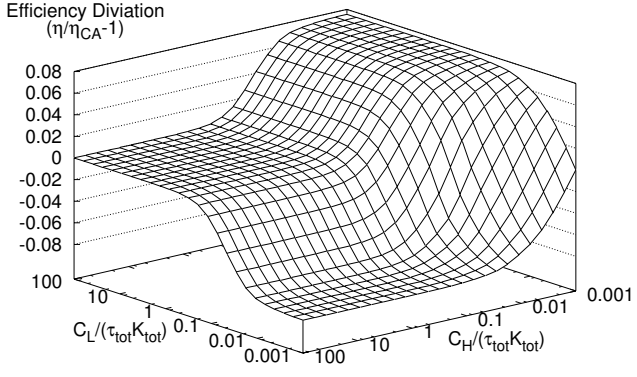

Figure 2.8: Optimal work output and efficiency versus polytropic heat capacities.

This finding is quite remarkable since the Curzon-Ahlborn efficiency has been reoccuring in numerous publications and studies of many different systems, in particular in cases of linear heat transport laws. The above results show that the Curzon-Ahlborn efficiency can not be used as an universal figure for heat engines optimized for maximum work output although it still can serve as a rough estimate of the efficiency for such engines. The numerical calculations further suggest that one should try to allocate the more isothermal-like heat transfer branch to the cold reservoir in order to improve the efficiency.

Optimal branch temperatures versus polytropic heat capacities

Figure 2.9 shows the optimal start temperature $T_{1\mathrm{H}}$ and $T_{1\mathrm{L}}$ of the upper and lower heat transfer branch, respectively. The region of $C_{\mathrm{H}}, C_{\mathrm{L}} > 0.1\tau_{\mathrm{tot}}K_{\mathrm{tot}}$ almost corresponds to two isothermal heat transfer branches of a Carnot cycle where the start and end temperature are the same within each branch. If C_{H} and C_{L} are approximately equal and are lower than $0.01\tau_{\mathrm{tot}}K_{\mathrm{tot}}$ then the optimal start temperatures of both branches become the same and the end temperatures become close to the reservoir temperature as can be seen in figure 2.6 b .

For all combinations of C_{H} and C_{L} the start temperature $T_{1\mathrm{H}}$ of the upper branch is higher than the start temperature $T_{1\mathrm{L}}$ of the lower branch.

Optimal branch times and heat conductances versus polytropic heat capacities

Figure 2.10 shows the optimal allocation $\tau_{\mathrm{H}}/\tau_{\mathrm{L}}$ of the branch times and the optimal allocation $K_{\mathrm{H}}/K_{\mathrm{L}}$ of the heat conductances in one graph. This joint display is possible since the dependence of the optimized $\tau_{\mathrm{H}}/\tau_{\mathrm{L}}$ and $K_{\mathrm{H}}/K_{\mathrm{L}}$ allocations on the polytropic heat capacities C_{H} and C_{L} turns out to be the same. This feature is a consequence of the symmetry of the optimization problem with respect to the branch times and heat conductances.

For the region of almost isothermal heat transfer branches, where $C_{\mathrm{H}} > 0.1\tau_{\mathrm{tot}}K_{\mathrm{tot}}$ and $C_{\mathrm{L}} > 0.1\tau_{\mathrm{tot}}K_{\mathrm{tot}}$, as well as for the line of equal polytropic heat transfer branches, where $C_{\mathrm{H}} = C_{\mathrm{L}}$, the optimum allocation of the branch times and conductances is an equal allocation to both heat transfer branches.

In case of $C_{\mathrm{H}} \gg 0.1\tau_{\mathrm{tot}}K_{\mathrm{tot}}$ and $C_{\mathrm{L}} \ll 0.1\tau_{\mathrm{tot}}K_{\mathrm{tot}}$, a larger proportion of the available branch time and conductance should be allocated to the upper heat transfer branch than to the lower heat transfer branch and vice versa, if $C_{\mathrm{H}} \ll 0.1\tau_{\mathrm{tot}}K_{\mathrm{tot}}$ and $C_{\mathrm{L}} \gg 0.1\tau_{\mathrm{tot}}K_{\mathrm{tot}}$.

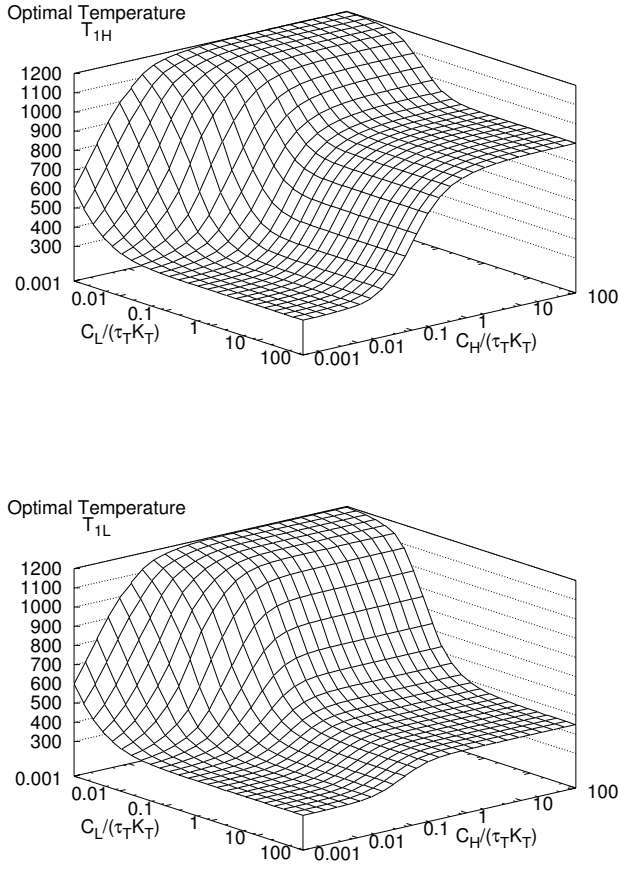

Figure 2.9: Optimal start temperatures of the upper and lower heat transfer branch versus the polytropic heat capacities.

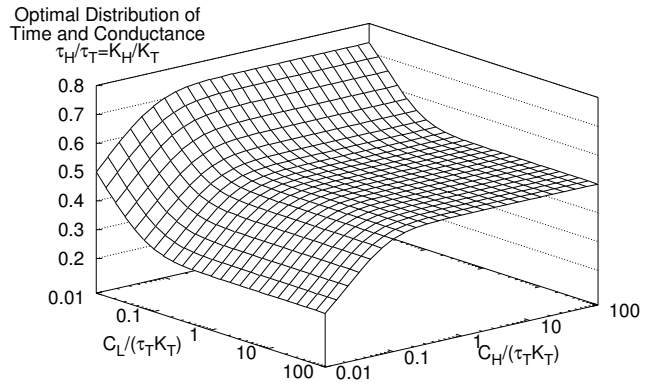

Figure 2.10: Plot of the optimal allocation of branch times and heat conductances versus polytropic heat capacities

2.5 Summary

Endoreversible engine cycles with two adiabatic and two heat transfer branches have been investigated and optimized for maximum work output. The heat transfer branches are described as general polytropic processes which include common standard branches, like isotherms, isobars, and isochors, as special cases. Thus the considered model is capable to describe technologically important cycles like the Brayton cycle and Otto cycle. The study further accounts for the finite heat capacity of the working fluid and the finite-time character of the heat transfer processes.

Analytic expressions for the maximized work output, for the corresponding optimal temperatures of the working fluid, for the optimal allocation of the heat conductances and of the durations of the heat transfer processes have been obtained in case of equal polytropic degrees of both polytropic branches. If both polytropic degrees are equal the efficiency at maximum work is found to coincide with the Curzon-Ahlborn efficiency, $\eta^* = 1 - \sqrt{T_{0\mathrm{L}}/T_{0\mathrm{H}}}$, of an endoreversible Carnot engine and does not depend on the degree of the polytropic processes or other design parameters.

Then the open problem whether the Curzon-Ahlborn efficiency is applicable in the case of different polytropic degrees on the two heat exchanging branches is investigated. The answer to this problem is quite important as it might shed light on the range of validity of the Curzon-Ahlborn efficiency. An analytic solution to this ques-

tion was not possible. The question had to be resolved by numerical methods.

The results of the numerical calculations showed that the efficiency of the polytropic engine significantly deviates from the Curzon-Ahlborn efficiency if the branches are of a different type. This is quite surprising since the existing literature suggests that the linearity of the heat conduction law is the main criterion for an applicability of the Curzon–Ahlborn efficiency. But instead it turned out that the exponents of the polytropic branches are crucial in this context.

Additionally, the numerical calculations yielded optimal solutions for performance and process parameters. It was demonstrated how the work output of the engine can be improved by allocating the conductances and times of the heat transfer processes in an optimal way. The calculations further showed that the performance of the heat engine increases for large absolute values of the polytropic heat capacity.

Chapter 3

Optimal allocation of heat-exchanger costs

Finite and therefore irreversible heat flows in thermal systems are often interfaced by heat exchangers which play an important role for the performance and costs of such systems. Several papers have addressed the question of how to allocate a given heat transfer equipment to the hot and the cold sides of heat engines [37, 50, 51] and refrigerators [51, 57–60] to achieve, for instance, a maximum of work output, efficiency, or coefficient of performance or to minimize the entropy production of the system. The cited studies arrived at the conclusion that the thermal conductance of the heat exchangers should be split evenly between the hot and cold ends to achieve an optimal performance of the investigated devices. This result is the same regardless if the system is a cyclic or a stationary operating one, as long as the heat transfer laws are linear.

However, it is not genrally known wether these results are still valid for systems where the heat transfer laws are non-linear. It further is not clear how the optimal allocation of the heat exchanger inventory is affected if the the actual expenditures for heat exchangers obey a complete different dependency for the hot and cold side of a device. For real-world applications capital investment costs are often the restricting factor on the design of heat exchanger inventory. In a power plant, for example, the capital investment costs per unit of thermal conductance or heat exchanger area are certainly much less for a cooling tower than for a heat exchanger within the chemically aggressive atmosphere of a hot furnace chamber. This illustrates why a more general description is needed to account for actual costs of heat exchangers in thermodynamic systems with generally non-linear heat transfer.

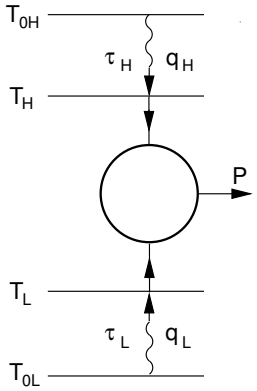

Figure 3.1: Model of a energy converting system with heat exchangers to hot and cold reservoirs at constant temperatures $T_{0\mathrm{H}}$ and $T_{0\mathrm{L}}$, respectively, a reversible subsystem with a work contact (P) operating between internal temperatures of T_{H} and T_{L}.

In the following non-linear cost functions are introduced for each of the heat exchangers in order to account for the capital investments needed to achieve a certain flow of heat through each of the heat exchangers. The optimal performance of a generalized energy converting system is subsequently determined under the constraint of limited financial resources for the total heat exchanger inventory. The present study is not limited to costs alone as restricting resource. It also is applicable to the problem of optimal allocation of weights, sizes or any other parameter associated with heat exchangers, if the dependency between this parameter and the flow of heat through a heat exchanger is known.

3.1 Model of a energy converting system

Figure 3.1 shows an endoreversible model with two heat reservoirs at constant temperatures $T_{0\mathrm{H}}$ and $T_{0\mathrm{L}}$ and a reversible operating, energy converting subsystem. The model is likewise capable to describe heat engines, refrigerators and heat pumps, if the signs of the heat flows q_{H} and q_{L} and of the power flow P are chosen appropriately. For heat engines, the upper heat exchanger transfers the heat q_{H} to the energy converting subsystem which produces the power P and discharges the heat $-q_{\mathrm{L}}$ to the cold reservoir via a second heat exchanger. The cases of refrigerators and heat pumps are simply retrieved by changing the signs of power and heat flows to the opposite of the heat engine case.

For all three instances of the model it is assumed that the heat flows q_i ($i \in \{\mathrm{H}, \mathrm{L}\}$) between the energy converting subsystem and the heat reservoirs are functions of the

costs c_i for heat exchangers and the temperatures on either side of the heat exchangers:

$$q_i(c_i, T_{0i}, T_i) = k_i(c_i)\varphi_i(T_{0i}, T_i) \quad i \in \{\mathrm{H}, \mathrm{L}\} \; . \tag{3.1}$$

The functions φ_i represent the types of heat transfer, and have to meet the requirements for sensible heat transfer laws as defined in equation (1.15). Common examples are linear heat transfer, where $\varphi_i(T_{0i}, T_i) = T_{0i} - T_i$, and radiative heat transfer, where $\varphi_i(T_{0i}, T_i) = T_{0i}^4 - T_i^4$; further examples are found in the appendix B.

The term $k_i(c_i)$ describes the dependence of the heat transfer on the amount c_i of invested capital. The units and physical meaning of $k_i(c_i)$ essentially depend on the form of the heat transfer laws. Therefore $k_i(c_i)$ is referred to as *heat transfer coefficient* here, to avoid confusion with properties occurring in a heat transport law of particular type. In case of a linear heat transport law, for example, $k_i(c_i)$ is equivalent to the heat conductance of the heat exchangers.

The following analysis is performed for two modes of operation:

- stationary conditions (see section 1.3.2) where the energy converting subsystem contacts both heat reservoirs simultaneously with different temperatures at different contact points;
- cyclic conditions (see section 1.3.2) where the energy converting subsystem takes only one temperature at a time and alternately connects to either one of the two heat reservoirs during the contact times $\tau_\mathrm{H} = \gamma_\mathrm{H}\tau_\mathrm{tot}$ and $\tau_\mathrm{L} = \gamma_\mathrm{H}\tau_\mathrm{tot}$ where τ_tot is the total cycle time and the parts of time are restricted by

$$\gamma_\mathrm{H} + \gamma_\mathrm{L} = 1 \, , \quad \gamma_\mathrm{H} \geq 0 \quad \gamma_\mathrm{L} \geq 0 \; . \tag{3.2}$$

The average power and entropy production rates are defined as

$$\overline{P} = \frac{1}{\tau_\mathrm{tot}} \int_0^{\tau_\mathrm{tot}} P \, \mathrm{d}t \; , \quad \text{and} \tag{3.3}$$

$$\overline{s} = \frac{1}{\tau_\mathrm{tot}} \int_0^{\tau_\mathrm{tot}} s \, \mathrm{d}t \; , \tag{3.4}$$

respectively. In case of stationary conditions, where the rates are constant in time, it follows that $P = \overline{P}$ and $s = \overline{s}$ at every moment of time.

3.2 Optimizing for a minimum of entropy production

The thermodynamic system in figure 3.1 is optimized for minimal entropy production subject to a given average power $\overline{P}$. With this constraint some optimization

objectives become equivalent. In particular, the minimization of entropy production is equivalent to the optimization of the efficiency η if the system is operating as an engine, or to the maximization of the coefficients of performance (COP) if the system is operated as a refrigerator or heat pump. The prove of this equivalences has been published elsewhere [31] and can be found in appendix D of this thesis.

3.2.1 Problem statement

The problem of finding the optimal allocation of heat exchanger costs in a thermal system (Fig.3.1) is formulated as:

> Determine the values of the fluid temperatures T_{H}, T_{L}, the parts γ_{H}, γ_{L} of the cycle time during which the working fluid is in contact with one of the reservoirs, and the heat exchangers costs c_{H}, c_{L}, such that the average rate of produced entropy $\overline{s}$ is minimized for given total costs c_{tot} of the heat exchanger inventory and given average power $\overline{P}$ exchanged with the system.

The average entropy increase within the reversible, energy converting subsystem is equal to zero. This allows to reduce the minimization problem to the problem of minimizing the average increase of the reservoirs entropy, or, which is equivalent, to the problem of maximizing the expression

$$-\overline{s} = \gamma_{\mathrm{H}} \frac{k_{\mathrm{H}}(c_{\mathrm{H}})\varphi_{\mathrm{H}}(T_{\mathrm{H}})}{T_{0\mathrm{H}}} + \gamma_{\mathrm{L}} \frac{k_{\mathrm{L}}(c_{\mathrm{L}})\varphi_{\mathrm{L}}(T_{\mathrm{L}})}{T_{0\mathrm{L}}} \rightarrow \max_{T_i, c_i, \gamma_i} . \tag{3.5}$$

The six controls of this optimization problem are two internal temperatures T_i, two costs c_i of the heat exchangers and two parts γ_i of the cycle time where $i \in \{\mathrm{H}, \mathrm{L}\}$. The case of stationary conditions does not require an optimization with respect to γ_{H} and γ_{L} since the energy converting subsystem is in permanent contact with both heat reservoirs during the whole cycle time τ_{tot} so that Therefore stationary correspond to $\gamma_{\mathrm{H}} = \gamma_{\mathrm{L}} = 1$.

The set of admissible solutions of the problem is restricted by balance equations for the reversible, energy converting subsystem. These balance equations where introduced in section 1.1.4. Here the entropy balance is written in time averaged form as

$$\gamma_{\mathrm{H}} \frac{k_{\mathrm{H}}(c_{\mathrm{H}})\varphi_{\mathrm{H}}(T_{\mathrm{H}})}{T_{\mathrm{H}}} + \gamma_{\mathrm{L}} \frac{k_{\mathrm{L}}(c_{\mathrm{L}})\varphi_{\mathrm{L}}(T_{\mathrm{L}})}{T_{\mathrm{L}}} = 0 \; ; \tag{3.6}$$

and the energy balance in time averaged form as

$$\gamma_{\mathrm{H}} k_{\mathrm{H}}(c_{\mathrm{H}})\varphi_{\mathrm{H}}(T_{\mathrm{H}}) + \gamma_{\mathrm{L}} k_{\mathrm{L}}(c_{\mathrm{L}})\varphi_{\mathrm{L}}(T_{\mathrm{L}}) = \overline{P} \; . \tag{3.7}$$

A further constraint is the fixed total cost c_{tot} of the heat exchangers which is the sum of costs of the two individual heat exchangers

$$c_{\mathrm{H}} + c_{\mathrm{L}} = c_{\mathrm{tot}} \ . \tag{3.8}$$

3.2.2 Optimality conditions

The Lagrange function for the optimization problem follows from equations (3.2), (3.5), (3.6), (3.7) and (3.8) and is written as

$$\mathcal{L} = \gamma_{\mathrm{H}}\mathcal{L}_{\mathrm{H}} + \gamma_{\mathrm{L}}\mathcal{L}_{\mathrm{L}} + \lambda_{\mathrm{c}}(c_{\mathrm{H}} + c_{\mathrm{L}}) + \lambda_{\gamma}(\gamma_{\mathrm{H}} + \gamma_{\mathrm{L}}) \ , \tag{3.9}$$

where

$$\mathcal{L}_i = k_i(c_i)\varphi_i(T_i)\Lambda_i(\lambda, T_i) \ , \tag{3.10}$$

$$\Lambda_i(\lambda, T_i) = \frac{\lambda_0}{T_{0\mathrm{i}}} + \frac{\lambda_1}{T_i} + \lambda_2 \ , \qquad i \in \{\mathrm{H}, \mathrm{L}\} \ . \tag{3.11}$$

If the system operates at stationary conditions, the restriction (3.2) on the cycle times is omitted and λ_γ is set to zero.

The optimality conditions for the fluid temperatures, $\partial\mathcal{L}/\partial T_i = 0$, can be written as

$$\frac{\partial\varphi_i}{\partial T_i}\Lambda_i = \lambda_1\frac{\varphi_i}{T_i^2} \ , \quad i \in \{\mathrm{H}, \mathrm{L}\} \ . \tag{3.12}$$

Note that in order to shorten the notation the above and the following expressions do not explicitly state the dependencies $\varphi_i = \varphi_i(T_i)$ and $k_i = k_i(c_i)$.

The optimality conditions for the costs of heat exchangers, $\partial\mathcal{L}/\partial c_i = 0$, are combined to

$$\gamma_{\mathrm{H}}\frac{\mathrm{d}k_{\mathrm{H}}}{\mathrm{d}c_{\mathrm{H}}}\varphi_{\mathrm{H}}\Lambda_{\mathrm{H}} = \gamma_{\mathrm{L}}\frac{\mathrm{d}k_{\mathrm{L}}}{\mathrm{d}c_{\mathrm{L}}}\varphi_{\mathrm{L}}\Lambda_{\mathrm{L}} \ . \tag{3.13}$$

In case of cyclic conditions one additional has the conditions $\partial\mathcal{L}/\partial\gamma_i = 0$ ($i \in \{\mathrm{H}, \mathrm{L}\}$), for the γ optimality. These two conditions are used to obtain

$$\frac{\Lambda_{\mathrm{L}}}{\Lambda_{\mathrm{H}}} = \frac{k_{\mathrm{H}}\varphi_{\mathrm{H}}}{k_{\mathrm{L}}\varphi_{\mathrm{L}}} \ . \tag{3.14}$$

3.2.3 Optimal cost allocation

In order to derive the optimal cost allocation the ratio of the two representations ($i \in \{\mathrm{H}, \mathrm{L}\}$) of equation (3.12) is taken:

$$\frac{\Lambda_{\mathrm{L}}}{\Lambda_{\mathrm{H}}} = \frac{\partial\varphi_{\mathrm{H}}/\partial T_{\mathrm{H}}}{\partial\varphi_{\mathrm{L}}/\partial T_{\mathrm{L}}}\frac{\varphi_{\mathrm{L}}}{\varphi_{\mathrm{H}}}\left(\frac{T_{\mathrm{H}}}{T_{\mathrm{L}}}\right)^2 \ . \tag{3.15}$$

The ratio $\Lambda_\mathrm{L}/\Lambda_\mathrm{H}$ is found from condition (3.13) as

$$\frac{\Lambda_\mathrm{L}}{\Lambda_\mathrm{H}} = \frac{\gamma_\mathrm{H}\varphi_\mathrm{H}}{\gamma_\mathrm{L}\varphi_\mathrm{L}} \frac{\mathrm{d}k_\mathrm{H}/\mathrm{d}c_\mathrm{H}}{\mathrm{d}k_\mathrm{L}/\mathrm{d}c_\mathrm{L}} \,. \tag{3.16}$$

This equation is combined with equation (3.15) to yield the expression

$$\frac{\mathrm{d}k_\mathrm{H}/\mathrm{d}c_\mathrm{H}}{\mathrm{d}k_\mathrm{L}/\mathrm{d}c_\mathrm{L}} = \frac{\gamma_\mathrm{L}}{\gamma_\mathrm{H}} \frac{\partial\varphi_\mathrm{H}/\partial T_\mathrm{H}}{\partial\varphi_\mathrm{L}/\partial T_\mathrm{L}} \left(\frac{\varphi_\mathrm{L}T_\mathrm{H}}{\varphi_\mathrm{H}T_\mathrm{L}}\right)^2 \,, \tag{3.17}$$

which, by eliminating the quadratic term using equation (3.6), further simplifies to

$$\frac{\mathrm{d}k_\mathrm{H}/\mathrm{d}c_\mathrm{H}}{\mathrm{d}k_\mathrm{L}/\mathrm{d}c_\mathrm{L}} = \frac{\gamma_\mathrm{H}}{\gamma_\mathrm{L}} \frac{\partial\varphi_\mathrm{H}/\partial T_\mathrm{H}}{\partial\varphi_\mathrm{L}/\partial T_\mathrm{L}} \left(\frac{k_\mathrm{H}}{k_\mathrm{L}}\right)^2 \,. \tag{3.18}$$

In case of cyclic conditions, equation (3.14) is substituted into equation (3.16) to calculate the optimal $\gamma_\mathrm{L}/\gamma_\mathrm{H}$ ratio as

$$\frac{\gamma_\mathrm{H}}{\gamma_\mathrm{L}} = \frac{\mathrm{d}k_\mathrm{L}/\mathrm{d}c_\mathrm{L}}{\mathrm{d}k_\mathrm{H}/\mathrm{d}c_\mathrm{H}} \frac{k_\mathrm{H}}{k_\mathrm{L}} \,. \tag{3.19}$$

This ratio is inserted into equation (3.18) to derive the condition for the optimal allocation of the costs in case of a cyclic system:

$$\left(\frac{\mathrm{d}k_\mathrm{H}/\mathrm{d}c_\mathrm{H}}{\mathrm{d}k_\mathrm{L}/\mathrm{d}c_\mathrm{L}}\right)^2 = \frac{\partial\varphi_\mathrm{H}/\partial T_\mathrm{H}}{\partial\varphi_\mathrm{L}/\partial T_\mathrm{L}} \left(\frac{k_\mathrm{H}}{k_\mathrm{L}}\right)^3 \,. \tag{3.20}$$

The analogous expression for stationary conditions,

$$\frac{\mathrm{d}k_\mathrm{H}/\mathrm{d}c_\mathrm{H}}{\mathrm{d}k_\mathrm{L}/\mathrm{d}c_\mathrm{L}} = \frac{\partial\varphi_\mathrm{H}/\partial T_\mathrm{H}}{\partial\varphi_\mathrm{L}/\partial T_\mathrm{L}} \left(\frac{k_\mathrm{H}}{k_\mathrm{L}}\right)^2 \,, \tag{3.21}$$

is derived by directly substituting $\gamma_\mathrm{H} = \gamma_\mathrm{L} = 1$ into equation (3.18).

The last formula (3.21) is the desired result for the optimal allocation of heat exchanger costs c_H and c_L in case of stationary conditions. This formula significantly differs from the corresponding formula (3.20) in case of cyclic conditions.

Both formulas are equally valid for heat engines, refrigerators and heat pumps and can be used with any laws of heat transfer $k_i(c_i)\varphi_\mathrm{i}(T_{0i}, T_i)$ ($i \in \{\mathrm{H}, \mathrm{L}\}$).

In general, formulae (3.21) and (3.20) are evaluated by inserting the optimal values of the fluid temperatures $T^*_\mathrm{H}(k_\mathrm{H}, k_\mathrm{L})$ and $T^*_\mathrm{L}(k_\mathrm{H}, k_\mathrm{L})$. Expressions for these temperatures are either determined directly from condition (3.12) together with equations (3.2), (3.6), (3.7) and (3.14), or calculated for a system optimized with respect to T_H and T_L in case of given k_H and k_L, or found in the literature, for example in [64–67].

3.3 Examples

In all following examples a cost function of the quite general form

$$k_i = \beta_i c_i^{a_i} \ , \quad i \in \{\mathrm{H}, \mathrm{L}\} \ . \tag{3.22}$$

is assumed for both heat exchangers. The heat transfer coefficient at the i-th side of the system is proportional to the a_i-th power of the respective cost of the heat exchanger. Proportionality between the the cost c_i and the heat transfer coefficient β_i corresponds to $a_i = 1$. A system where the marginal costs are decreasing for increasing heat transfer coefficients corresponds to $a_i > 1$, while a system where the marginal costs are decreasing for increasing heat transfer coefficients corresponds to $a_i < 1$.

The derivatives of the cost function $k_i(c_i)$ with respect to c_i is determined as

$$\frac{\mathrm{d}k_i}{\mathrm{d}c_i} = \frac{a_i k_i}{c_i} \ . \tag{3.23}$$

3.3.1 Linear heat transfer

Consider the case of linear heat transfer laws where the heat flows are proportional to the difference of temperatures:

$$\varphi_i = T_{0i} - T_i \ , \quad i \in \{\mathrm{H}, \mathrm{L}\} \ . \tag{3.24}$$

Then the derivatives $\partial\varphi_i / \partial T_i$ are equal to -1 and the expressions for the optimal cost allocation are directly derived from equation (3.20) and (3.21) as

$$\frac{\mathrm{d}k_\mathrm{H}/\mathrm{d}c_\mathrm{H}}{\mathrm{d}k_\mathrm{L}/\mathrm{d}c_\mathrm{L}} = \begin{cases} \left(\frac{k_\mathrm{H}}{k_\mathrm{L}}\right)^{3/2} & \text{for cyclic conditions} \\ \left(\frac{k_\mathrm{H}}{k_\mathrm{L}}\right)^{2} & \text{for stationary conditions.} \end{cases} \tag{3.25}$$

By inserting the cost function (3.22) and their derivatives (3.23) into the optimality conditions (3.25) one finds

$$\frac{\beta_\mathrm{H}}{\beta_\mathrm{L}} = \left(\frac{a_\mathrm{H}}{a_\mathrm{L}}\right)^2 \frac{c_\mathrm{L}^{a_\mathrm{L}+2}}{c_\mathrm{H}^{a_\mathrm{H}+2}} \tag{3.26}$$

for cyclic conditions and

$$\frac{\beta_\mathrm{H}}{\beta_\mathrm{L}} = \frac{a_\mathrm{H}}{a_\mathrm{L}} \frac{c_\mathrm{L}^{a_\mathrm{L}+1}}{c_\mathrm{H}^{a_\mathrm{H}+1}} \tag{3.27}$$

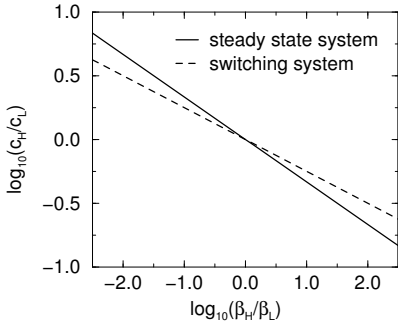

Figure 3.2: The optimal allocation of the heat exchanger costs $c_\mathrm{H}/c_\mathrm{L}$ is plotted versus the ratio $\beta_\mathrm{H}/\beta_\mathrm{L}$ (see text) for an engine with a linear law of heat transfer and a quadratic dependency between the costs and the heat transfer coefficients.

for stationary conditions.

If the exponents a_H and a_L are equal, then the optimal allocation of the costs is easily determined from the above equation as

$$\frac{c_\mathrm{H}}{c_\mathrm{L}} = \left(\frac{\beta_\mathrm{H}}{\beta_\mathrm{L}}\right)^{-b} \tag{3.28}$$

for equal exponents $a = a_\mathrm{H} = a_\mathrm{L}$ with $b = 1/(a+1)$ for stationary conditions and $b = 1/(a+2)$ for cyclic conditions.

If the ratio $\beta_\mathrm{H}/\beta_\mathrm{L} = 1$ then $c_\mathrm{H}/c_\mathrm{L} = 1$ for any exponent a, regardless of if the system is operating at stationary or cyclic conditions.

Figure 3.2 plots the optimal ratio $c_\mathrm{H}/c_\mathrm{L}$ of the heat exchanger costs as a function of the ratio $\beta_\mathrm{H}/\beta_\mathrm{L}$ in case of a quadratic dependence ($a = 2$) between the cost c_i and the heat transfer coefficient k_i. The cost ratio $c_\mathrm{H}/c_\mathrm{L}$ is less sensitive to variations in the ratio $\beta_\mathrm{H}/\beta_\mathrm{L}$ in case of cyclic conditions than in case of stationary conditions. This is also true for other values of the power a as long as $a > -1$, which should be the case for all physically sensible systems.

If the degrees a_H and a_L are different solutions of equation (3.26) and (3.27) generally have to be calculated numerically.

3.3.2 Heat engine with an inverse law of heat transfer operating at cyclic conditions

Consider a heat engine operating at cyclic conditions with a inverse law of heat transfer in both branches. This kind of heat transfer is also known as Fourier law of heat transfer (see appendix B.3).

The temperature part of the equation (3.1) for the heat flow in each branch is written as

$$\varphi_i(T_{0i}, T_i) = \frac{1}{T_i} - \frac{1}{T_{0i}} \ , \quad i \in \{\mathrm{H}, \mathrm{L}\} \ . \tag{3.29}$$

Then the equation (3.20) for the optimal cost allocation takes the form

$$\frac{\mathrm{d}k_\mathrm{H}/\mathrm{d}c_\mathrm{H}}{\mathrm{d}k_\mathrm{L}/\mathrm{d}c_\mathrm{L}} = \frac{T_\mathrm{L}}{T_\mathrm{H}} \left(\frac{k_\mathrm{H}}{k_\mathrm{L}}\right)^{3/2} \ . \tag{3.30}$$

In order to evaluate this expression the temperature T_H and T_L at the operating point where the power output reaches its maximum need to be determined first. The solution of this problem is known [31], and presented in appendix E.

The optimal temperatures are found in equation (E.10) and are inserted into equation (3.30) to obtain an expression for the optimal cost allocation

$$\frac{\mathrm{d}k_\mathrm{H}/\mathrm{d}c_\mathrm{H}}{\mathrm{d}k_\mathrm{L}/\mathrm{d}c_\mathrm{L}} = \frac{\dfrac{2\sqrt{k_\mathrm{H}} + \sqrt{k_\mathrm{L}}}{T_{0\mathrm{H}}} + \dfrac{\sqrt{k_\mathrm{L}}}{T_{0\mathrm{L}}}}{\dfrac{\sqrt{k_\mathrm{H}} + 2\sqrt{k_\mathrm{L}}}{T_{0\mathrm{L}}} + \dfrac{\sqrt{k_\mathrm{H}}}{T_{0\mathrm{H}}}} \left(\frac{k_\mathrm{H}}{k_\mathrm{L}}\right)^{3/2} \ . \tag{3.31}$$

This nonlinear equation generally has to be solved numerically for a given cost function $k_i(c_i)$ to find the optimal cost ratio $c_\mathrm{H}/c_\mathrm{L}$ versus the ratio $\beta_\mathrm{H}/\beta_\mathrm{L}$.

The cost function (3.22) and their derivatives (3.23) are substituted into equation (3.31). The resulting expression can be written as

$$\frac{T_{0\mathrm{H}}}{T_{0\mathrm{L}}} \left(\sqrt{k_\mathrm{H} k_\mathrm{L}}(a_\mathrm{H} c_\mathrm{L} - a_\mathrm{L} c_\mathrm{H}) + 2 a_\mathrm{H} k_\mathrm{L} c_\mathrm{L}\right) = \sqrt{k_\mathrm{H} k_\mathrm{L}}(a_\mathrm{L} c_\mathrm{H} - a_\mathrm{H} c_\mathrm{L}) + 2 a_\mathrm{L} k_\mathrm{H} c_\mathrm{H} \ . \tag{3.32}$$

Dividing this equation by k_L, c_L and a_L yields, after some more algebraic transformations, an expression which only contains ratios, $T_\mathrm{H}/T_\mathrm{L}$, $k_\mathrm{H}/k_\mathrm{L}$ $c_\mathrm{H}/c_\mathrm{L}$, and $a_\mathrm{H}/a_\mathrm{L}$:

$$\sqrt{\frac{k_\mathrm{H}}{k_\mathrm{L}}} \left(\frac{a_\mathrm{H}}{a_\mathrm{L}} - \frac{c_\mathrm{H}}{c_\mathrm{L}}\right) \left(1 + \frac{T_{0\mathrm{H}}}{T_{0\mathrm{L}}}\right) = 2 \left(\frac{k_\mathrm{H}}{k_\mathrm{L}} \frac{c_\mathrm{H}}{c_\mathrm{L}} - \frac{a_\mathrm{H}}{a_\mathrm{L}} \frac{T_{0\mathrm{H}}}{T_{0\mathrm{L}}}\right) \ . \tag{3.33}$$

Now take a closer look at the case of equal exponents $a = a_\mathrm{H} = a_\mathrm{L}$. With this assumption and the cost relationships (3.22) the above equation (3.33) transforms to

$$\sqrt{\frac{\beta_\mathrm{H}}{\beta_\mathrm{L}} \left(\frac{c_\mathrm{H}}{c_\mathrm{L}}\right)^a} \left(1 - \frac{c_\mathrm{H}}{c_\mathrm{L}}\right) \left(1 + \frac{T_{0\mathrm{H}}}{T_{0\mathrm{L}}}\right) = 2 \left[\frac{\beta_\mathrm{H}}{\beta_\mathrm{L}} \left(\frac{c_\mathrm{H}}{c_\mathrm{L}}\right)^{a+1} - \frac{T_{0\mathrm{H}}}{T_{0\mathrm{L}}}\right] \ . \tag{3.34}$$

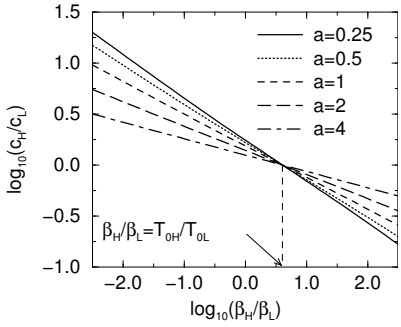

Figure 3.3: The optimal $c_{\mathrm{H}}/c_{\mathrm{L}}$ versus $\beta_{\mathrm{H}}/\beta_{\mathrm{L}}$ relationship is plotted for different exponents a of the cost function (3.22) for the case of heat engine operating at cyclic conditions and an inverse heat transfer law in both branches. Here, the ratio of the source temperature $T_{0\mathrm{H}}/T_{0\mathrm{L}}$ is equal to 4.

This equation is evaluated numerically to calculated the optimal $c_{\mathrm{H}}/c_{\mathrm{L}}$ versus $\beta_{\mathrm{H}}/\beta_{\mathrm{L}}$ relationship as depicted in figure 3.3. Note that the point of an equal cost allocation, where $c_{\mathrm{H}}/c_{\mathrm{L}} = 1$, is independent of the exponent a and always occurs at $\beta_{\mathrm{H}}/\beta_{\mathrm{L}} = T_{0\mathrm{H}}/T_{0\mathrm{L}}$ as can be seen from equation (3.34).

3.4 Summary

This chapter considered the problem of allocating a given amount of investment to the heat exchanger inventory of a generalized thermal system. An open question in this area is whether in this case the often observed even split of the heat exchanger inventory between the hot and the cold side remains the optimal solution. To analyze this question a model is considered which is equally well suited to describe heat engines, refrigerators, and heat pumps. The expressions obtained are valid for stationary as well as cyclic operating conditions. Several examples illustrated how the formulae derived in this paper can be applied to a wide variety of thermodynamic systems.

The new result obtained here is that there exists a significant difference between stationary and cyclic operating systems. It was shown in a general fashion how this difference influences the optimal allocation of the heat exchanger costs. The ramifications of this finding with respect to different heat transfer laws will be subject of further studies.

Chapter 4

Heat engines with several heat reservoirs

Heat engines with several heat sources are common for many real-world applications such as industrial heat-recovery systems and solar energy installations. In such installations several different heat sources are present, which provide heat at different rates, and, even more important, at different temperatures.

In this chapter an endoreversible model is used to investigate these kind of heat engines. The average power output is used as a criterion of thermodynamical perfection. Methods of averaged nonlinear programming [68–70], which are already well established for the optimization of thermal systems with two heat reservoirs [31, 71, 72], are applied to determine the maximum possible average power output and optimal contact functions between the heat reservoirs and a power converting subsystem.

4.1 Model

A model of an endoreversible heat engine with multiple heat reservoirs is depicted in figure 4.1. It consists of a power converting subsystem with a working fluid at one unique temperature $T(t)$ at each moment of time and N sources at constant temperatures T_{0i} where $i \in \{1, N\}$. The heat transfer laws for each source have the form

$$\tilde{q}_i(T_{0i}, T, \theta_i) = \theta_i q_i(T_{0i}, T), \quad i \in \{1, N\} \; . \tag{4.1}$$

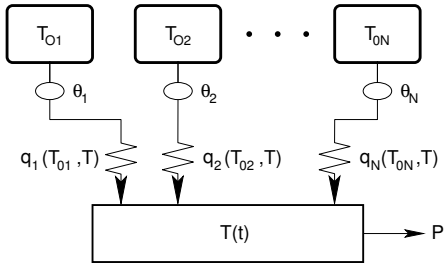

Figure 4.1: Schematics of an endoreversible heat engine with multiple heat reservoirs. The working fluid in the engine subsystem has one temperature $T(t)$ at a time and may contact one or more heat reservoirs, counted by i, at temperatures T_{0i} via the contacts $\theta_i \in [0,1]$ exchanging the heats q_i.

The contact functions θ_i are equal to one if the working fluid is fully connected with the i-th reservoir, and are equal to zero if there is no contact. A further requirement is that the heat transfer laws are well defined according to expression (1.15) in section 1.1.5 and that the working fluid is characterized by one unique value of temperature at each moment of time. The fluid temperature $T(t)$ and the contact functions $\theta_i(T_{0i}, T)$ are taken as the $N+1$ controls of the system. The system is operated at cyclic conditions and in a cycle fashion with a fixed cycle time τ_{tot}.

4.2 Problem formalization

The system is optimized for a maximum average power output $\bar{P}$. This is equivalent to the maximization of the time-averaged sum of the heat flows

$$q_\Sigma(\boldsymbol{T}_0, T, \boldsymbol{\theta}) = \sum_{i=1}^{N} \tilde{q}_i(T_{0i}, T, \theta_i) \ , \tag{4.2}$$

where the vector $\boldsymbol{\theta}$ of the contact functions and the vector $\boldsymbol{T}_0$ of the reservoir temperature are defined as

$$\boldsymbol{\theta} = (\theta_1, \theta_2, \ldots, \theta_N) \quad \text{and} \tag{4.3}$$

$$\boldsymbol{T}_0 = (T_{01}, T_{02}, \ldots, T_{0N}) \ , \ . \tag{4.4}$$

The optimization problem can be formalized as the maximization of the functional

$$I = \bar{P} = \overline{q_\Sigma}\,(\boldsymbol{T}_0, T, \theta) = \frac{1}{\tau_{\mathrm{tot}}} \int_0^{\tau_{\mathrm{tot}}} q_\Sigma(\boldsymbol{T}_0, T, \theta)\,\mathrm{d}t \rightarrow \max_{T, \boldsymbol{\theta}} \tag{4.5}$$

subject to the restriction of balanced entropy

$$\overline{s_\Sigma}\,(\boldsymbol{T}_0, T, \theta) = \frac{1}{\tau_{\rm tot}} \int_0^{\tau_{\rm tot}} \frac{1}{T} q_\Sigma(\boldsymbol{T}_0, T, \theta)\,{\rm d}t = 0\ . \tag{4.6}$$

This restriction is due to the endoreversibility of the system.

The controls of the process are the temperature T of the working fluid and the the elements of the vector $\boldsymbol{\theta} = (\theta_1, \theta_2, \ldots, \theta_N)$ of the contact functions. These elements satisfy the conditions

$$0 \le \theta_i(t) \le 1\ , \quad i \in \{1, N\}\ . \tag{4.7}$$

4.3 Optimal contact functions

Equations (4.5–4.7) define a problem of averaged nonlinear programming. The optimality conditions for such a kind of problem have the form [68–70]

$$\mathcal{L} = \sum_{i=1}^{N} \theta_i q_i(T_{0i}, T)\Big[1 - \frac{\lambda}{T}\Big] \to \max_{T,\boldsymbol{\theta}}\ \min_{\lambda}\ . \tag{4.8}$$

At first consider the variation of $\mathcal{L}$ with respect to each component $\theta_i(T_{0i}, T)$ of the contact vector $\boldsymbol{\theta}$. The Lagrange function $\mathcal{L}$ is linear dependent on each component θ_i, so that the condition of maximum, $(\partial\mathcal{L}/\partial\theta_i)\delta\theta_i \le 0$, is only fulfilled at the boundary of the admissible range of θ_i. The boundary values $\{0{,}1\}$ of θ_i correspond to either positive or negative values of $\delta\theta_i$ and, via $(\partial\mathcal{L}/\partial\theta_i)\delta\theta_i \le 0$, determine a rule for the contact functions:

$$\theta_i(T_{0i}, T) = \begin{cases} 1 & \text{if} \quad \left[1 - \frac{\lambda}{T}\right] q_i(T_{0i}, T) > 0 \\ 0 & \text{if} \quad \left[1 - \frac{\lambda}{T}\right] q_i(T_{0i}, T) < 0 \end{cases} \qquad i \in \{1, N\}\ . \tag{4.9}$$

Take a closer look at this rule. If T is less than λ then $q_i(T_{0i}, T)$ needs to be negative. Then the working fluid is in contact with reservoirs which serve as heat sinks and thus fulfill the condition $T_{0i} < T$. In the contrary case, if T is larger than λ, the heat flow $q_i(T_{0i}, T)$ should be positive. This implies the condition $T_{0i} > T$. The working fluid then connects to reservoirs which act as heat sources. As a consequence the rule (4.9) divides the set of N heat reservoirs into two subsets of *hot* and *cold* reservoirs. Depending on the value of T (greater or less than λ) the working fluid in the power converting subsystem is either connected to reservoirs of the hot or cold set.

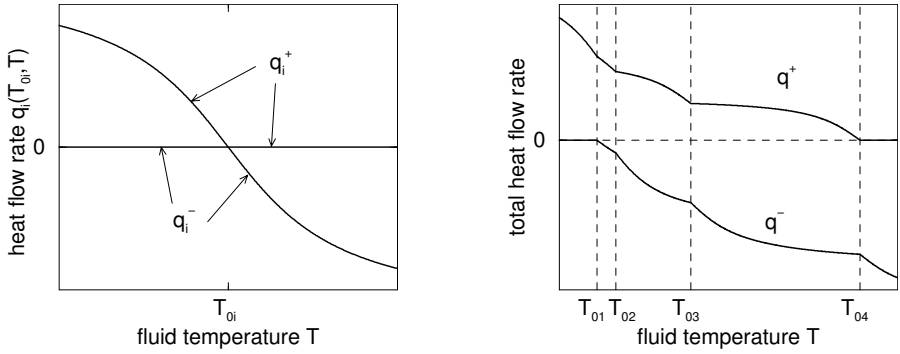

Figure 4.2: Construction of heat transfer functions for an example of four heat reservoirs at different temperatures T_{0i} ($i \in \{1, \ldots, N\}$). The heat flow rates q_i from each of the reservoirs i are splitted into heat input functions $q_i^+(T_{0i}, T)$ and output functions $q_i^-(T_{0i}, T)$ and are respectively summed up to a total heat input function $q^-(\boldsymbol{T}_0, T)$ and a total heat output function $q^+(\boldsymbol{T}_0, T)$.

4.4 Construction of heating and cooling functions

To determine the heat flows resulting from the above rule, the heat transfer function for each reservoir is separated into heat input and output functions

$$q_i^+(T_{0i}, T) = \begin{cases} q_i(T_{0i}, T)\,, & \text{if} \quad T_{0i} \geq T, \\ 0\,, & \text{if} \quad T_{0i} < T, \end{cases} \tag{4.10}$$

$$q_i^-(T_{0i}, T) = \begin{cases} 0\,, & \text{if} \quad T_{0i} > T, \\ q_i(T_{0i}, T)\,, & \text{if} \quad T_{0i} \leq T, \end{cases} \tag{4.11}$$

for each $i \in \{1, N\}$. The total rate of heat input to and from the working fluid are calculated as the sum of all contributions $q_i^+(\boldsymbol{T}_0, T)$ and $q_i^-(\boldsymbol{T}_0, T)$,

$$q^+(\boldsymbol{T}_0, T) = \sum_{i=1}^{N} q_i^+(T_{0i}, T) \tag{4.12}$$

$$q^-(\boldsymbol{T}_0, T) = \sum_{i=1}^{N} q_i^-(T_{0i}, T)\,. \tag{4.13}$$

Figure 4.2 illustrates the construction of heating and cooling functions for an example of four heat reservoirs at different temperatures $T_{01} < T_{02} < T_{03} < T_{04}$ and a non-linear heat transfer law. Definitions (4.10 – 4.13) and rule (4.9) can be used to

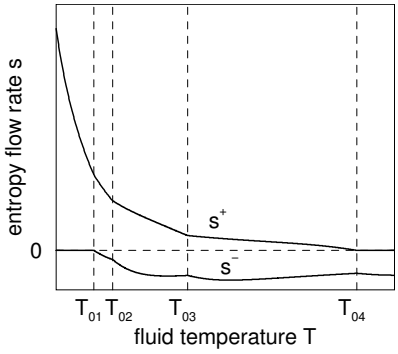

Figure 4.3: The entropy inflow $s^+(\boldsymbol{T}_0, T)$ and outflow $s^-(\boldsymbol{T}_0, T)$ versus the temperature T of the working fluid corresponding to respective total rate of heat input q^+ and output q^- of figure 4.2.

introduce a function of total heat exchange

$$q_\Sigma(\boldsymbol{T}_0, T) = \sum_{i=1}^{N} \theta_i q_i(T_{0i}, T) = \begin{cases} q^+(\boldsymbol{T}_0, T)\,, & \text{if} \quad T > \lambda \\ q^-(\boldsymbol{T}_0, T)\,, & \text{if} \quad T < \lambda \end{cases} \tag{4.14}$$

which shows a discontinuity at $T = \lambda$ where q_Σ jumps from q^- to q^+.

The heat exchange causes an entropy change of the working fluid. The rates of entropy flow to the working fluid are easily obtained by dividing the corresponding heat exchange rate by the current temperature of the working fluid. In particular, the total rate of entropy increase of the working fluid is

$$s_\Sigma(\boldsymbol{T}_0, T) = \frac{q_\Sigma(\boldsymbol{T}_0, T)}{T} = \begin{cases} s^+(\boldsymbol{T}_0, T)\,, & \text{if} \quad T > \lambda \\ s^-(\boldsymbol{T}_0, T)\,, & \text{if} \quad T < \lambda \end{cases}\,, \tag{4.15}$$

where

$$s^+(\boldsymbol{T}_0, T) = \frac{q^+(\boldsymbol{T}_0, T)}{T} \qquad \text{and} \qquad s^-(\boldsymbol{T}_0, T) = \frac{q^-(\boldsymbol{T}_0, T)}{T}\,. \tag{4.16}$$

The graphs of these functions are depicted in figure 4.3.

The functions q^+ and s^+ are independent of the value of λ and are functions of T. Additionally, the heat flow q^+ is a monotonous function of T. It is therefore possible to define a relationship $s^+(q^+)$ by calculating corresponding values of q^+ and s^+ for different values of T. The same can be done for q^- and s^- to construct the relationship $s^-(q^-)$. Both relationships $s^+(q^+)$ and $s^-(q^-)$ cover distinct ranges with exception of the origin as the only common point. Because of this $s^+(q^+)$ and $s^-(q^-)$, can be combined to one relation $s_\Sigma(q_\Sigma)$ as illustrated in figure 4.4.

Note that the objective functional (4.5) of the optimization problem contains $q_\Sigma(\boldsymbol{T}_0, T)$ as integrand and the restriction (4.6) contains $s_\Sigma(\boldsymbol{T}_0, T)$ as integrand.

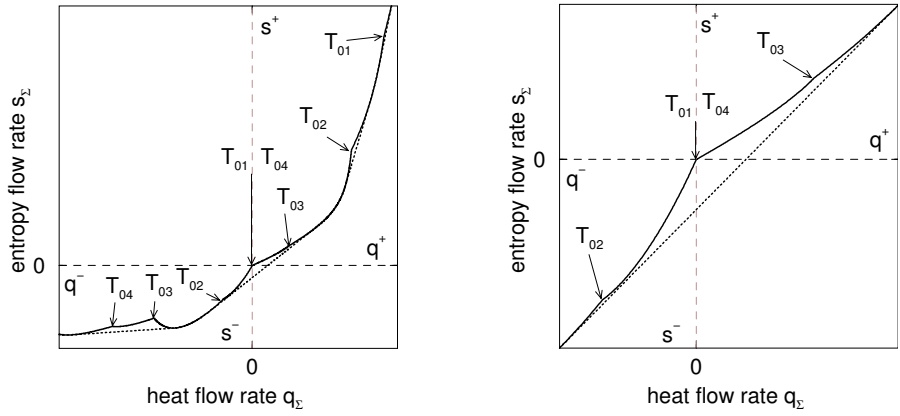

Figure 4.4: Overview (left) and detail (right) of the relation between the rates of heat and entropy flow $s_\Sigma(q_\Sigma)$ which consists of two branches $s^+(q^+)$ and $s^-(q^-)$. The dotted line is the downward convex hull of $s_\Sigma(q_\Sigma)$.

4.5 Base values for the temperatures of the working fluid

The theory of averaged programming [68, 69] states that the solution for the optimal controls are piecewise constant step functions taking values out of a set of no more than $m+1$ *base points* where m is the number of constraints of the problem (see [70], p. 78 ff). There is only one constraint (4.6) here, and consequently there are no more than two base points for the temperature T. These base points are located at points where the function $s_\Sigma(q_\Sigma)$ touches a linear part of its convex hull (see [70], p. 75).

The downward convex hull can be determined numerically by calculating the minimum of all linear interpolations of any two, not necessarily distinct points of a (discretized) function $s_\Sigma(q_\Sigma)$. Figure 4.4 shows the result of such a calculation. It illustrates that points corresponding to a temperature T equal to one of the reservoir temperatures T_{0i} ($i \in \{1, N\}$) are not on the convex hull since contacts functions of the heat reservoirs jump between zero and one at reservoir temperatures. The discontinuities of the contact functions result in an increase of the slope of $s_\Sigma(q_\Sigma)$ and kinks in the curve of $s_\Sigma(q_\Sigma)$.

The two base points of the fluid temperature are referred to as T_1 and T_2 in the following. If the function $s_\Sigma(q_\Sigma)$ is located on its convex hull at $s_\Sigma = 0$, the two base points T_1 and T_2 are identical and there is actually only one base point. Without loss of generality the following proceeds with two (not necessarily distinct) base

points. The Lagrange function (4.8) reaches its maximum at the base points so that the optimality condition $\partial\mathcal{L}/\partial T = 0$, which can be written as

$$\lambda = \frac{\partial q_\Sigma(\boldsymbol{T}_0, T)}{\partial T} T \left(\frac{\partial q_\Sigma(\boldsymbol{T}_0, T)}{\partial T} - \frac{q_\Sigma(\boldsymbol{T}_0, T)}{T} \right)^{-1} , \tag{4.17}$$

is fulfilled at $T = T_1$ and $T = T_2$. The base values are the only values allowed for the the temperature T of the working fluid. The temperature of the working fluid T has to switch between the base value T_1 and T_2 during the cycle of duration τ_{tot}. It attains the base value T_1 during the time $\tau_1 = \gamma_1 \tau_{\mathrm{tot}}$ and it attains the base value T_2 during the time $\tau_2 = \gamma_2 \tau_{\mathrm{tot}}$. This is the behavior of a system operating at cyclic conditions as explained in section 1.3.2.

Thus the distribution of T is know and can be used to evaluate the restriction (4.6) on the averaged rate of entropy change as (see [70], p. 66)

$$\gamma_1 \frac{q_\Sigma(\boldsymbol{T}_0, T_1)}{T_1} + \gamma_2 \frac{q_\Sigma(\boldsymbol{T}_0, T_2)}{T_2} = 0 , \tag{4.18}$$

with

$$\gamma_1 + \gamma_2 = 1,\ \gamma_1 \geq 0,\ \gamma_2 \geq 0 . \tag{4.19}$$

Another relationship is found from the condition that the Lagrangian attains its global maximum at each of its base points (see [70], p. 72). This condition, here written as $\mathcal{L}(\lambda, T_1) = \mathcal{L}(\lambda, T_2)$, yields

$$q_\Sigma(\boldsymbol{T}_0, T_1) \left[1 - \frac{\lambda}{T_1} \right] = q_\Sigma(\boldsymbol{T}_0, T_2) \left[1 - \frac{\lambda}{T_2} \right] . \tag{4.20}$$

Equations (4.17-4.20) are sufficient to determine the values of λ, T_1, T_2, γ_1, and γ_2 for given laws of heat conduction $q_i(T_{0i}, T)$ and reservoir temperatures T_{0i}. These equations are used to analytically or numerically calculate optimal solutions.

4.6 Hot, cold, and unused reservoirs

Equation (4.18) can be used to obtain the ratio of the parts of time

$$\frac{\gamma_2}{\gamma_1} = -\frac{T_2 q_\Sigma(\boldsymbol{T}_0, T_1)}{T_1 q_\Sigma(\boldsymbol{T}_0, T_2)} . \tag{4.21}$$

The ratio $q_\Sigma(\boldsymbol{T}_0, T_1)/q_\Sigma(\boldsymbol{T}_0, T_2)$ in the above equation is eliminated with equation (4.20). The resulting expression is further simplified with condition (4.19) to

$$\lambda = \gamma_1 T_2 + \gamma_2 T_1 . \tag{4.22}$$

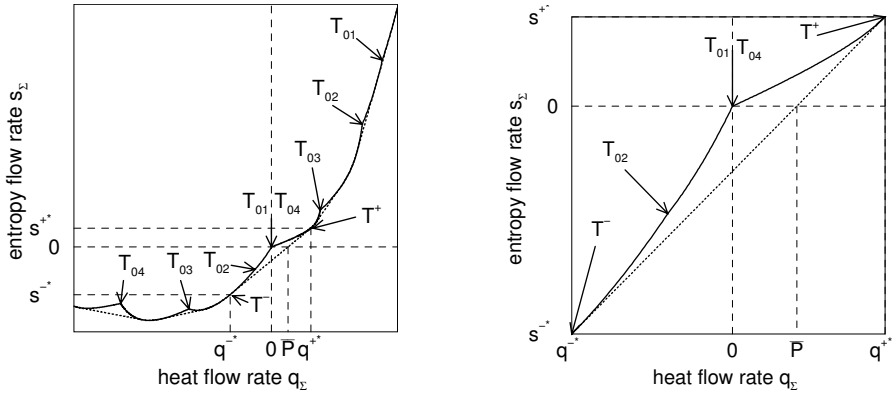

Figure 4.5: The optimal solution for cyclic process is the average of the two base points at $T = T^-$ and $T = T^+$ corresponding to heat and entropy outflow (q^{-*},s^{-*}) and inflow (q^{+*},s^{+*}), respectively. This leads to an average power output $\bar{P}$.

It is immediately clear from condition (4.19) that the value of λ is between the values of the base points T_1 and T_2. The cases where one or two of the base points are equal to λ is of little interest here since this would correspond to zero heat input or output as can be seen from equations (4.17) and (4.20). It therefore can be assumed that one base value, referred to as T^+ here, is larger than λ and the other one, referred to as T^- here, is smaller than λ.

The rule (4.9) for the contact function implies that the base value T^+ is associated with heat input from reservoirs with temperatures larger than T^+ while the value T^- is associated with heat output to reservoirs at temperatures smaller than T^-. All reservoirs with temperatures in the range between T^- and T^+ are therefore never connected during a cycle; these reservoirs are referred to as *unused reservoirs*.

4.6.1 Solution graph

The solutions for the example presented in figure 4.2 to 4.4 demonstrates how used and unused reservoirs can be distinguished from each other and how optimal solutions are obtained. Figure 4.5 again shows the $s_\Sigma(q_\Sigma)$ relation of figure 4.4 but now with the solution drawn into it.

The base points can be determined geometrically. Start at the origin where the restriction $s = 0$ is fulfilled and travel in two contrary direction on the $s_\Sigma(q_\Sigma)$ curve

until the downward convex hull of $s_\Sigma(q_\Sigma)$ is touched. The two points are the base points of the optimization problem and are located at the lower left and upper right corner of the right graph in figure 4.5. The heat flows at the base points are

$$q^{+*} = q^+(\boldsymbol{T}_0, T^+) = q_\Sigma(\boldsymbol{T}_0, T^+) \quad \text{and} \tag{4.23}$$

$$q^{-*} = q^-(\boldsymbol{T}_0, T^-) = q_\Sigma(\boldsymbol{T}_0, T^-)\,, \tag{4.24}$$

and correspond to the two base values T^- and T^+ of the working fluid's temperature T. All points in the negative branch of the graph from the origin to the base point (q^{-*}, s^{-*}) correspond to temperatures lower than T^- and all points in the positive branch of the graph from the origin to the base point (q^{+*}, s^{+*}) correspond to temperatures larger than T^+. This means that reservoirs with temperatures outside the range (q^{-*}, s^{-*}) and (q^{+*}, s^{+*}) are unused reservoirs and are never contacted by the working fluid.

In the present example, the working fluid alternately operates at the temperature T^- where it rejects heat to the two coldest reservoirs (T_{02} and T_{01}) and at the temperature T^+ where it receives heat from the hottest reservoir (T_{04}). The reservoir with the intermediate temperature T_{03} never connects to the working fluid, it is an unused reservoir.

4.6.2 Solution for parts of time

The parts of time γ^+ and γ^- spent at either base points can be determined analytically by substituting λ in equation (4.20) using equation (4.17). By considering the notation for the two base points T^+ and T^- one obtains

$$\left(\frac{T^- q^{+*}}{T^+ q^{-*}}\right)^2 = \frac{(\partial q^+/\partial T)|_{T^+}}{(\partial q^-/\partial T)|_{T^-}}\,. \tag{4.25}$$

Then the left side of the above equation is substituted by equation (4.21) and the square root is taken to obtain an expression for the ratio of the parts

$$\frac{\gamma^-}{\gamma^+} = \sqrt{\frac{-(\partial q^+/\partial T)|_{T^+}}{-(\partial q^-/\partial T)|_{T^-}}}\,. \tag{4.26}$$

The values for each part are readily derived using equation (4.18) to obtain

$$\gamma^+ = \frac{\sqrt{-(\partial q^-/\partial T)|_{T^-}}}{\sqrt{-(\partial q^+/\partial T)|_{T^+}} + \sqrt{-(\partial q^-/\partial T)|_{T^-}}} \tag{4.27}$$

$$\gamma^- = \frac{\sqrt{-(\partial q^+/\partial T)|_{T^+}}}{\sqrt{-(\partial q^+/\partial T)|_{T^+}} + \sqrt{-(\partial q^-/\partial T)|_{T^-}}}\,. \tag{4.28}$$

This result is very useful, since the parts of time γ^- and γ^+ are easily calculated analytically after the base values $T^-$and T^+ are determined.

4.7 Synopsis of algorithm

Altogether the algorithm to calculate the optimal solution corresponding to maximum power output is as follows

- For the entire range of temperatures calculate the sum of all positive heat $q_i^+(T_{0i}, T)$ and entropy flows $s_i^+(T_{0i}, T)$ from all reservoirs and construct the relation $s^+(q^+)$.
- Do the same for all negative heat $q_i^-(T_{0i}, T)$ and entropy flows $q_i^-(T_{0i}, T)$ to obtain $s^-(q^-)$.
- Combine the two relations $s^+(q^+)$ and $s^-(q^-)$ into one relationship $s_\Sigma(q_\Sigma)$.
- Determine the downward convex hull of $s_\Sigma(q_\Sigma)$.
- Determine the base points (q^{+*}, s^{+*}) and (q^{-*}, s^{-*}) as the touching points between the graph $s_\Sigma(q_\Sigma)$ and the downward convex hull.
- Calculate the base values T^+ and T^- for the temperature of the working fluid using expressions (4.23) and (4.24), respectively.
- Assign the heat reservoirs to sets of hot, cold and unused reservoirs: all reservoirs with temperatures larger than T^+ are in the hot set, all reservoirs with temperatures smaller than T^- are in the cold set, and all remaining reservoirs are in the set of unused reservoirs which will be never connected by the working fluid.
- Calculate the parts γ^+ and γ^- of time during which the respective reservoirs of the hot and cold cold set connect to the working fluid by using the expressions (4.27) and (4.28).
- Determine the power output of the optimized system with expression

$$\bar{P} = \gamma^+ q^+(\boldsymbol{T}_0, T^+) + \gamma^- q^-(\boldsymbol{T}_0, T^-) \; . \tag{4.29}$$

4.8 Summary

In this chapter a power-producing thermal systems which exchanges heat with several (two or more) heat reservoirs via irreversible heat transfer processes was considered. One of the interesting questions for such systems is how the different heat reservoirs are used in an optimal fashion. The system was optimized for maximum power output in case of cyclic conditions. The optimal solution provides rules that state which reservoirs need to be contacted for how long, to achieve an maximum of average power output of the system. Most interestingly, it was shown that there are systems where some reservoirs should not be connected at all in order to achieve an optimal performance of the system. These reservoirs were referred to as *unused reservoirs*. An algorithm was presented which allowed to identify unused reservoirs and to calculate optimized contact times between the *used* reservoirs and the power-producing subsystem.

Chapter 5

Path-optimization of a Diesel engine

Improvements in the design of internal combustion engines to increase their efficiency are becoming more and more important for economical and ecological reasons. The following approach explores the general possibility of improving the efficiency of Diesel engines by optimizing the motion of the pistons within the cylinders of these engines. The idea is to abstract Diesel engines enough to make them treatable but at the same time to include all major loss terms and also employ empirical knowledge on the heat transfer. The focus of this chapter is thus not primarily on the technical realization of the engine as such, but on the thermodynamic processes taking place inside of Diesel engines.

In this manner Diesel engines were investigated by K. H. Hoffmann, S. Watowich, R. S. Berry, and P. Blaudeck [74, 75]. All these studies, including the one presented in this chapter and in [76], have in common that they consider engines with a four–stroke cycle of successive intake, compression, power and exhaust stroke, which operate at constant number of revolutions per minute and with a fixed fuel consumption per cycle. The working fluid of the engines can be assumed to consist of an ideal gas [86] which is in internal equilibrium all the time. Engines are therefore modeled in the manner of endoreversible systems. The thermodynamic processes are optimized to yield maximum work per cycle.

The exhaust and intake are of minor importance for the overall performance of Diesel engines since the changes in pressure and temperature are at least one order of magnitude smaller than during the compression and power strokes. The present study

therefore only considers the compression and power stroke of a Diesel engine and optimizes both strokes together.

The aim of this investigation is to improve the modeling of the heat transfer as well as the gas properties. Different from previous studies [73–75] the present analysis does not rely on a simple linear heat transfer law to describe the heat leak through the walls of the cylinder of the engine; it rather employs an empirically verified model for the heat leak. This model is based on a study conducted by Annand [77] and takes a macroscopic view of the heat transfer process. It considers basic gas properties and dimensionless, scalable quantities for the description of the fluid flow patterns inside the cylinder [78–82]. Annand's formulae are in good agreement with a wide range of experimentally measured data. The heat leak should by modeled accurately because it is one of the most important loss terms in internal combustion engines, since the temperature between working fluid and of the cylinder walls become quite large.

5.1 Model

Conventional Diesel engines are designed around one or more cylindric combustion chambers, closed at one end, in which a close-fitting piston slides. The outer side of the piston is attached to a crankshaft by a connecting rod. The crankshaft transforms the reciprocating motion of the piston into a rotary motion. If the combustion chamber is an ideally shaped cylinder with a bore d, where the volume V of the cylinder is related to the distance x between the head of the piston and the top of the cylinder as

$$V = \pi d(d/2 + x) \; . \tag{5.1}$$

If the distance between the crankshaft and the cylinder is large, the motion of the piston during the compression and power stroke is well approximated by a sinusoidal function

$$x(t) = \frac{1}{2}(x_{\mathrm{f}} + x_{\min}) + \frac{1}{2}(x_{\mathrm{f}} - x_{\min}) \cos(2\pi t/t_{\mathrm{tot}}) \; . \tag{5.2}$$

Here, x_{f} and $x_{\min}$ are the respective maximum and minimum positions of the piston and t_{tot} is the total duration of the compression and power stroke together. An engine with sinusoidal piston motion is referred to as a conventional engine in the following.

In contrast to the conventional engine one can consider a mode of operation where the piston path $x(t)$ is taken as a time-parameterized function to optimize the work output of the engine. Note that quite arbitrary piston motions have indeed been realized in practice for example by Kristiansen Cycle Engines Ltd. who used a contoured plate to guide the piston on the desired path (see [83] pp. 45 ff).

Geometry	
bore (inside diameter of cylinder) [m]	$d = 7.98 \times 10^{-2}$
piston position [m]	x
max. piston position (bottom dead center) [m]	$x_{\mathrm{f}} = 8.0 \times 10^{-2}$
min. piston position (top dead center) [m]	$x_{\min} = 0.5 \times 10^{-2}$
volume [m^3]	$V = \pi x d^2/4 =$
stroke volume [m^3]	$V_{\mathrm{stroke}} = 375\,\mathrm{cm}^3$
wall area [m^2]	$A = \pi d(d/2 + x)$
friction coefficient [$\mathrm{N\,s\,m^{-1}}$]	$\alpha = 12.9$
revolutions per minute [$(60\,\mathrm{s})^{-1}$]	≈ 3600
Time for compression and power stroke [s]	$t_{\mathrm{tot}} = 17 \times 10^{-3}$
Temperatures	
temperature [K]	T
initially [K]	$T_0 = 300$
average wall temperature [K]	$T_{\mathrm{w}} = 600$
Combustion	
ignition time [s]	t_{z}
burn time [s]	$t_{\mathrm{b}} = 1.0 \times 10^{-3}$
heat of combustion [$\mathrm{J\,mol^{-1}}$]	$\mathcal{Q}_{\mathrm{c}} = 5.57 \times 10^4$
number of moles [mol]	N
initially [mol]	$N_{\mathrm{i}} = 0.0144$
after total combustion [mol]	$N_{\mathrm{f}} = 0.0157$
heat capacity at constant volume [$\mathrm{J\,K^{-1}mol^{-1}}$]	C
initially (see section 5.1.3)	C_{i}
after total combustion (see section 5.1.3)	C_{f}

Table 5.1: Geometry and temperature properties of a Diesel engine.

5.1.1 Frictional losses

On a well-lubricated sliding surface, the frictional forces are proportional to the piston velocity v [84]. This yields a frictional loss rate of mechanical energy which is proportional to the square of v written as

$$w_{\mathrm{f}} = \alpha v^2 \ . \tag{5.3}$$

Here the frictional loss rate is assumed to have the above simple form with a constant friction coefficient α during the compression and power stroke. The heat produced by friction is assumed to be immediately removed by the engines cooling system and does not heat the working fluid in the combustion chamber.

5.1.2 Combustion

In modern Diesel engines, fuel is injected into the cylinder at the end of the compression stroke and evaporates in the hot compressed air. After a short delay the fuel ignites and starts to burn rapidly causing a sharp rise in temperature and pressure. The remaining fuel relatively slowly burns as it evaporates and diffuses into oxygen-rich regions. In moderately and heavily loaded engines, the combustion process continues well until the end of the power stroke.

The finite combustion rate is one of the main features of a Diesel engine and here is approximated by a time-dependent reaction coordinate

$$\xi(t) = \begin{cases} 0 & \text{for} \quad t < t_{\mathrm{z}} \\ 1 + [(t - t_{\mathrm{z}})/t_{\mathrm{b}} - 1] \exp[(t_{\mathrm{z}} - t)/t_{\mathrm{b}}] & \text{for} \quad t \geq t_{\mathrm{z}} \ , \end{cases} \tag{5.4}$$

with a characteristic combustion time t_{b}. The reaction coordinate $\xi(t)$ describes the extent of the combustion which starts at the ignition time t_{z}. Total combustion is achieved at $t \to \infty$ and results in $\xi = 1$. This simple model was found by Kleinschmidt [85] as an approximation of the heat production curves of real Diesel engines. The working fluid is treated as an ideal gas with time dependent

$$\text{mole number} \qquad N(t) \ = N_{\mathrm{i}} + (N_{\mathrm{f}} - N_{\mathrm{i}})\xi(t) \tag{5.5}$$

$$\text{heat capacity} \qquad C(t,T) \ = C_{\mathrm{i}}(T) + (C_{\mathrm{f}}(T) - C_{\mathrm{i}}(T))\xi(t) \ . \tag{5.6}$$

The heat capacity C is at constant volume. The variations of N and C also change the internal energy NCT of the working fluid and therefore need to be considered in the energy balance.

Gas properties	
gas constant [$\mathrm{J\,K^{-1}mol^{-1}}$]	$R = 8.314$
thermal conductivity [$\mathrm{J/K^{-1}m^{-1}s^{-1}}$]	κ
of air	$\kappa_\mathrm{a} = 3.17 \times 10^{-4} T^{0.772}$
of combustion products	$\kappa_\mathrm{c} = 2.02 \times 10^{-4} T^{0.837}$
viscosity [$\mathrm{kg\,m^{-1}s^{-1}}$]	ν
of air	$\nu_\mathrm{a} = 0.612 \times 10^{-6} T^{0.604}$
of combustion products	$\nu_\mathrm{c} = 0.355 \times 10^{-6} T^{0.679}$
heat capacity at constant pressure [$\mathrm{J\,K^{-1}mol^{-1}}$]	C_p
of air (300K$< T <$ 700K)	$C_\mathrm{p,a} = 0.573 T^{0.097}$
of air (700K$\leq T <$ 2200K)	$C_\mathrm{p,a} = 0.392 T^{0.155}$
of combustion products (700K$\leq T <$ 2200K)	$C_\mathrm{p,c} = 0.267 T^{0.226}$
fuel–air equivalence ratio [1]	$\Lambda = 1.2$
Heat leak	
Reynolds number [1]	$\mathcal{R} = \rho \bar{v} d / \nu$
density [$\mathrm{kg/m^3}$]	$\rho = 29 \times 10^{-3} N/V$
average piston speed [m/s]	$\bar{v} = 2(x_\mathrm{f} - x_\mathrm{min})/t_\mathrm{tot}$
Stefan-Boltzmann constant [$\mathrm{Wm^{-2}K^{-4}}$]	$\sigma = 5.67 \times 10^{-8}$
convective constant [1]	$a = 0.540$
exponent of the Reynolds number [1]	$b = 0.7$
radiative constant during power stroke [1]	$c = 0.1$

Table 5.2: Gas and heat leak properties of a Diesel engine.

The rate of heat produced during the combustion is described by the heating function

$$q_\mathrm{comb}(t) = \mathcal{Q}_\mathrm{c} N_\mathrm{i} \dot{\xi}(t) \,, \tag{5.7}$$

where $\mathcal{Q}_\mathrm{c}$ is the heat per mole of the air-fuel mixture.

These formulae are a continuous approximation for the combustion process in real engines [85].

5.1.3 Empiric gas properties

The thermal conductivity κ, the viscosity ν, and the heat capacity at constant pressure C_p of the working fluid shows a considerable dependence on the temperature T. These dependencies are well approximated by power functions [86] and are listed in table 5.2. In this table the subscript ‘a’ refers to the case of dry air, the subscript ‘c’

refers to the case of fully combusted gases for a stoichiometric mixture of air and fuel where the fuel has a hydrogen to carbon ratio of 85/15. Commonly Diesel engines operate with an excess of air and therefore use a non-stoichiometric mixture of air and fuel. The degree of 'non-stoichiometry' is expressed by the *fuel-air equivalence ratio* Λ, which is defined as the actual air–fuel ratio divided by the stoichiometric air–fuel ration. The value of Λ typically ranges from 1.2 to 2.0 where $\Lambda = 1.2$ is found in fully loaded, $\Lambda = 1.5$ in three-quarter loaded and $\Lambda = 2.0$ in half loaded Diesel engines. Here $\Lambda = 1.2$ is used.

The values of thermal conductivity κ, the viscosity ν and the heat capacity at constant pressure C_p of the working fluid after total combustion are obtained by linear interpolation as

$$X_{\mathrm{f}} = \frac{(\Lambda - 1)X_{\mathrm{a}} + X_{\mathrm{c}}}{\Lambda} \,, \tag{5.8}$$

where X is a placeholder for κ, ν and C_p. Before the combustion has started the initial value of a property X is $X_{\mathrm{i}} = X_{\mathrm{a}}$. Note the heat capacities at constant volume are calculated from there counterparts at constant pressure by subtracting the gas constant R

$$C_{\mathrm{i}}(T) = C_{\mathrm{p,a}} - R \tag{5.9}$$

$$C_{\mathrm{f}}(T) = \frac{(\Lambda - 1)C_{\mathrm{p,a}} + C_{\mathrm{p,c}}(T)}{\Lambda} - R \,. \tag{5.10}$$

During the combustion the value of a property X depends on the reaction coordinate $\xi(t)$, as defined by equation (5.4), so that the value X generally is given by

$$X(t, T) = X_{\mathrm{i}}(T) + [X_{\mathrm{i}}(T) - X_{\mathrm{f}}(t)]\, \xi(t). \tag{5.11}$$

If the temperature and time dependence of the gas properties is considered the working fluid may still be treated as an ideal, semi-perfect gas.

5.1.4 Heat leak

In combustion engines thermal energy flows to the cylinder's walls by heat conduction and convection of the working fluid. During the combustion of the working fluid, the luminous flame is causing an additional contribution to the heat leak by radiating energy towards the cooler cylinder walls. In effect, thermal energy leaves the cylinder and is further conducted through the cylinder wall to the cooling system of the engine. Consequently the heat transfer rate is subject to quite large variations during the cycle and depends on various properties of the working fluid as well as on flow patterns inside the cylinder.

Contribution of convection and conduction

The convective and conductive part of the heat leak is described by a formula found by Annand [77]. The rate of heat loss is proportional to both, the exposed internal surface area of the piston cylinder

$$A = \pi d(d/2 + x) \tag{5.12}$$

and the difference between fluid temperature T and surface temperature T_{w}, and is written as

$$q_{\mathrm{c}} = A k_{\mathrm{a}}(T, x)\,[T - T_{\mathrm{w}}]\ . \tag{5.13}$$

The non-constant heat transfer coefficient

$$k_{\mathrm{a}}(T, x, t) = a\frac{\kappa(T)}{d}\mathcal{R}^{b}(T, x) \tag{5.14}$$

is a function of the thermal conductivity $\kappa(T)$ and the Reynolds number $\mathcal{R}(T, x, t)$ and depends on the fluid temperature T, the position x of the piston and the time, since the gas properties are variables of time during the combustion. The formula also contains the inside diameter d of the cylinder and the constants a and b as fixed, design-dependent parameters. The value of the convective constant a is typically in the range between 0.35 and 0.8 and depends on the conditions of convection in the cylinder. Low values of a correspond to 'quiet' combustion and high values of a were measured for combustion chambers which are specially optimized for fast combustion. Basically, the thermal conductivity κ incorporates the temperature dependence of the heat conduction into the modeling while the Reynolds number $\mathcal{R}$ introduces the influence of flow patterns on the convective part of the heat transfer. A summary of the empirical values of these properties is shown in table 5.2.

Contribution of radiation

If the combustion process has not started, the air-fuel mixture is quasi transparent for heat radiation and the heat leak out of the cylinder is, for all practical purposes, entirely conductive and convective.

During the power stroke, when the mixture burns, solid incandescent carbon particles appear as intermediate combustion products and radiate heat towards the cooler cylinder wall. The carbon particles are in strong convective contact with their environment and thus are often assumed to have the same temperatures as the working fluid. Since the carbon content in Diesel fuels is high, the predominant sources of radiative energy are the carbon particles. Chemical luminescence, which corresponds to a much higher effective temperature, is relatively weaker and can be ignored. Even

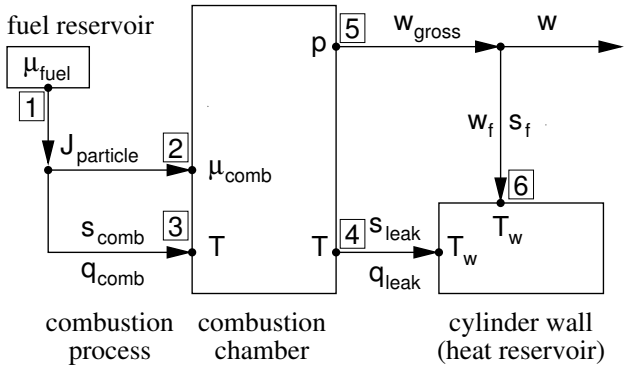

Figure 5.1: Endoreversible model of a Diesel engine

if only the radiation from the carbon particles at gas temperature is considered, exact calculations of the radiative heat transfer are very difficult. Such calculations involve the computation of integrals with respect to cylinder volume, surface area, and wavelength and requiring detailed data about the temperatures, concentration and geometry of the carbon particles as well as their spectral absorptivity during the combustion process.

Again Annand has provided a formula [77], based on the well known expression for blackbody radiation, to estimate the radiative heat transfer

$$q_{\mathrm{r}} = Ac\sigma(T^4 - T_{\mathrm{w}}^4) \; . \tag{5.15}$$

Here, a so-called radiative constant c incorporates all the unknown factors into a single number. During the compression stroke, where the radiative heat transfer is negligible, c is set to zero. The value for c during the power stroke has been obtained from experimental data and typically is in the range between 0.04 to 0.32 for Diesel engines [77]. In the following $c = 0.1$ is assumed.

Altogether the total rate of heat loss q_{leak} through the cylinder walls consist of a contribution q_{c} which is caused by conduction and convection and a contribution q_{r} which is caused by radiation:

$$q_{\mathrm{leak}} = q_{\mathrm{c}} + q_{\mathrm{r}} \; . \tag{5.16}$$

5.1.5 Endoreversible model

Figure 5.1 shows an endoreversible representation of the Diesel engine modeled in this chapter. The combustion process is formally described as a particle flux from a 'fuel reservoir' to the combustion chamber. The particle flux J_{particle} of 'fuel particles' emerges from contact 1 at high chemical potential μ_{fuel} and enters the combustion chamber at contact 2 at low chemical potential μ_{comb}. According to section 1.1.1 the particle flux is associated with an outflux of energy $\mu_{\mathrm{fuel}} J_{\mathrm{particle}}$ at contact 1 and an influx of energy $\mu_{\mathrm{comb}} J_{\mathrm{particle}}$ at contact 2. Since combustion is an irreversible interaction entropy is produced. The corresponding flux s_{comb} of entropy carries the energy flux q_{comb} to contact 3 of the combustion chamber. The heat q_{comb} is the difference of the energy fluxes carried by the particle flux J_{particle} and can be identified as the heat produced by combustion of fuel. The properties of the empirical heating function (5.7) are identified with the properties of the endoreversible model as

$$q_{\mathrm{comb}} = \underbrace{(\mu_{\mathrm{fuel}} - \mu_{\mathrm{comb}})}_{\mathcal{Q}_{\mathrm{c}}} \underbrace{J_{\mathrm{particle}}}_{N_{\mathrm{i}}\dot{\xi}(t)} \ . \tag{5.17}$$

The heat leak is modeled using contact point 4 where an entropy flow $s_{\mathrm{leak}} = q_{\mathrm{leak}}/T$ leaves the combustion chamber to the cylinder wall. The cylinder wall serves as a heat reservoir at constant temperature T_{w}. A flux of work w_{gross} leaves the combustion chamber at contact 5 which is assigned the pressure p of the working fluid as intensity. The pressure p can be expressed as

$$p = \frac{NRT}{V} \tag{5.18}$$

because the working fluid is an ideal gas. The flux of work w_{gross} is carried by the flux $\dot{V}$, which is the derivative of the volume V of the combustion chamber with respect to time t. The flux of work can be written as

$$w_{\mathrm{gross}} = p\dot{V} = \frac{NRT}{x} v \tag{5.19}$$

with the velocity $v = \dot{x}$ of the piston.

A part of the work flux w_{gross} is irreversibly transformed to heat w_{f} by friction and carried to the cylinder walls by the entropy flux s_{f}. The utilizable work flux w is then given by

$$w = w_{\mathrm{gross}} - w_{\mathrm{f}} \ . \tag{5.20}$$

5.1.6 Internal energy and equations of state

The temporal change of internal energy is the sum of work and heat fluxes out and into the combustion chamber

$$\frac{\mathrm{d}}{\mathrm{d}t}U = q_{\mathrm{comb}} - q_{\mathrm{leak}} - w \ . \tag{5.21}$$

The total derivative of the internal energy U with respect to time can be evaluated as

$$\frac{\mathrm{d}}{\mathrm{d}t}U = \frac{\mathrm{d}}{\mathrm{d}t}(NCT) = \frac{\partial N}{\partial t}CT + N\frac{\partial C}{\partial t}T + N\left(\frac{\partial C}{\partial T}T + C\right)\frac{\mathrm{d}T}{\mathrm{d}t} \ . \tag{5.22}$$

Both, the mole number $N = N(t)$ and the heat capacity $C = C(t, T)$ of the working fluid are functions of time and change their values during the combustion process according to equation (5.5) and (5.6), respectively. Inserting the respective expressions (5.5) and (5.6) for $N(t)$ and $C(t, T)$ into equation (5.22) yields

$$\frac{\mathrm{d}}{\mathrm{d}t}U = NC\frac{\mathrm{d}T}{\mathrm{d}t} + \dot{\xi}[C(N_{\mathrm{f}} - N_{\mathrm{i}}) + N(C_{\mathrm{f}} - C_{\mathrm{i}})]T + TN\frac{\partial C}{\partial T}\frac{\mathrm{d}T}{\mathrm{d}t} \ . \tag{5.23}$$

This equation and equation (5.21) are combined to calculate the derivative $\dot{T} = \mathrm{d}T/\mathrm{d}t$ of the temperature with respect to time as

$$\dot{T} = \frac{q_{\mathrm{comb}} - q_{\mathrm{leak}} - w - \dot{\xi}T[C(N_{\mathrm{f}} - N_{\mathrm{i}}) + N(C_{\mathrm{f}} - C_{\mathrm{i}})]}{NC + NT(\partial C/\partial T)} \ . \tag{5.24}$$

5.2 Optimization

The goal of the optimization in question is to find a path $x(t)$ of the piston which maximizes the total net output of mechanical work W during the compression and power stroke. The work output W is expressed by the integral of equation (5.20) as

$$W = \int_0^{t_{\mathrm{tot}}} \left(\frac{NRT}{x}v - \alpha v^2\right) \mathrm{d}t \ . \tag{5.25}$$

The optimization is subject to boundary conditions and constraints:

- The total duration t_{tot} of the compression and power stroke is fixed.
- The start and end position of the piston are equal and fixed, $x(0) = x(t_{\mathrm{tot}}) = x_{\mathrm{f}}$, and the piston is not allowed to go beyond this maximum value.

- The lowest accessible position $x_{\min}$ of the piston leads to a compression ratio of 1:16 for the engine.

- The wall temperature of the cylinder T_{w}, as well as the initial temperature of the working fluid T_0, is given while the end temperature of the fluid is allowed to vary freely.

The values of these and further parameters are found in table 5.1.

Since the amount of fuel and the cycle time are fixed, the path which yields maximum work also maximizes the average power output and the thermodynamic efficiency of the engine.

The temperature and piston position are state variables and subject to the equations of state

$$\dot{T} = \frac{q_{\mathrm{comb}} - NRTv/x - q_{\mathrm{leak}} - \dot{\xi}[C(N_{\mathrm{f}} - N_{\mathrm{i}}) + N(C_{\mathrm{f}} - C_{\mathrm{i}})]T}{NC + NT(\partial C/\partial T)} \tag{5.26}$$

$$\dot{x} = v\,. \tag{5.27}$$

The optimization problem is solved with control theory (see [25–27], for example). The Hamiltonian of the optimization problem is

$$H = \frac{NRT}{x}v - \alpha v^2 + \lambda_1 \dot{T} + \lambda_2 v + \mathcal{P}(x) \tag{5.28}$$

with the adjoint variables λ_1 and λ_2. An appropriate penalty function

$$\mathcal{P}(x) = -\alpha v^2 \left(\frac{x'_{\min}}{x}\right)^{n_x} \tag{5.29}$$

ensures that the constraints on the piston position x is kept. The exponent n_x typically is in the range of 10 to 70 and specifies the 'smoothness' of the constraint. Large values of n_x correspond to a 'sharp' constraint. The parameter $x'_{\min}$ is found by a fitting procedure such that the actual boundary value $x_{\min}$ is met (if possible) but never violated.

Control theory provides differential equations for adjoint variables as

$$\begin{aligned}\dot{\lambda}_1 &= -\frac{\partial H}{\partial T} = -\frac{NRv}{x} \\ &\quad + \frac{\lambda_1}{NC + NT(\partial C/\partial T)} \Bigg\{ NRv/x + \frac{\partial q_{\mathrm{leak}}}{\partial T} \\ &\quad + \dot{\xi} \Bigg[\left(C + T\frac{\partial C}{\partial T} \right) (N_{\mathrm{f}} - N_{\mathrm{i}}) + N(C_{\mathrm{f}} - C_{\mathrm{i}}) \\ &\quad + TN \left(\frac{\partial C_{\mathrm{f}}}{\partial T} - \frac{\partial C_{\mathrm{i}}}{\partial T} \right) \Bigg] + N \left[2\frac{\partial C}{\partial T} + \frac{\partial^2 C}{\partial^2 T} T \right] \dot{T} \Bigg\} \qquad (5.30) \\ \dot{\lambda}_2 &= -\frac{\partial H}{\partial x} = \frac{NRT}{x^2} v + \frac{\lambda_1}{NC + NT(\partial C/\partial T)} \left(-\frac{NRT}{x^2} v + \frac{\partial q_{\mathrm{leak}}}{\partial x} \right) \\ &\quad - \frac{\alpha v^2}{x} n_x \left(\frac{x'_{\min}}{x} \right)^{n_x} . \qquad (5.31)\end{aligned}$$

The Pontryagin maximum principle [25] requires that H is maximized with respect to v. Solving $\partial H/\partial v = 0$ with respect to the piston velocity v yields

$$v = \frac{\lambda_2 - NRT/x\{\lambda_1/[NC + NT(\partial C/\partial T)] - 1\}}{2\alpha[1 + (x'_{\min}/x)^{n_x}]} . \qquad (5.32)$$

By inserting the expression (5.32) for v into the equations of the adjoint variables, (5.30) and (5.31) and considering the equations of state (5.26) and (5.27) a closed system of four nonlinear differential equations is obtained. This set of differential equations is solved numerically using an adaptive step-size controlled scheme ([56] pp. 714 ff).

The boundary conditions of the set of differential equations are the initial and final position of the piston ($x(t_{\mathrm{tot}}) = x_{\mathrm{f}}$) and the initial value of the fluid temperature $T(0) = T_0$. The final temperature $T(t_{\mathrm{tot}})$ is allowed to freely vary, which is equivalent to $\lambda_1(t_{\mathrm{tot}}) = 0$. In order to meet the two boundary conditions at $t = t_{\mathrm{tot}}$ the initial values of the adjoint variables λ_1 and λ_2 have to be adjusted to the correct values. These values are found using a shooting method ([56] pp. 757 ff) which systematically solves the set of ordinary differential equations for different initial values of λ_1 and λ_2 until the boundary conditions are fulfilled within a reasonable accuracy.

Another parameter whose optimal value should be determined is the optimal ignition time $t_{\mathrm{z}}^{\mathrm{opt}}$. This value is found by systematically calculating the optimal path and corresponding work output for various ignition times t_{z}. The ignition time which gives the largest work output is $t_{\mathrm{z}}^{\mathrm{opt}}$.

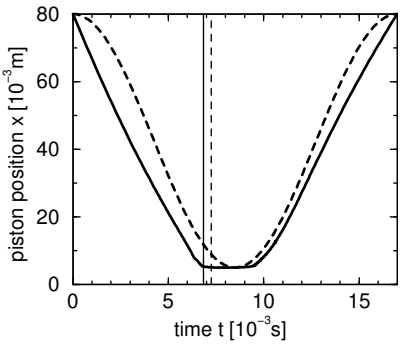

Figure 5.2: Piston path of conventional Diesel engine (dashed line) compared to a path-optimized Diesel engine (solid line). The thin, vertical lines mark the ignition times.

5.3 Results

Piston paths for the simultaneously optimized compression and power stroke are calculated for engines with path optimized and conventional sinusoidal piston motion.

5.3.1 Optimal path

The piston motion of the path-optimized Diesel engine shows significant differences to the sinusoidal piston motion of a conventional engine, as can be seen from figure 5.2. The sinusoidal piston motion starts at the bottom dead center with slope zero corresponding to a zero velocity, accelerates and then reaches its maximum speed in the middle of the compression stroke. At the end of the compression stroke, near the top dead center, the velocity decreases to zero again. The optimal ignition time for the conventional engine was determined as $t_z^{\mathrm{opt}} = 7.25\,\mathrm{ms}$.

The trajectory of the path optimized engine starts with a finite velocity and proceeds on a straight line of constant velocity. This behavior minimizes the losses due to friction since the frictional loss rate is proportional to the square of the velocity.

However, because of the heat leak and the volume work of the piston, the optimal path slightly deviates from a straight line. Initially, the walls of the cylinder are hotter than the working fluid and the cold gas receives heat from the walls until the temperature of the working fluid becomes higher than the temperature of wall and the direction of the heat flow switches. Both, the heat losses and compression work are minimized simultaneously if the minimum piston position is reached just before the ignition of the fuel.

The path-optimized engine completes its compression stroke at the optimized ignition

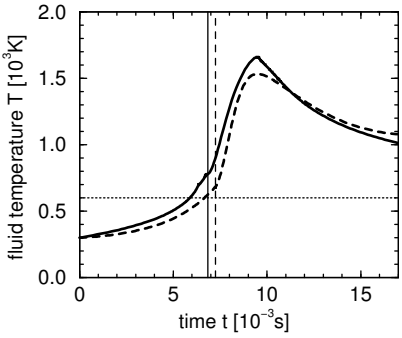

Figure 5.3: Temperature of the working fluid for conventional Diesel engine (dashed line) compared to the path-optimized Diesel engine (solid line). The thin, vertical lines mark the times of ignition; the thin dotted line marks the temperature of the cylinder wall

time $t_z^* = 6.84\,\mathrm{ms}$ where the piston is decelerating to standstill at the highest possible rate. Subsequently, a zero-velocity phase is entered where the piston remains at its minimum position. The zero-velocity phase is a consequence of the existence of a minimal piston position $x_{\min}$. Without this constraint the optimized system would move the piston to positions x smaller than $x_{\min}$ which would result in an extreme rise of temperature and pressure. The zero-velocity phase is followed by an acceleration phase where the volume increases again. As a consequence of this expansion the rise of the temperature is limited even though the combustion within the cylinder continues.

5.3.2 Fluid temperature

Compared to the sinusoidal piston motion, the path optimization of the piston motion increases the peak temperatures and decreases the exhaust temperatures as can be seen from figure 5.3. The lower exhaust temperatures of the optimized engine are a consequence of both, increased heat losses due to higher temperatures during the peak of combustion and a faster power stroke.

5.3.3 Heat loss

The heat loss rate q_{leak}, which is depicted in figure 5.4 is indeed very sensitive to the temperature T of the fluid. It is negative at the begin of the compression stroke, where the cylinder wall is hotter than the working fluid, becomes positive shortly before the ignition of the fuel and peaks during the burning of the fuel.

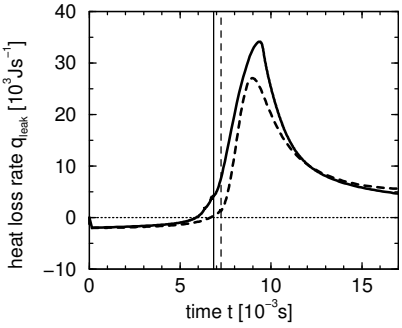

Figure 5.4: Heat loss for conventional Diesel engine (dashed line) compared to the path-optimized Diesel engine (solid line). The thin, vertical lines mark the times of ignition.

	conventional	optimized	difference
ignition time t_z^{opt}	7.25 ms	6.84 ms	
work output W	282.17 J	295.75 J	4.8 %
friction loss W_{fric}	21.06 J	20.70 J	-1.7 %
total heat loss Q_{leak}	103.92 J	129.17 J	24.3 %
heat loss Q_{c}	101.43 J	126.68 J	24.9 %
heat loss Q_{r}	2.49 J	2.49 J	0.0 %
efficiency $\eta = W/Q_{\mathrm{comb}}$	35.2%	36.9%	4.8 %
maximum pressure p_{max}	6.97 MPa	7.94 MPa	13.9 %
maximum temperature T_{max}	1532 K	1659 K	8.3 %
final temperature $T(t_{\mathrm{tot}})$	1079 K	1012 K	-6.6 %

Table 5.3: Results for the conventional and path-optimized Diesel engine

5.4 Summary

Table 5.3 compares the net work output W, several loss terms, the efficiency η, and some important temperatures of the path-optimized engine versus the conventional engine. The work output and total heat losses have been calculated by integrating the respective rates. The by far dominating loss term is due to the heat leak through the cylinder of the engine. The path optimization even increases the heat losses; this is mainly caused by the higher temperatures during the power stroke. A large proportion of the total heat $Q_{\mathrm{comb}} = 801.5\,\mathrm{J}$ produced by combustion is lost through the heat leak; the percentage increases from 13 percent in case of conventional engine to 16 percent in case of a path-optimized engine. Friction dissipates only about 7 percent of the available volume work of the working fluid.

Relative to the conventional sinusoidal case, the work output and efficiency of the

engine were improved through path optimization by 4.8 percent. This improvement was bought by higher peak temperatures and peak pressure and lower exhaust temperatures of the path-optimized engine compared to the conventional engine. A low exhaust temperature might not be always desirable, if for example the residual energy of the exhaust gases are utilized by a turbocharger.

Compared to previous studies where the path-optimization yielded an improvement in work output of up to 20 % the present study predictions an improvement of about 5 %. This is due to the improved modeling of the heat transfer and of the gas properties. This improved accuracy is necessary since the heat leak is one of the most important loss mechanism of the Diesel engine. Thus this refined engine model leads to a much more realistic estimation of the possible improvements of Diesel engines.

Chapter 6

Summary

Endoreversible thermodynamics views a thermodynamic system as a network of internally reversible subsystems which exchange energy in an irreversible fashion. Thus it becomes possible to include irreversibilities into the description of thermodynamic processes, and also to account for non-equilibrium between subsystems while preserving many advantages of classical reversible thermodynamics at the same time. This thesis provides a framework for the endoreversible description and evaluation of thermodynamic systems. It especially considers the finite time character of processes and distinguishes between three kinds of operating conditions:

- *stationary conditions* where all fluxes and intensities of a system are constant in time.
- *cyclic conditions* where a system is allowed to switch between different branches of constant intensities.
- *dynamic conditions* where the system is allowed to evolve along a quite arbitrary path rather than sticking to rigid branches. The temporal behavior of such a system is not strictly predetermined but for example indirectly influenced by controls, initial and final conditions.

The theoretical framework has been applied to the analysis of a number of open problems in the field of endoreversible thermodynamics. This lead to new and sometimes surprising results:

Endoreversible engine cycles with two adiabatic and two generalized heat transfer branches operating at cyclic conditions were optimized for maximum work output.

The heat transfer branches were described as general polytropic processes which include common standard branches, like isotherms, isobars and isochors, as special cases. The finite heat capacity of the working fluid and the finite-time character of the heat transfer processes was considered. The optimization yielded analytic expressions for the maximized work output, the corresponding optimal values for the temperatures of the working fluid as well as the optimal allocation of the heat conductances and the durations of the heat transfer processes. The efficiency at maximum work was found to coincide with the Curzon-Ahlborn efficiency for endoreversible Carnot engines, if the degrees of the two polytropic heat transfer branches are equal.

For an unequal degree of the two polytropic heat transfer branches the study yields the new result that the efficiency of the optimized engine generally deviates from the Curzon-Ahlborn efficiency.

This and several other new results were obtained by a numerically solution of the optimization problem. The analysis demonstrated for the first time how the work output of this engine can be improved by allocating the conductances and times of the heat transfer processes in an optimal way. Since the setup of the model is very general, the results are applicable to a broader class of heat engines than considered up to now in the literature.

Another interesting result was obtained regarding the optimal allocation for the heat exchanger inventory. Thus the optimal allocation of a given amount of capital to the heat exchanger inventory of a generalized thermal system was considered. This economic problem was set up for the case where the dependence between the cost of the heat exchanger equipment and the corresponding heat transfer coefficient is a nonlinear function, a case not treated thoroughly before.

The considered model is equally well suited to describe the operation of heat engines, refrigerators and heat pumps. All instances of the model were operation-optimized for the minimization of entropy production. The expressions obtained for the optimal cost allocation are suited for arbitrary laws of heat transfer, arbitrary cost functions and stationary as well as cyclic operating conditions. The results show a very distinct difference between cyclic and stationary operations independent of the heat transfer laws used. The generality of the result is a surprising but convenient feature.

A further study considered a power-producing thermal system which exchanges heat with several (two or more) heat reservoirs via irreversible heat transfer processes. Heat engines with several heat reservoirs are common for many real-world applications such as industrial heat-recovery systems and solar energy installations. The system was optimized for maximum power output in case of cyclic conditions. The optimal solution provided rules that state which reservoirs need to be contacted for how long, to achieve a maximum of average power output of the system.

Most interestingly it was shown that there are systems where some reservoirs should not be connected at all in order to achieve an optimal performance of the system. These reservoirs were referred to as *unused reservoirs*. An algorithm was presented which allowed to identify unused reservoirs and to calculate optimized contact times between the *used* reservoirs and the power-producing subsystem.

Finally the thesis addressed the problem of optimizing the piston motion of a Diesel engine to achieve a maximum of work output for a given fuel input. Improvements of the efficiency of internal combustion engines like the Diesel engine are very important for economical and ecological reasons. Thus all options of improvement should be investigated. Here an endoreversible model of the Diesel engine was set up which considered the full dynamics of the system and accounted for the temporal variations of the heat produced by the combustion process, the basic flow pattern within the engine's cylinder, the temperature dependence of the viscosity, thermal conductivity, and heat capacity of the working fluid and losses due to friction and heat leak through the cylinder walls.

The piston trajectory for both, the compression and power stroke of the models were simultaneously optimized using a control theory method and a variety of numerical algorithms. The optimization procedure was systematically repeated to find the optimum ignition time for both, the conventionally and the path optimized engine, separately. Compared to the conventional Diesel engine with sinusoidal piston motion the work output and efficiency of the path optimized engine improved by about 5 percent. The path optimization caused increased heat losses; yet it also improved the utilization of the composition heat so that the overall work output was improved. Even though the mean feature of the results remain unchanged, the actual numbers obtained here give a much more realistic picture of the potential of process optimization in the Diesel engine.

Appendix A

The Curzon–Ahlborn heat engine

The *Curzon–Ahlborn heat engine* as introduced by Curzon and Ahlborn [11], probably is the best known endoreversible system. It is depicted in figure A.2 and consists of three reversible subsystems and two irreversible interactions. Two of the subsystems are heat reservoirs and serve as heat sources and heat sinks at constant temperatures $T_{0\mathrm{H}}$ and $T_{0\mathrm{L}}$, respectively. The third subsystem is a reversible Carnot engine which produces the work W during one cycle by alternately absorbing the heat Q_{H} from the hot reservoir during the time τ_{H} and rejecting the heat Q_{L} to the low temperature reservoir during the time τ_{L}.

A.1 Work characteristic

The entropy-temperature diagram of the reversible engine is a Carnot cycle made up of two isothermal heat transfer branches and two adiabatic branches. The time τ_{tot} needed to complete one cycle and the total time τ_{a} spent in the adiabatic branches ($1 \rightarrow 2$ and $3 \rightarrow 4$) are taken as fixed values while the times spent in the isothermal branches ($2 \rightarrow 3$ and $4 \rightarrow 1$) are allowed to vary within the restriction that all branch times should sum up to the total cycle time

$$\tau_{\mathrm{tot}} = \tau_{\mathrm{H}} + \tau_{\mathrm{L}} + \tau_{\mathrm{a}} \; . \tag{A.1}$$

The reversible engine subsystem operates between the temperatures T_{H} and T_{L} and is coupled to the heat reservoirs via irreversible heat conduction described by linear

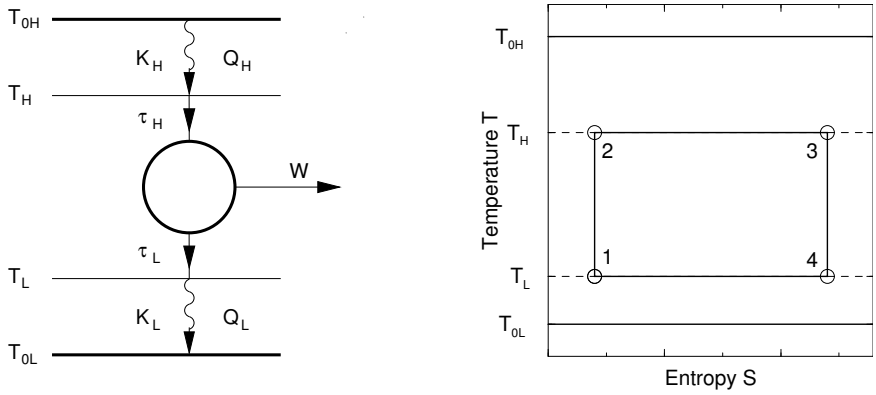

Figure A.1: Curzon–Ahlborn model of an endoreversible heat engine with reversible Carnot heat engine connected to a cold and hot heat reservoir via finite-rate heat transfer. The corresponding TS-diagram is shown at the right.

heat transfer laws

$$Q_{\mathrm{H}} = K_{\mathrm{H}}\tau_{\mathrm{H}}(T_{0\mathrm{H}} - T_{\mathrm{H}}) \tag{A.2}$$

$$Q_{\mathrm{L}} = K_{\mathrm{L}}\tau_{\mathrm{L}}(T_{\mathrm{L}} - T_{0\mathrm{L}})\ . \tag{A.3}$$

The exchanged heats Q_{H} and Q_{L} are proportional to temperature differences and the respective thermal conductances K_{H} and K_{L} are finite.

The reversible engine subsystem dissipates or looses no energy during a cycle so that the exchanged energies obey the balance equation (1.16), here written as

$$0 = Q_{\mathrm{H}} - Q_{\mathrm{L}} - W\ . \tag{A.4}$$

Entropy is created and carried away during the heat transfer process but no entropy is produced inside the reversible engine subsystem so that the balance equation (1.17) is applied to obtain

$$0 = \Delta S_{\mathrm{H}} - \Delta S_{\mathrm{L}} = \frac{Q_{\mathrm{H}}}{T_{\mathrm{H}}} - \frac{Q_{\mathrm{L}}}{T_{\mathrm{L}}}\ . \tag{A.5}$$

This model certainly is very simple, if one thinks about real heat engines, yet it incorporates some essential features common to most heat engines: finite, irreversible heat transfer and finite time operation.

At first, two important properties of the engine are introduced: The Carnot efficiency

$$\eta_{\mathrm{C}} = 1 - T_{0\mathrm{L}}/T_{0\mathrm{H}} \tag{A.6}$$

as the upper bound for any engine operating between the two reservoirs at temperatures $T_{0\mathrm{L}}$ and $T_{0\mathrm{H}}$ and the efficiency of the engine subsystem,

$$\eta = 1 - T_{\mathrm{L}}/T_{\mathrm{H}} \;=\; W/Q_{\mathrm{H}} \;, \tag{A.7}$$

which in fact is the efficiency of the entire endoreversible system and is equal to the fraction of heat Q_{H} actually converted into work W.

Using the definion of efficiency and equation (A.2) the work output of the system is expressed as

$$W = Q_{\mathrm{H}}\eta = K_{\mathrm{H}} t_{0\mathrm{H}} (T_{0\mathrm{H}} - T_{\mathrm{H}})\eta \,. \tag{A.8}$$

From equation (A.5) follows

$$T_{\mathrm{L}}/T_{\mathrm{H}} = Q_{\mathrm{L}}/Q_{\mathrm{H}} \;, \tag{A.9}$$

which, by applying equations (A.2), (A.3), (A.6) and (A.7) is transformed to

$$(1-\eta) = \frac{K_{\mathrm{L}}\tau_{\mathrm{L}}[T_{\mathrm{H}}(1-\eta) - T_{0\mathrm{H}}(1-\eta_{\mathrm{C}})]}{K_{\mathrm{H}}\tau_{\mathrm{H}}(T_{0\mathrm{H}} - T_{\mathrm{H}})} \tag{A.10}$$

and subsequently solved for the unknown temperature T_{H}:

$$T_{\mathrm{H}} = T_{0\mathrm{H}} \frac{K_{\mathrm{H}}\tau_{\mathrm{H}}(1-\eta) + K_{\mathrm{L}}\tau_{\mathrm{L}}(1-\eta_{\mathrm{C}})}{(K_{\mathrm{H}}\tau_{\mathrm{H}} + K_{\mathrm{L}}\tau_{\mathrm{L}})(1-\eta)} \;. \tag{A.11}$$

After inserting this result into equation (A.8) and substituting τ_{L} with equation (A.1) an expression for the work output is obtained:

$$W(\tau_{\mathrm{H}}, \eta, K_{\mathrm{H}}, K_{\mathrm{L}}) = T_{0\mathrm{H}} \frac{K_{\mathrm{H}}\tau_{\mathrm{H}} K_{\mathrm{L}}(\tau - \tau_{\mathrm{H}} - \tau_{\mathrm{a}})}{K_{\mathrm{H}}\tau_{\mathrm{H}} + K_{\mathrm{L}}(\tau - \tau_{\mathrm{H}} - \tau_{\mathrm{a}})} \eta \frac{\eta_{\mathrm{C}} - \eta}{1-\eta} \;. \tag{A.12}$$

This work characteristics describes all possible modes of operations of the Curzon–Ahlborn engine with respect to four independent parameters: the duration τ_{H} of the upper heat transfer branch, the efficiency η and the heat transfer coefficients K_{H} and K_{L}. Here, the reservoir temperatures $T_{0\mathrm{H}}$ and $T_{0\mathrm{L}}$, the cycle time τ_{tot} and the duration τ_{a} of the adiabatic branches are given constants.

A.2 Maximization of work output

The problem of finding the maximum possible work output W with respect to the four independent parameters can be treated as a problem of unconstrained optimization. Note that instead of introducing physical constraints like positiveness of temperatures

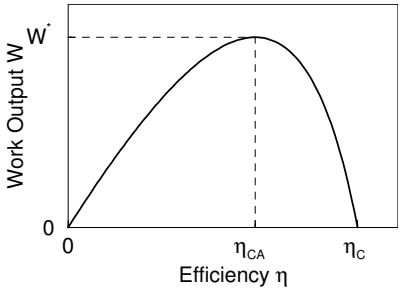

Figure A.2: The work output W of the Curzon–Ahlborn engine reaches its maximum W^* at the Curzon–Ahlborn efficiency η_{CA} and vanishes at the Carnot efficiency η_{C}.

and times into the optimization problem one can solve a simplified optimization problem first and then check if and which of the mathematical solutions are compatible with reality.

A qualitative plot of the work output W versus the efficiency η within a sensible range for the efficiency η between zero and the Carnot efficiency η_{C} and positive τ_{tot}, τ_{H}, τ_{a}, K_{H}, K_{L}, $T_{0\mathrm{H}}$, and $T_{0\mathrm{H}}$ reveals a convex function with one maximum, W^*, as depicted in figure A.2. Note that the shape of this function is independent of the values of the parameters of the system.

One necessary condition for an extremum, $\partial W/\partial\eta = 0$, solved for η, yields the famous *Curzon–Ahlborn efficiency*

$$\eta_{\mathrm{CA}} = 1 - \sqrt{T_{\mathrm{L}}/T_{\mathrm{H}}}\,. \tag{A.13}$$

This result is quite remarkable because η_{CA} does not depend on the size of the conductances or the branch times. One should however notice that the Curzon–Ahlborn efficiency η_{CA} is a bound for only a special class of heat engines operating at maximum power in contrast to the Carnot efficiency η_{C}, which is the ultimate limit for any heat engine.

The work output W of the Curzon–Ahlborn engine can further be optimized with respect to the branch time τ_{H}. The necessary optimality condition, $\partial W/\partial\tau_{\mathrm{H}} = 0$, provides a relation between the optimal branch times τ_{L}^* and τ_{H} and the conductances,

$$\tau_{\mathrm{H}}^*/\tau_{\mathrm{L}}^* = \sqrt{K_{\mathrm{L}}/K_{\mathrm{H}}}\,, \tag{A.14}$$

where $\tau_{\mathrm{L}}^* = \tau_{\mathrm{tot}} - \tau_{\mathrm{a}} - \tau_{\mathrm{H}}^*$.

The work output, maximized with respect to the first two degrees of freedom, is then written as

$$W(\tau_{\mathrm{H}}^*, \eta^*, K_{\mathrm{H}}, K_{\mathrm{L}}) = \frac{(\tau - \tau_{\mathrm{a}})K_{\mathrm{H}}K_{\mathrm{L}}}{\left(\sqrt{K_{\mathrm{H}}} + \sqrt{K_{\mathrm{L}}}\right)^2}\left(\sqrt{T_{0\mathrm{H}}} - \sqrt{T_{0\mathrm{L}}}\right)^2. \tag{A.15}$$

This optimized work output $W_{\max}$ is still a function of the conductances K_{H} and K_{L}.

A.3 Optimal allocation of conductances, conductivities and areas

With no limits on the conductances K_{H} and K_{L} the work output W can take any desired value. Therefore at least one more independent constraint is needed to obtain a non-trivial optimization problem.

A typical question extensively considered in the literature [37, 50–52] concerns the optimal allocation of the conductances K_{H} and K_{L} for given total heat conductance

$$K = K_{\mathrm{H}} + K_{\mathrm{L}} \; . \tag{A.16}$$

This constraint is easily introduced into the already partially optimized work characteristics (A.15) since it does neither depend on η nor on τ_{H}. By substituting K_{L} in equation (A.15) using equation (A.16) and applying the optimality condition $\partial W_{\max}/\partial K_{\mathrm{L}} = 0$ the optimal allocation of the conductances is found as

$$K_{\mathrm{H}}^{*} = K_{\mathrm{L}}^{*} = K/2 \; . \tag{A.17}$$

The fully optimized work output of the Curzon-Ahlborn engine is finally obtained as

$$W(\tau_{\mathrm{H}}^{*}, \eta^{*}, K_{\mathrm{H}}^{*}) = \frac{(\tau - \tau_a)K}{8} \left(\sqrt{T_{0\mathrm{H}}} - \sqrt{T_{0\mathrm{L}}} \right)^2 \; . \tag{A.18}$$

The optimization of the Curzon–Ahlborn engine can be refined even further into the realm of optimal design. Each of the conductances can be splitted into a product of respective surface areas A_{H}, A_{L} and conductivities κ_{H}, κ_{L}:

$$K_{\mathrm{H}} = \kappa_{\mathrm{H}} A_{\mathrm{H}} \quad \text{and} \quad K_{\mathrm{L}} = \kappa_{\mathrm{L}} A_{\mathrm{L}} \; . \tag{A.19}$$

In case of given conductivities κ_{H}, κ_{L} and constrained total area

$$A_{\mathrm{tot}} = A_{\mathrm{H}} + A_{\mathrm{H}} \tag{A.20}$$

of the heat exchangers one can ask for a power-optimal allocation of the areas A_{H} and A_{L}. The required calculation are straight forward and presented elsewhere [53]. The resulting optimality condition for the areas are

$$\frac{A_{\mathrm{L}}^{*}}{A_{\mathrm{H}}^{*}} = \sqrt{\frac{\kappa_{\mathrm{H}}}{\kappa_{\mathrm{L}}}} \; . \tag{A.21}$$

Note that the above results have been obtained for a reciprocating engine where both the contact times and conductances are optimized independently. There exist alternative ways to evaluate the Curzon-Ahlborn models, namely for systems operating at stationary conditions, which yield different results (see [87, 88] for example).

Appendix B

Heat transfer laws

The form of the heat transfer law significantly influences the results obtained in the modeling of thermodynamic systems. This appendix gives brief overview of commonly used heat transfer laws and also discusses the physical relevance and meaning of these laws. Further details on practical aspects of heat transfer are found in textbooks [89–92].

B.1 Linear law

The most commonly applied expression for the heat transport is a linear one

$$q = A\alpha\Delta T \,, \tag{B.1}$$

where A is a characteristic area and α is known as the heat transfer coefficient. Note that many textbooks, especially in engineering, use the letter h for the heat transfer coefficient. This linear expression is motivated from the observation that a heat flow is driven by a characteristic temperature difference ΔT and (in some cases) is proportional to this temperature difference. The expression (B.1) is commonly known as *Newton's law of cooling*.

Originally *Newton's law of cooling* states that the rate of heat loss per unit area from a body is directly proportional to the temperature difference between the body and the surrounding fluid medium in contact with the body. This concept appeared in a paper read by Newton at the Royal Society on 28 May 1701 and was published anonymously [93]. There are, however strong reasons to believe that the idea of a

heat transfer law of this kind have been formulated earlier by Fourier [94]. In order to not enter a discussion on the history of science here, the above expression is referred to as *linear heat transfer law* within this thesis.

It is an important question for the modeling of thermodynamic processes if and under what circumstances a constant heat transfer coefficient can be regarded as realistic and can be justified by physical models.

For some cases of forced laminar and turbulent convection, a linear law is in good agreement with reality [95,96]. As an explanation for the linear dependence consider the solid body to be surrounded by a boundary layer of resting fluid through which the heat energy has to be conducted before being carried away by the flowing fluid outside this layer. For uniform layers the heat transfer coefficient α can be understood as the ratio between the thermal conductivity of the fluid and the mean thickness of the boundary layer. This intuitive picture is confirmed by detailed models for heat transport from a wall of uniform temperature to a fluid moved by a forced, laminar flow [95,96].

The heat transport in solids usually is dominated by conduction. Then the local density of heat flow

$$j_{\mathrm{q}} = -\lambda \nabla T \tag{B.2}$$

is proportional to the temperature gradient. The proportional factor is the thermal conductivity λ. If λ does not show a strong dependence on the temperature and the conditions are quasistatic, the locally linear heat transfer relation (B.2) may also lead to a globally linear relationship between a heat flow q and a characteristic temperature difference. The linear law (B.1) is indeed often applied to describe the heat transfer in bulk materials.

The linear dependence between heat flow and temperature difference frequently occurs as the first term of the Taylor expansion of a more general, non–linear heat transfer law. This means that for small temperature differences it may be possible to approximate the heat transport by equation (B.1).

One should, however, keep in mind that a linear heat transport law is not universal although it is simple and has been in common use for a long time. Deviations from the linear law already have been known in the 18th century shortly after Newton's time (see [97], page 238). Often a linear law can only serve as a crude approximation. Real heat transport processes can show a complicated dependence on state variables, geometry, flow patterns, material constants and boundary condition. There exists a number of simple and realistic examples for systems where the concept of a linear heat transfer law is misleading, fails completely or even is incorrect as an approximation [96].

However, if one does not know the details of a heat transfer process or wants to be

as general as possible, at least for small ΔT, the simple linear heat transfer law often is the best choice of all alternatives. This is one of the reasons why in the theoretical analysis of thermodynamic systems the linear heat transfer law is widely used and particularly has been applied to study endoreversible models of engines, coolers and heaters [11, 13, 15–17, 28, 30, 55, 98–105].

B.2 Dulong–Petit law

A more appropriate yet still global description of the heat transfer is provided by the so–called Dulong–Petit law

$$q/A = K(\Delta T)^n \ . \tag{B.3}$$

The origin of this expression dates back to 1818 when Dulong and Petit had conducted a number of experiments that arrived at a series of laws which related different cases of heat transfer to different values of n [106].

Recent theoretical studies have also found laws of the Dulong–Petit type for certain situation of heat transfer. Theoretical studies of a vertical plate at constant temperature in contact with a naturally convecting fluid yielded a value of $n = 5/4$ for laminar and a value of $n = 4/3$ for turbulent convection [96, 107]. The nonlinearity of the heat transfer in case of natural convection is not surprising since the fluid motion itself is caused by a temperature dependence of the fluid's density.

Another example for situation where the Dulong–Petit law applies well is the heat transfer during the film condensation of a resting vapor at a vertical wall. If the vapor is not overheated, the theory (see [108]) gives

$$q/A \propto \Delta T^{3/4} \ , \tag{B.4}$$

where ΔT is the difference between the boiling temperature of the fluid and the temperature of the wall.

The Dulong–Petit law may also be useful to phenomenological describe a situation where the heat transfer between two subsystems has conductive as well as radiative components. Typical value of the exponent n are in the range between 1.1 and 1.6 depending on the portion of the radiative heat transfer compared to the total heat transfer [55, 64, 95].

The Dulong–Petit law has been applied to describe the heat transfer of endoreversible models of heat engines and refrigerators [64, 109–111].

B.3 Inverse law

The heat conduction in metals at very low temperatures usually shows a proportionality to the difference of inverse temperatures

$$q = K(1/T_2 - 1/T_1) \; . \tag{B.5}$$

This relation is often found in conjunction with linear irreversible thermodynamics, where the difference of the inverse temperatures is the force corresponding to the heat flux and K is an Onsager coefficient.

Although the above expression (B.5) is known as *Fourier heat transfer law* it is referred to as *inverse heat transfer law* within this thesis. This is done to avoid confusion since some textbooks use the term *Fourier heat transfer law* to designate a linear law of heat transfer as described by equation (B.1).

The inverse heat transfer law it has been used within a number of studies on endoreversible systems [32, 112–114].

B.4 Generalized and exotic heat transfer laws

A generalized, nonlinear heat transfer law of the form

$$q = K(T_1^n - T_2^n) \tag{B.6}$$

includes the linear ($n = 1$), inverse ($n = -1$), and radiative ($n = 4$) heat transfer laws as special cases. There are several studies in the literature where an expression of the above kind has been used to describe the heat transfer between subsystems [19, 49, 65, 67, 87, 112, 115, 116]. Most of these studies are not so much concerned about real physical situations where such laws may occur but instead focus on the analytical treatment of theoretical models.

An example for a quite extraordinary heat transfer laws is provided by Orlov [32] who investigated the maximum efficiency and the respective optimal cycle of an endoreversible engine where the heat transfer was governed by the expression

$$q = K_1 \left(\frac{1}{T_1} - \frac{1}{T_2} \right) + K_2 \left(\frac{1}{T_1} - \frac{1}{T_2} \right)^9 \; . \tag{B.7}$$

B.5 Stefan–Boltzmann law

Electromagnetic radiation from a hot body like the sun or sooth particles can serve as a source of heat. For some systems, in particular those operating at high temperatures, radiation is the major transfer mechanism for heat. Radiative heat transfer is typically described by the Stefan-Boltzmann law of black-body radiation where the heat flux between two radiating bodies at temperature T_1 and T_2 is given by

$$q = K\sigma(T_1^4 - T_2^4) \; . \tag{B.8}$$

Here, $\sigma = 5.67 \times 10^{-8}\,\mathrm{Wm^{-2}K^{-4}}$ is defined as the Stefan-Boltzmann constant. The constant K incorporates the emittance of the two radiating bodies and geometry factors.

The linear approximation of equation (B.8),

$$q = 4K\sigma T_1^3(T_1 - T_2) \; , \tag{B.9}$$

is valid for small temperature differences where $(T_1 - T_2) \to 0$, and defines a case where the heat transfer can be described by a linear law if T_1 is constant.

Typical applications, where radiative heat transfer is involved are solar collectors and solar-thermal heat engines [117]. In particular, endoreversible solar thermal models have been discussed in the literature [2,19,53,102,118–129]. Other examples include internal combustion engines where hot sooth particles radiate heat towards the cooler cylinder wall.

Appendix C

Optimized polytropic engine: numerical results

The following parameters and performance measures are calculated for the fully optimized polytropic heat engine of section 2.4.2 in chapter 2. The calculations are performed for an engine operating at temperatures $T_{0\mathrm{H}} = 1200$ and $T_{0\mathrm{L}} = 300$ of the upper and lower reservoir, respectively. This corresponds to a Curzon–Ahlborn efficiency of $\eta_{\mathrm{CA}} = 0.5$. Results are computed for 81 different combinations of the polytropic heat capacities $\widehat{C}_{\mathrm{H}}$ and $\widehat{C}_{\mathrm{L}}$ over the range of 0.01 to 100 using an accuracy of $\varepsilon = 10^{-9}$ and 32 bit arithmetic.

Tables C.1, C.2, and C.3. show that for equal polytropic heat capacities $\widehat{C}_{\mathrm{H}}$ and $\widehat{C}_{\mathrm{L}}$ the efficiency η^* of the optimized engine is identical to the Curzon–Ahlborn efficiency η_{CA}. For the case of unequal $\widehat{C}_{\mathrm{H}}$ and $\widehat{C}_{\mathrm{L}}$ the efficiency varies between 0.462 and 0.535. The maximum possible work output of $\widehat{W}^* = 37.5$ is obtained for large values of $\widehat{C}_{\mathrm{H}}$ and $\widehat{C}_{\mathrm{L}}$, where the start and end temperatures of both, the upper heat transfer branch ($T_{1\mathrm{H}}$ and $T_{2\mathrm{H}}$) and the lower heat transfer branch ($T_{1\mathrm{L}}$ and $T_{2\mathrm{L}}$) are almost identical and the heat transfer processes are therefore very close to isotherms. The values of the optimal, scaled branch times $\widehat{\tau}^*_{\mathrm{H}}$ and the optimal, scaled heat conductances $\widehat{K}^*_{\mathrm{H}}$ were found to be identical within the available numerical accuracy. This is understandable since the optimization problem is symmetric with respect to $\widehat{\tau}^*_{\mathrm{H}}$ and $\widehat{K}^*_{\mathrm{H}}$.

$\widehat{C}_{\mathrm{H}}$	$\widehat{C}_{\mathrm{L}}$	$\widehat{K}^*_{\mathrm{H}}, \widehat{\tau}^*_{\mathrm{H}}$	$T^*_{1\mathrm{L}}$	$T^*_{2\mathrm{L}}$	$T^*_{1\mathrm{H}}$	$T^*_{2\mathrm{H}}$	$\widehat{W}^*$	η^*
100	100.00	0.500000	450.2	449.8	899.6	900.4	37.500	0.50000
100	30.00	0.500000	450.6	449.4	899.6	900.4	37.500	0.50000
100	10.00	0.500004	451.9	448.1	899.6	900.4	37.499	0.50000
100	3.00	0.500043	456.3	443.8	899.7	900.5	37.493	0.49998
100	1.00	0.500384	469.6	432.1	900.5	901.3	37.435	0.49986
100	0.30	0.504131	520.6	397.2	909.1	909.9	36.801	0.49847
100	0.10	0.529445	679.6	341.5	963.1	963.8	32.496	0.49007
100	0.03	0.622592	988.9	306.0	1099.9	1100.3	18.229	0.47083
100	0.01	0.733435	1140.1	300.7	1170.9	1171.1	7.213	0.46217
30	100.00	0.500000	450.2	449.8	898.7	901.2	37.500	0.50000
30	30.00	0.500000	450.6	449.4	898.8	901.3	37.500	0.50000
30	10.00	0.500003	451.9	448.1	898.8	901.3	37.499	0.50000
30	3.00	0.500042	456.3	443.8	898.8	901.3	37.493	0.49998
30	1.00	0.500384	469.6	432.1	899.6	902.1	37.435	0.49986
30	0.30	0.504131	520.6	397.2	908.3	910.7	36.801	0.49847
30	0.10	0.529444	679.6	341.5	962.3	964.6	32.496	0.49007
30	0.03	0.622591	988.9	306.0	1099.5	1100.8	18.229	0.47084
30	0.01	0.733435	1140.1	300.7	1170.7	1171.3	7.213	0.46217
10	100.00	0.50000	450.2	449.8	896.2	903.7	37.499	0.50000
10	30.00	0.50000	450.6	449.4	896.2	903.7	37.499	0.50000
10	10.00	0.50000	451.9	448.1	896.3	903.8	37.498	0.50000
10	3.00	0.50004	456.3	443.8	896.3	903.8	37.492	0.49999
10	1.00	0.50038	469.6	432.1	897.1	904.6	37.434	0.49986
10	0.30	0.50413	520.6	397.2	905.8	913.2	36.800	0.49848
10	0.10	0.52944	679.6	341.5	960.1	966.8	32.495	0.49007
10	0.03	0.62259	988.8	306.0	1098.2	1102.0	18.228	0.47084
10	0.01	0.73343	1140.0	300.7	1170.2	1171.8	7.213	0.46217

Table C.1: Parameters for optimized polytropic engines for different values of the scaled polytropic heat capacities $\widehat{C}_{\mathrm{H}}$ and $\widehat{C}_{\mathrm{L}}$.

$\widehat{C}_{\mathrm{H}}$	$\widehat{C}_{\mathrm{L}}$	$\widehat{K}^*_{\mathrm{H}}, \widehat{\tau}^*_{\mathrm{H}}$	$T^*_{1\mathrm{L}}$	$T^*_{2\mathrm{L}}$	$T^*_{1\mathrm{H}}$	$T^*_{2\mathrm{H}}$	$\widehat{W}^*$	η^*
3.00	100.00	0.49996	450.1	449.7	887.4	912.4	37.486	0.50002
3.00	30.00	0.49996	450.5	449.3	887.4	912.4	37.486	0.50002
3.00	10.00	0.49996	451.8	448.0	887.4	912.4	37.485	0.50002
3.00	3.00	0.50000	456.2	443.8	887.5	912.5	37.478	0.50000
3.00	1.00	0.50034	469.5	432.0	888.3	913.3	37.421	0.49987
3.00	0.30	0.50409	520.5	397.1	897.1	921.7	36.787	0.49849
3.00	0.10	0.52940	679.4	341.4	952.3	974.4	32.484	0.49009
3.00	0.03	0.62254	988.6	306.0	1093.5	1106.5	18.224	0.47085
3.00	0.01	0.73339	1139.9	300.7	1168.3	1173.5	7.212	0.46217
1.00	100.00	0.49962	449.4	449.0	861.8	936.5	37.371	0.50014
1.00	30.00	0.49962	449.8	448.5	861.8	936.5	37.370	0.50014
1.00	10.00	0.50038	451.0	447.3	861.8	936.5	37.370	0.50014
1.00	3.00	0.49966	455.5	443.0	861.9	936.6	37.363	0.50013
1.00	1.00	0.50000	468.7	431.3	862.7	937.3	37.306	0.50000
1.00	0.30	0.50375	519.5	396.6	871.8	945.4	36.675	0.49862
1.00	0.10	0.52905	678.0	341.1	929.4	995.4	32.390	0.49022
1.00	0.03	0.62216	986.8	305.9	1079.7	1118.3	18.185	0.47095
1.00	0.01	0.73299	1138.7	300.7	1162.5	1178.1	7.203	0.46223
0.30	100.00	0.49587	441.5	441.1	770.7	1010.8	36.135	0.50153
0.03	30.00	0.37747	330.4	330.0	365.7	1192.8	13.100	0.52797
0.30	10.00	0.49588	443.1	439.5	770.7	1010.9	36.134	0.50153
0.30	3.00	0.49591	447.4	435.4	770.8	1010.9	36.128	0.50151
0.30	1.00	0.49626	460.1	424.2	771.7	1011.5	36.073	0.50139
0.30	0.30	0.50000	509.1	390.9	781.8	1018.2	35.471	0.50000
0.30	0.10	0.52526	662.6	338.1	846.2	1058.9	31.379	0.49158
0.30	0.03	0.61799	967.5	305.2	1025.8	1151.2	17.768	0.47209
0.30	0.01	0.27121	1126.3	300.5	1138.2	1189.5	7.116	0.46288

Table C.2: Parameters for optimized polytropic engines for different values of the scaled polytropic heat capacities $\widehat{C}_{\mathrm{H}}$ and $\widehat{C}_{\mathrm{L}}$.

$\widehat{C}_{\mathrm{H}}$	$\widehat{C}_{\mathrm{L}}$	$\widehat{K}^*_{\mathrm{H}}, \widehat{\tau}^*_{\mathrm{H}}$	$T^*_{1\mathrm{L}}$	$T^*_{2\mathrm{L}}$	$T^*_{1\mathrm{H}}$	$T^*_{2\mathrm{H}}$	$\widehat{W}^*$	η^*
0.10	100.00	0.47061	399.3	399.0	563.6	1130.5	28.908	0.50995
0.10	30.00	0.47061	399.6	398.7	563.6	1130.5	28.908	0.50995
0.10	10.00	0.47062	400.5	397.7	563.7	1130.5	28.908	0.51000
0.10	3.00	0.47066	403.8	394.6	563.8	1130.6	28.903	0.50993
0.10	1.00	0.47100	413.7	385.9	564.7	1130.9	28.863	0.50981
0.10	0.30	0.47478	452.4	360.7	575.4	1134.4	28.424	0.50843
0.10	0.10	0.50000	577.2	322.8	645.5	1154.5	25.449	0.50000
0.10	0.03	0.59144	857.1	302.1	870.4	1190.0	15.316	0.47916
0.10	0.01	0.70330	1056.0	300.1	1057.3	1199.0	6.615	0.46672
0.03	100.00	0.37747	330.3	330.2	365.7	1192.8	13.101	0.52798
0.03	30.00	0.37747	330.4	330.0	365.7	1192.8	13.100	0.52797
0.03	10.00	0.37748	330.8	329.6	365.7	1192.8	13.100	0.52797
0.03	3.00	0.37752	332.2	328.3	365.8	1192.8	13.099	0.52796
0.03	1.00	0.37790	336.5	324.8	366.4	1192.9	13.087	0.52786
0.03	0.30	0.38206	353.9	315.1	373.7	1193.6	12.958	0.52677
0.03	0.10	0.40857	415.2	303.5	421.1	1197.0	12.107	0.52008
0.03	0.03	0.50000	599.9	300.1	600.1	1199.9	8.996	0.50000
0.03	0.01	0.61858	848.5	300.0	848.5	1200.0	5.059	0.47978
0.01	100.00	0.26657	307.6	307.6	315.7	1199.3	4.730	0.53528
0.01	30.00	0.26657	307.7	307.6	315.7	1199.3	4.730	0.53528
0.01	10.00	0.26658	307.8	307.4	315.7	1199.3	4.730	0.53528
0.01	3.00	0.26662	308.3	307.0	315.7	1199.3	4.730	0.53527
0.01	1.00	0.26701	309.9	305.8	316.0	1199.3	4.727	0.53522
0.01	0.03	0.38142	424.3	300.0	424.3	1200.0	4.029	0.51943
0.01	0.30	0.27122	316.5	302.8	319.6	1199.4	4.704	0.53463
0.01	0.10	0.29670	340.6	300.3	340.9	1199.9	4.563	0.53122
0.01	0.01	0.50000	600.0	300.0	600.0	1200.0	3.000	0.50000

Table C.3: Parameters for optimized polytropic engines for different values of the scaled polytropic heat capacities $\widehat{C}_{\mathrm{H}}$ and $\widehat{C}_{\mathrm{L}}$.

Appendix D

Equivalence of performance measures

The following proof has been adapted from a work of Rozonoer and Tsirlin [31] to the problem and notation presented in chapter 3 of this thesis.

For a system as depicted in figure 3.1 it is shown that under the constraint of a given average power $\overline{P}$ the minimization of the entropy production is equivalent to the maximization of the efficiency or the coefficients of performance.

The total entropy ΔS produced during the cycle time τ_{tot} is the sum of the entropy increment of the two heat reservoirs since the net contribution of the reversible operating compartment is zero during one cycle. This is written as

$$\Delta S = -\left[\frac{Q_{\mathrm{H}}}{T_{0\mathrm{H}}} + \frac{Q_{\mathrm{L}}}{T_{0\mathrm{L}}}\right], \tag{D.1}$$

where $Q_i = \int_0^{\tau_{\mathrm{tot}}} q_i \mathrm{d}t$ are the amounts of heat obtained by the fluid from the i-th source during one cycle and T_{0i} are the temperatures of the reservoirs ($i \in \{\mathrm{H}, \mathrm{L}\}$).

The total work $W = \int_0^{\tau_{\mathrm{tot}}} P \,\mathrm{d}t = \tau_{\mathrm{tot}} \overline{P}$ of one cycle is obtained by energy balance

$$Q_{\mathrm{H}} + Q_{\mathrm{L}} = W \ . \tag{D.2}$$

This work W is positive for heat engines and negative for heat pumps and refrigerators. By solving equation (D.2) for Q_{L} and substituting the resulting expression into equation (D.1) one finds

$$\Delta S = Q_{\mathrm{H}} \left(\frac{1}{T_{0\mathrm{L}}} - \frac{1}{T_{0\mathrm{H}}}\right) - \frac{W}{T_{0\mathrm{L}}} \ . \tag{D.3}$$

The efficiency η of a heat engine is equal to W/Q_{H}. Hence, from (D.3) one obtains a monotonous dependency between ΔS and η is derived as

$$\Delta S = \frac{W}{\eta}\left(\frac{1}{T_{0\mathrm{L}}} - \frac{1}{T_{0\mathrm{H}}}\right) - \frac{W}{T_{0\mathrm{L}}} \,. \tag{D.4}$$

Since $T_{0\mathrm{H}}$, $T_{0\mathrm{L}}$ and W are fixed, such a dependency implies for the model of figure 3.1 that the maximization of the efficiency of a heat engine subject to given average power output is equivalent to the minimization of its entropy production.

The definitions of the coefficients of performance (COP) for refrigerators and heat pumps are

$$\mathrm{COP}_{\mathrm{R}} = \frac{Q_{\mathrm{L}}}{W} \,, \quad \text{and} \quad \mathrm{COP}_{\mathrm{HP}} = -\frac{Q_{\mathrm{H}}}{W} \,, \tag{D.5}$$

respectively. Taking into account that both COPs,

$$\mathrm{COP}_{\mathrm{R}} = 1 - \frac{1}{\eta} \,, \qquad \mathrm{COP}_{\mathrm{HP}} = -\frac{1}{\eta} \,, \tag{D.6}$$

are monotonic increasing functions of η, it becomes clear that the same reasoning as for the heat engine also applies to refrigerators and heat pumps. The maximization of COPs and minimization of entropy are therefore equivalent for the model used in chapter 3 of this thesis.

Appendix E

Fluid temperatures for engines with inverse heat transfer

This section studies an endoreversible system as depicted in figure 3.1 in chapter 3. This system is operated as an heat engine, with given heat conductances (which can be either optimal or not) and an inverse law of heat conduction on the hot and cold heat reservoirs. The problem of maximizing the average power output $\overline{P}$ can be written as

$$\gamma_{\mathrm{H}} k_{\mathrm{H}} \left(\frac{1}{T_{\mathrm{H}}} - \frac{1}{T_{0\mathrm{H}}} \right) + \gamma_{\mathrm{L}} k_{\mathrm{L}} \left(\frac{1}{T_{\mathrm{L}}} - \frac{1}{T_{0\mathrm{L}}} \right) \longrightarrow \max_{T_{\mathrm{H}}, T_{\mathrm{L}}, \gamma_{\mathrm{H}}, \gamma_{\mathrm{L}}} , \tag{E.1}$$

subject to the endoreversibility condition

$$\gamma_{\mathrm{H}} \frac{k_{\mathrm{H}}(1/T_{\mathrm{H}} - 1/T_{0\mathrm{H}})}{T_{\mathrm{H}}} + \gamma_{\mathrm{L}} \frac{k_{\mathrm{L}}(1/T_{\mathrm{L}} - 1/T_{0\mathrm{L}})}{T_{\mathrm{L}}} = 0 \, . \tag{E.2}$$

The parts γ_{H} and γ_{L} of the cycle time are either restricted by

$$\gamma_{\mathrm{H}} + \gamma_{\mathrm{L}} = 1, \quad \gamma_{\mathrm{H}} \geq 0, \quad \gamma_{\mathrm{L}} \geq 0 \tag{E.3}$$

for cyclic conditions (see section 1.3.2) or by $\gamma_{\mathrm{H}} = \gamma_{\mathrm{L}} = 1$ for stationary conditions (see section 1.3.2).

The Lagrange function of the optimization problem is

$$\mathcal{L} = \gamma_{\mathrm{H}} \mathcal{L}_{\mathrm{H}} + \gamma_{\mathrm{L}} \mathcal{L}_{\mathrm{L}} + \lambda_{\gamma} (\gamma_{\mathrm{H}} + \gamma_{\mathrm{L}}), \tag{E.4}$$

where

$$\mathcal{L}_i = k_i \left(\frac{1}{T_i} - \frac{1}{T_{0i}} \right) \left[1 - \frac{\lambda}{T_i} \right] , \qquad i \in \{\mathrm{H}, \mathrm{L}\} . \tag{E.5}$$

Note that $\lambda_\gamma = 0$ for stationary conditions. The necessary conditions of optimality with respect to T_i yields:

$$\frac{\partial \mathcal{L}_i}{\partial T_\mathrm{i}} = 0 \quad \Rightarrow \quad \frac{1}{T_\mathrm{i}} = \frac{1}{2} \left[\frac{1}{T_{0\mathrm{i}}} + \frac{1}{\lambda} \right] , \qquad i \in \{\mathrm{H}, \mathrm{L}\} . \tag{E.6}$$

In order to find the optimal temperatures the value of $1/\lambda$ needs to be determined.

E.1 Stationary conditions

In case of stationary operating conditions the two instances of equation (E.6) are substituted into condition (E.2) and solved for $1/\lambda$:

$$\frac{1}{\lambda} = \sqrt{\frac{k_\mathrm{H}/T_{0\mathrm{H}}^2 + k_\mathrm{L}/T_{0\mathrm{L}}^2}{k_\mathrm{H} + k_\mathrm{L}}} . \tag{E.7}$$

This expression is subsequently inserted into equation (E.6) to calculate the optimal temperatures as

$$T_i^* = 2 \left[\frac{1}{T_{0i}} + \sqrt{\frac{k_\mathrm{H}/T_{0\mathrm{H}}^2 + k_\mathrm{L}/T_{0\mathrm{L}}^2}{k_\mathrm{H} + k_\mathrm{L}}} \right]^{-1} , \qquad i \in \{\mathrm{H}, \mathrm{L}\} . \tag{E.8}$$

E.2 Cyclic conditions

In case of cyclic conditions the value of $1/\lambda$ is found by combining the two optimality conditions, $\partial \mathcal{L}/\partial \gamma_i$, $i \in \{\mathrm{H}, \mathrm{L}\}$. The two instances of equation (E.6) are then substituted into the resulting expression which is finally transformed to

$$\frac{1}{\lambda} = \frac{\sqrt{k_\mathrm{H}}/T_{0\mathrm{H}} + \sqrt{k_\mathrm{L}}/T_{0\mathrm{L}}}{\sqrt{k_\mathrm{H}} + \sqrt{k_\mathrm{L}}} . \tag{E.9}$$

So the optimal temperatures of the fluid are determined from equations (E.6) as

$$T_i^* = 2 \left[\frac{1}{T_{0i}} + \frac{\sqrt{k_\mathrm{H}}/T_{0\mathrm{H}} + \sqrt{k_\mathrm{L}}/T_{0\mathrm{L}}}{\sqrt{k_\mathrm{H}} + \sqrt{k_\mathrm{L}}} \right]^{-1} , \qquad i \in \{\mathrm{H}, \mathrm{L}\} . \tag{E.10}$$

The result is well known and has, for example, been published in reference [31].

Bibliography

[1] Carnot, S. *Réflexions sur la puissance motrice du feu et sur les machines propres á développer cette puissance*. Paris, 1824. In French, Bachelier, Paris, 1824; Fox, R. (ed.), Libraire Philosophique J. Vrin, Paris 1978, see also On the Motive Power of Heat, American Society of Mechanical Engineers, 1943.

[2] Müser, H. Behandlung von Elektronenprozessen in Halbleiterrandschichten. *Zeitschrift für Physik*, 148:380–390, 1957. In German.

[3] Novikov, I. I. The efficiency of atomic power stations. *Atomnaya Energiya*, 3:409, 1957. (in Russian).

[4] Novikov, I. I. The efficiency of atomic power stations. *Journal Nuclear Energy II*, 7:125–128, 1958. Translated from Atomnaya Energiya, 3 (1957), 409.

[5] Vukalovich, M. P. and Novikov, I. I. *Thermodynamics*. Mashinostroenie, Moscow, 1972.

[6] El-Wakil, M. M. *Nuclear Power Engineering*, pages 162–165. McGraw-Hill, New York, 1962.

[7] El-Wakil, M. M. *Nuclear Energy Conversion*, pages 31–35. International Textbook Company, Scranton, PA, 1971.

[8] Novikov, I. I. and Voskresenskii, K. D. *Thermodynamics and Heat Transfer*. Atomizat, Moscow, 1977.

[9] Chambadal, M. P. Le choix du cycle thermique dans une usine generatrice nucleaire. *Revue Generale de L'Electricite*, 67(6):332, 1958.

[10] Chambadal, P. *Evolution et Applications du Concept d'Entropie*, chapter 30. Dunod, Paris, 1963.

[11] Curzon, F. L. and Ahlborn, B. Efficiency of a carnot engine at maximum power output. *American Journal of Physics*, 43:22, 1975.

[12] Andresen, B., Berry, R. S., Nitzan, A., and Salamon, P. Thermodynamics in finite time. I. the step-Carnot cycle. *Physical Review A*, 15(5):2086–2093, 1977.

[13] Salamon, P., Andresen, B., and Berry, R. S. Thermodynamics in finite time. II. potentials for finite-time processes. *Physical Review A*, 15(5):2094–2102, 1977.

[14] Salamon, P., Nitzan, A., Andresen, B., and Berry, R. S. Minimum entropy production and the optimization of heat engines. *Physical Review A*, 21(6):2115, 1980.

[15] Salamon, P. and Nitzan, A. Finite time optimizations of a newton's law Carnot cycle. *Journal of Chemical Physics*, 74(6):3546–3560, 1981.

[16] Rubin, M. H. Optimal configuration of a class of irreversible heat engines. I. *Physical Review A*, 19(3):1272, 1979.

[17] Ondrechen, M. J., Rubin, M. H., and Band, Y. B. The generalized Carnot cycle - a working fluid operation in finite-time between finite heat sources and sinks. *Journal of Chemical Physics*, 78:4721–4727, 1983.

[18] De Vos, A. and Pauwels, H. On the thermodynamic limit of photovoltaic energy conversion. *Applied Physics*, 25:119–125, 1981.

[19] De Vos, A. Reflections on the power delivered by endoreversible engines. *Journal of Physics D: Applied Physics*, 20:232–236, 1987.

[20] De Vos, A., Landsberg, P. T., Baruch, P., and Parrott, J. E. Entropy fluxes, endoreversibility, and solar energy conversion. *Journal of Applied Physics*, 74(6):3631–3637, 1993.

[21] Gordon, J. M. Maximum power point characteristics of a heat engine as a thermodynamic problem. *American Journal of Physics*, 57:1136–1142, 1989.

[22] Sieniutycz, S. and Berry, R. S. Canonical formalism, fundamental equation, and generalized thermomechanics for irreversible fluids with heat-transfer. *Physical Review E*, 47(3):1765–1783, 1993.

[23] Hoffmann, K. H., Burzler, J. M., and Schubert, S. Endoreversible thermodynamics. *Journal of Non-Equilibrium Thermodynamics*, 22(4):311–355, 1997.

[24] Falk, G. and Ruppel, W. *Energie und Entropie*. Springer, Berlin, 1976.

[25] Pontryagin, L., Boltyanski, V., Gamkrelidze, R., and Mishtchenko, E. *The Mathematical Theory of Optimal Processes*. Interscience, New York, 1962.

[26] Gregory, J. and Lin, C. *Constrained Optimization in the Calculus of Variations and Optimal Control Theory*. Van Nostrand Reinhold, New York, 1993.

[27] Hocking, L. M. *Optimal Control*. Clarendon Press, Oxford, 1991.

[28] Rubin, M. H. Optimal configuration of a class of irreversible heat engines. II. *Physical Review A*, 19(3):1277, 1979.

[29] Rubin, M. H. Optimal configuration on an irreversible heat engine with fixed compression ratio. *Physical Review A*, 22(4):1741, 1980.

[30] Rubin, M. H. and Andresen, B. Optimal staging of endoreversible heat engines. *Journal of Applied Physics*, 53(1):1–7, 1982.

[31] Rozonoer, L. I. and Tsirlin, A. M. Optimal control of thermodynamic processes III. *Automation and Remote Control USSR*, 44(1):314–326, 1983. Translated from Avtomatika i Telemekhanika.

[32] Orlov, V. N. Optimum irreversible Carnot cycle containing three isotherms. *Sov. Phys. Dokl.*, 30:506–508, 1985.

[33] Angulo-Brown, F. An ecological optimization criterion for finite-time heat engines. *Journal of Applied Physics*, 69(11):7465–7469, 1991.

[34] Gordon, J. M. and Huleihil, M. On optimizing maximum-power heat engines. *Journal of Applied Physics*, 69(1):1–7, 1991.

[35] Chen, J. and Yan, Z. Unified description of endoreversible cycles. *Physical Review A*, 39(8):4140, 1989.

[36] Lee, W. Y. and Kim, S. S. Finite-time optimizations of a heat engine. *Energy*, 15(11):979–985, 1990.

[37] Lee, W. Y. and Kim, S. S. Power optimization of an irreversible heat engine. *Energy*, 16(7):1051–1058, 1991.

[38] Yan, Z. J. and Chen, L. X. Optimal performance of an endoreversible cycle operating between a heat source and sink of finite capacities. *Journal of Physics A: Mathematical and General*, 30(23):8119–8127, 1997.

[39] Pathria, R. K., Nulton, J. D., and Salamon, P. A finite-time heat engine with fixed-capacity heat transfers. *Journal of Physics A: Mathematical and General*, 29(21):6925–6937, 1996.

[40] Landsberg, P. T. and Leff, H. S. Thermodynamic cycles with nearly universal maximum-work efficiencies. *Journal of Physics A: Mathematical and General*, 22:4019–4025, 1989.

[41] Callen, H. *Thermodynamics and an Introduction in Thermostatics*. Wiley & Sons, New York, 2nd edition, 1985.

[42] Elsner, N. *Grundlagen der Technischen Thermodynamik*. Akademie-Verlag, Berlin, 1985.

[43] Moran, M. J. and Shapiro, H. N. *Fundamentals of Engineering Thermodynamics*. Wiley & Sons, New York, 2nd edition, 1993.

[44] Spalding, D. B. and Cole, E. H. *Engineering Thermodynamics*. Adward Arnold, London, 3rd edition, 1973.

[45] Stephan, K. and Mayinger, F. *Thermodynamik - Band 1 Einstoffsysteme*. Springer, Berlin, 13th edition, 1990.

[46] Wylen, G. J. V. and Sonntag, R. E. *Fundamentals of Classical Thermodynamics*. Wiley & Sons, New York, 3rd edition, 1986.

[47] Granet, I. *Elementary Applied Thermodynamics*. Wiley & Sons, 1965.

[48] Obert, E. F. and Young, R. L. *Thermodynamik der Verbrennungskraftmaschine*. McGraw-Hill, New York – Toronto – London, 1962.

[49] Gordon, J. M. Observations on efficiency of heat engines operating at maximum power. *American Journal of Physics*, 58(4):370–375, 1990.

[50] Bejan, A. Theory of heat transfer-irreversible power plants. *International Journal of Heat and Mass Transfer*, 31(6):1211–1219, 1988.

[51] Bejan, A. Power and refrigeration plants for minimum heat exchanger inventory. *Journal of Energy Resources Technology*, 115:148–150, 1993.

[52] Bejan, A. Theory of heat-transfer irreversible power plants - II. the optimal allocation of heat-exchange equipment. *International Journal of Heat and Mass Transfer*, 37:433–444, 1995.

[53] Bejan, A. Power generation and refrigeration models with heat transfer irreversibilities. *Journal of the Heat Transfer Society Japan*, 33(128):68–75, 1994.

[54] Bejan, A. Entropy generation minimization: The new thermodynamics of finite-size devices and finite-time processes. *Journal of Applied Physics*, 79(3):1191–1218, 1996.

[55] Gutkowicz-Krusin, D., Procaccia, I., and Ross, J. On the efficiency of rate processes. power and efficiency of heat engines. *Journal of Chemical Physics*, 69(9):3898, 1978.

[56] Press, W. H., Teukolsky, S. A., Vetterling, W. T., and Flannery, B. P. *Numerical Recipes in C*. Cambridge University Press, Cambridge, 2nd edition, 1992.

[57] Bejan, A. Theory of heat transfer-irreversible refrigeration plants. *International Journal of Heat and Mass Transfer*, 32:1631–1639, 1989.

[58] Ibrahim, O. M., Klein, S. A., and Mitchell, J. W. A relation between thermodynamic performance and economics for heat engines. *ASME AES*, 24:15, 1991.

[59] Klein, S. A. Design considerations for refrigeraton cycles. *International Journal of Refrigeration – Revue Internationale du Froid*, 15:181–185, 1992.

[60] Radcenco, V., Vargas, J., Bejan, A., and Lim, J. Two design aspects of defrosting refrigerators. *International Journal of Refrigeration – Revue Internationale du Froid*, 18(2):76–86, 1995.

[61] Goth, Y. and Feidt, M. Thermodynamics - optimum coefficient of performance for endoreversible heat pump or refrigerating machine. *C. R. Acad. Sc. Paris*, 303(1):19, 1986. (in french).

[62] Chen, J. and Wu, C. Design considerations of primary performance parameters for irreversible refrigeration cycles. *International Journal of Ambient Energy*, 16(1):17, 1995.

[63] Chen, J. Optimal heat-transfer areas for endoreversible heat pumps. *Energy*, 19(10):1031–1036, 1994.

[64] Angulo-Brown, F. and Paez-Hernandez, R. Endoreversible thermal cycle with a nonlinear heat transfer law. *Journal of Applied Physics*, 74(4):2216–2219, 1993.

[65] Moukalled, F., Nuwayhid, R. Y., and Fattal, S. A universal model for studying the performance of Carnot-like engines at maximum power conditions. *International Journal of Energy Research*, 20:203–214, 1996.

[66] Chen, L., Sun, F., and Wu, C. The influence of heat-transfer law on the endoreversible carnot refrigerator. *Journal of the Institute of Energy*, 69(479):96–100, 1996.

[67] Wu, C., Chen, L. G., and Sun, F. R. Effect of heat transfer law on finite-time exergoeconomic performance of Carnot heat pump. *Energy Conversion and Management*, 39(7):579–588, 1998.

[68] Tsirlin, A. M. Conditions for optimality of the solution of averaged problems of mathematical programming. *Rossiĭskaya Akademiya Nauk. Doklady Akademii Nauk*, 323(1):43–47, 1992. ISSN 0869-5652. In Russian.

[69] Tsirlin, A. M. *Methods of Averaged Optimization and their Applications*. Nauka-Fizmatlit, 1997. In Russian.

[70] Berry, R. S., Kazakov, V., Sieniutycz, S., Szwast, Z., and Tsirlin, A. M. *Thermodynamic Optimisation of Finite-Time Processes*. Wiley & Sons, Chichester – New York, 2000.

[71] Rozonoer, L. I. and Tsirlin, A. M. Optimal control of thermodynamic processes I. *Automation and Remote Control USSR*, 44(1):55–62, 1983. Translated from Avtomatika i Telemekhanika.

[72] Rozonoer, L. I. and Tsirlin, A. M. Optimal control of thermodynamic processes II. *Automation and Remote Control USSR*, 44(1):209–220, 1983. Translated from Avtomatika i Telemekhanika.

[73] Mozurkewich, M. and Berry, R. S. Optimal paths for thermodynamic systems: The ideal otto cycle. *Journal of Applied Physics*, 53(1):34–42, 1982.

[74] Hoffmann, K. H., Watowich, S. J., and Berry, R. S. Optimal paths for thermodynamic systems: The ideal Diesel cycle. *Journal of Applied Physics*, 58(6):2125, 1985.

[75] Blaudeck, P. and Hoffmann, K. H. Optimzation of the power output for the compression and power stroke of the diesel engine. In *Proceedings of The International Conference ECOS'95*, volume 2, page 754. Istambul, Turkey, 1995.

[76] Burzler, J. M., Blaudeck, P., and Hoffmann, K. H. Optimal piston paths for diesel engines. In Sienuitycz, S. and Vos, A. D., editors, *Thermodynamics of energy conversion and transport*, pages 173–198. Springer, 2000.

[77] Annand, W. J. D. Heat transfer in the cylinder of reciprociating internal combustion engines. *Proceedings of the Institute of Mechanical Engineers*, 177(36):973–990, 1963.

[78] Nusselt, W. Der Wärmeübergang in den Verbrennungskraftmaschinen. *Zeitschrift des Vereins deutscher Ingenieure*, 67:692 and 708, 1923.

[79] Eichelberg, G. Temperaturverlauf und Wärmespannung in Verbrennungsmotoren. *Forsch. IngWes*, (263), 1923. In German.

[80] Overbye, V. D., Bennethum, J. E., Uyehara, O. A., and Myers, P. S. Unsteady heat transfer in engines. *Trans. Soc. automot. Engrs.*, 69:461, 1961.

[81] Woschni, G. Die Berechnung der Wandverluste und der thermischen Belastung der Bauteile von Dieselmotoren. *Motortechnische Zeitschrift*, 31(12):491–499, 1970. In German.

[82] Woschni, G. Experimental investigation of the heat transfer in internal combustion engines with insulated combustion chamber walls. pages Ch. 50, 53–65. 1989.

[83] Ferguson, C. F. *Internal Combustion Engines*. Wiley & Sons, New York, 1986.

[84] Taylor, C. F. *The Internal-Combustion Engine in Theory and Practice*, volume 1 and 2. MIT, Cambridge, MA, 1977.

[85] Kleinschmidt, W. Die Wärmeübertragung in aufgeladenen Dieselmotoren aus neuerer Sicht. 5. Aufladetechnische Konferenz, Augsburg, 1993.

[86] Pflaum, W. and Mollenhauer, K. *Wärmeübergang in der Verbrennungskraftmaschine*, volume 3 of *Die Verbrennungskraftmaschine*. Springer, Wien – New York, 1977.

[87] De Vos, A. Efficiency of some heat engines at maximum-power conditions. *American Journal of Physics*, 53:570–573, 1985.

[88] Bejan, A. *Advanced Engineering Thermodynamics*, volume 51. Wiley & Sons, New York, 1988.

[89] Rogers, G. and Mayhew, Y. *Engineering Thermodynamics - Work and Heat Transfer*. Longman and Scientific & Technical, New York, 1980.

[90] Bejan, A. *Heat Transfer*. Wiley & Sons, New York, 1983.

[91] Schack, A. *Der industrielle Wärmeübergang*. Verlag Stahleisen MBH, Düsseldorf, 1983. In German.

[92] Incropera, F. P. and Witt, D. P. D. *Fundamentals of Heat and Mass Transfer*. Wiley & Sons, 4th edition, 1996.

[93] Newton, I. A scale of the degrees of heat. *Philosophical Transactions*, March – May:824, 1701. See: David Brewster, Memoirs of the Life, Writings and Discoveries of Sir Isaac Newton (Constable, Edinburgh, 1885), Vol. 2, p.382.

[94] Adiutori, E. F. *A New Look at the Origin of the Heat Transfer Coefficient Concept*. Ventuno Press, 1988.

[95] O'Sullivan, C. T. Newton law of cooling – a critical assessment. *American Journal of Physics*, 58(10):956–960, 1990.

[96] Herwig, H. Critical note about a popular concept: The heat transfer coefficient h. *Forschung auf dem Gebiet des Ingenieurwesens*, 63:13–17, 1997. In German.

[97] Gillispie, G. C., editor. *Dictionary of Scientific Biography*, volume IV. Scribner, New York, 1971.

[98] Andresen, B., Salamon, P., and Berry, S. R. Thermodynamics in finite time: Extremals for imperfect heat engines. *Journal of Chemical Physics*, 66(4):1571, 1977.

[99] Blanchard, C. H. Coefficient of performance for a finite speed heat pump. *Journal of Applied Physics*, 51:2471–2472, 1980.

[100] Rebhan, E. and Ahlborn, B. Frequency-dependent performance of a nonideal Carnot engine. *American Journal of Physics*, 55(5):423–428, 1987.

[101] Chen, J. and Yan, Z. Optimal performance of an endoreversible-combined refrigeration cycle. *Journal of Applied Physics*, 63(10):4795–4798, 1988.

[102] Gordon, J. M. On optimized solar-driven heat engines. *Solar Energy*, 40:457–461, 1988.

[103] Andresen, B. Finite-time thermodynamics. In Sieniutycz, S. and Salamon, P., editors, *Finite-Time Thermodynamics and Thermoeconomics, Advances in Thermodynamics 4*, page 66. Taylor and Francis, New York, 1990.

[104] Orlov, V. N. and Berry, R. S. Analytical and numerical estimates of efficiency for an irreversible heat engine with distributed working fluid. *Physical Review A*, 45(19):7202–7206, 1992.

[105] Bejan, A. Models of power plants that generate minimum entropy while operating at maximum power. *American Journal of Physics*, 64(8):1054–1059, 1996.

[106] Dulong, P. and Petit, A. Recherches sur la mesure des températures et sur les lois de la communication de la chaleur. *Ann. Chim. Phys.*, 7:225–264, 1817. In French; see page 238 in [97].

[107] Gersten, K. and Herwig, H. *Strömungsmechanik/Grundlagen der Impuls-, Wärme- und Stoffübertragung aus asymptotischer Sicht*. Vieweg-Verlag, Braunschweig – Germany, 1992. In German.

[108] Stephan, K. *Wärmeübergang beim Kondensieren und beim Sieden*. Springer, Berlin – Heidelberg – New York, 1988. In German.

[109] Chen, W. Z., Sun, F. R., and Chen, L. G. The optimal relation of a carnot heat pump for the case $Q \propto \Delta T^n$. In *Proceedings of the International Energy Conference on Energy Conversion and Energy Source Engineering*, pages 18–20. Wuhan, China, 1990.

[110] Yan, Z. and Chen, J. A class of irreversible Carnot refrigeration cycles with a general heat tranfer law. *Journal of Physics D: Applied Physics*, 23:136–141, 1990.

[111] Chen, W. Z., Sun, F. R., Cheng, S. M., and Chen, L. G. Study on optimal performance and working temperatures of endoreversible forward and reverse carnot cycles. *International Journal of Energy Research*, 19:751, 1995.

[112] Chen, L. and Yan, Z. The effect of heat-transfer law on performance of a two-heat-source endoreversible cycle. *Journal of Chemical Physics*, 90(7):3740–3748, 1989.

[113] Chen, J. and Yan, Z. Optimal performance of endoreversible cycles for another linear heat transfer law. *Journal of Physics D: Applied Physics*, 26:1581–1586, 1993.

[114] Chen, L., Sun, F., and Chen, W. Optimal expansion of a heated working fluid in a cylinder with a movable on piston in the case of $q \propto \Delta(T^{-1})$s. *Chinese Journal of Mechanical Engineering*, 29:97, 1993.

[115] Nulton, J. D., Salamon, P., and Pathria, R. K. Carnot-like processes in finite time. I. theoretical limits. *American Journal of Physics*, 61(10):911–916, 1993.

[116] Moukalled, F., Nuwayhid, R. Y., and Noueihed, N. The efficiency of endoreversible heat engines with heat leak. *International Journal of Energy Research*, 19:377–389, 1995.

[117] De Vos, A. *Endoreversible Thermodynamics of Solar Energy Conversion*. Oxford University Press, Oxford, 1992.

[118] Castañs, M. Bases fisicas del aprovechamiento de la energia solar. *Revista de Geofísica*, 35:227–239, 1976.

[119] Bejan, A., Kearney, D. W., and Kreith, F. Second law analysis and synthesis of solar collector systems. *Journal of Solar Energy Engineering*, 103:23, 1981.

[120] Badescu, V. On the theoretical maximum efficiency of solar-radiation utilization. *Energy*, 14(9):571, 1989.

[121] Badescu, V. The theoretical maximum efficiency of solar converters with and without concentration. *Energy*, 14(4):237, 1989.

[122] Gordon, J. Nonequilibrium thermodynamics for solar energy application. In Sieniutycz, S. and Salamon, P., editors, *Finite-Time Thermodynamics and Thermoeconomics, Advances in Thermodynamics 4*, page 95. Taylor and Francis, New York, 1990.

[123] Lund, K. Application of finite-time thermodynamics to solar power conversion. In Sieniutycz, S. and Salamon, P., editors, *Finite-Time Thermodynamics and Thermoeconomics, Advances in Thermodynamics 4*, page 121. Taylor and Francis, New York, 1990.

[124] Badescu, V. Note concerning the maximal efficiency and the optimal operating temperature of solar converters with or without concentration. *Renewable Energy*, 1(1):131, 1991.

[125] Badescu, V. Maximum conversion efficiency for the utilization of diffuse solar radiation. *Energy*, 16(4):783, 1991.

[126] Badescu, V. A study concerning the opportunity of solar power generation in south-east rumania (dobrogea). *Energy Conversion and Management*, 33(11):971, 1992.

[127] Badescu, V. Thermodynamic conversion of the radiation flux emitted by a spherical source of black-body radiation. *International Journal of Energy Research*, 16:717, 1992.

[128] Göktun, S., Özakynak, S., and Yavuz, H. Design parameters of a radiative heat engine. *Energy*, 18(6):651–655, 1993.

[129] Blank, D. A. and Wu, C. Power optimization of an extraterrestrial, solar-radiant stirling heat engine. *Energy*, 20:523–530, 1995.

[130] De Vos, A. and Pauwels, H. Comment on a thermodynamical paradox presented by P. Würfel. *Journal of Physics C: Solid State Physics*, 16:6897–6909, 1983.

[131] Planck, M. Ueber irreversible strahlungsvorgänge. *Annalen der Physik*, 6:69–122, 1900. In German.

[132] Planck, M. Ueber das gesetz der energieverteilung im normalspektrum. *Annalen der Physik*, 4:719–737, 1901. In German.

[133] Planck, M. *Theorie der Wäremstrahlung*. Barth-Verlag, 1963. In German, reprint of the fifth edition of 1923.

[134] Siegel, R., Howell, J. R., and Lohrengel, J. *Wärmeübertragung durch Strahlung*, volume 1. Springer, Berlin, 1988. In German.

[135] Siegel, R. and Howell, J. R. *Thermal Radiation Heat Transfer*. McGraw-Hill, New York, 1972.

[136] Kabelac, S. *Thermodynamik der Strahlung*. Vieweg, Braunschweig/Wiesbaden, Germany, 1994. In German.

Thesen

- Reale thermodynamische Systeme zeichnen sich dadurch aus, dass Prozesse in endlichen Zeiten ablaufen bzw. dass endliche Prozessraten vorliegen. Diese irreversiblen Systeme lassen sich durch endoreversible Modelle beschreiben, d.h. durch eine Zerlegung in reversible Subsysteme, die miteinander in irreversibler Wechselwirkung stehen. Diese Beschreibung erlaubt eine teils analytische, teils numerische Bestimmung einer Vielzahl von Leistungsmerkmalen.

- Am Beispiel polytroper Kreisprozesse, die die herkömmlichen Zustandsänderungen wie Isothermen, Isobaren und Isochoren als Spezialfälle enthalten, wird der Einfluss endlicher Wärmekapazitäten und des Wärmeaustausches in endlicher Zeit untersucht. Unter diesen Voraussetzungen wird erstmals in dieser Allgemeinheit eine analytische Formel für die maximal erzielbare Ausgangsarbeit hergeleitet und sowohl die optimale Temperatur des Arbeitsmediums als auch die optimale Zuordnung der Wärmeleitfähigkeiten und die optimalen Kontaktzeiten zu den Wärmetauschern bestimmt.

- Es zeigt sich, dass die Wirkungsgrade dieser Kreisprozesse mit dem *Curzon-Ahlborn* Wirkungsgrad für endoreversible Carnot-Prozesse identisch sind, solange der Wärmeaustausch während polytroper Zustandsänderungen mit gleichen Polytropenexponenten stattfindet. Erstaunlicherweise ist im Fall gleicher Polytropenexponenten der Wirkungsgrad des Systems völlig unabhängig von dem Polytropenexponenten, den Wärmeleitungsgrößen und den Kontaktzeiten zu den Wärmetauschern.

  Bei unterschiedlichen Exponenten ergibt sich jedoch eine Abweichung vom Curzon-Ahlborn Wirkungsgrad, obwohl auch hier lineare Wärmeleitung vorliegt. Dies ist besonders interessant, da in der Literatur bislang gerade die Linearität des Wärmeleitungsgesetzes als entscheidend für die Gültigkeit des Curzon-Ahlborn Wirkungsgrads angesehen wird.

- Das ökonomische Optimierungsproblem der Verteilung der finanziellen Ressourcen auf die beiden Wärmetauscher eines allgemeinen thermischen Systems, das in der Lage ist, Wärmekraftmaschinen, Kühlschränke und Wärmepumpen zu beschreiben, wird untersucht. Sowohl für stationäre als auch zyklische Prozessführung wird bei vorgegebenen, aber nicht notwendigerweise linearen Wärmeleitungsgesetzen und Kostenfunktionen die Verteilung der Kosten auf die Wärmetauscher durch Minimierung der Entropieproduktionsrate optimiert. Hierbei zeigt sich, dass sich im Gegensatz zu linearen Wärmeleitungsgesetzen, bei denen die Kosten auf beide Austauscher

gleich verteilt werden, komplizierte Verteilungen ergeben und dass sich insbesondere ein bislang nicht dokumentierter Unterschied zwischen stationärer und zyklischer Prozessführung ergibt.

- Für einen reversiblen Kreisprozess, der im irreversiblen Kontakt mit mehreren Wärmebädern steht, wird mit der Methode der gemittelten nichtlinearen Programmierung ein Algorithmus entwickelt, der bei beliebiger Wahl des Wärmeleitungsgesetzes die optimalen Kontaktzeiten und Kontakttemperaturen zu den einzelnen Bädern unter der Voraussetzung einer maximalen mittleren Ausgangsleistung bestimmt. Interessanterweise zeigt sich, dass es unter diesen Bedingungen durchaus optimal sein kann, einige Wärmebäder nicht zu nutzen und sie zu keinem Zeitpunkt zu kontaktieren.

- Abschließend wird das Modell eines Dieselmotors untersucht, wobei erstmals neben einem realistischerem Wärmetransportgesetz auch die Temperaturabhängigkeit verschiedener Eigenschaften des Arbeitsgases berücksichtigt wird. Für dieses Modell wird die Kolbenbewegung mit dem Ziel einer maximalen Ausgangsleistung optimiert. Die Verbesserung der vom pfadoptimierten Dieselmotor gelieferten Arbeit beträgt im Vergleich zum konventionellen Motor mit sinusförmiger Kolbenbewegung circa 5 Prozent. Die in dieser Arbeit gewonnene Abschätzung für den Zuwachs an Ausgangsarbeit durch Optimierung der Kolbenführung berücksichtigt eine Vielzahl von Details, liefert so eine deutlich fundiertere und realistischere Abschätzung als bisher und zeigt dadurch die Grenzen der Pfadoptimierung auf.

Lebenslauf

Name	Josef Maximilian Burzler
Geburtstag	19. Juni 1969
Geburtsort	Regensburg
Familienstand	verheiratet, 2 Kinder

1989	**Abitur** am Werner-von-Siemens Gymnasium in Regensburg
1989 - 1990	**Wehrdienst** in Regensburg und Dillingen a. d. D.
1990 - 1996	**Studium der Diplomphysik** an Universität Regensburg ab 1993 gefördert durch das Cusanuswerk
1991	Studienaufenthalt an der Universität Leipzig
1993	Studentische Hilfskraft im Fachbereich Kristallographie und Radioaktivität der Universität Regensburg Forschungsprojekte mit Medizinern, Geologen und Herstellern kommerzieller Radon-Meßsysteme
1993 - 1995	**Auslandsstudium** an der Heriot-Watt University in Edinburgh; Simulation im Bereich Nichtlineare Optik in Zusammenarbeit mit Experimentalphysikern und Chemikern
1995 - 1996	Studentische Hilfskraft im Fachbereich Kristallographie und Radioaktivität: Betreuung von Vorlesungen und Übungen
23.03.1996	**Diplom in Physik**; Diplomarbeit zum Thema *Modellierung der Lichtausbreitung in optisch linearen und nichtlinearen Medien*; Zusatzzertifikat in Informatik
1996 - 1999	**Wissenschaftlicher Mitarbeiter** an der TU Chemnitz im Fachbereich *Theoretische Physik – Computerphysik*; mit Schwerpunkt *Optima und Grenzen thermodynamischer Prozesse*; Kooperation mit russischen und amerikanischen Wissenschaftlern; gefördert durch das Cusanuswerk
1999	Forschungsaufenthalt am Edinburgh Parallel Computing Centre: Projekt zur Optimierung von Dieselmotoren mit Supercomputer
1999 - 2002	**Software-Entwickler** und **Systemadministrator** bei der Adori AG in Regensburg
seit 2002	**Berater** und **Projektleiter** bei der UNIOPT AG in Regensburg

Wissenschaftliche Tagungen und Weiterbildung

1993 – 19. Radiometrisches Seminar, *Auswirkung von natürlichem Radon und seiner Zerfallsprodukte*, in Theuern

1995 – 23. Radiometrisches Seminar, *100 Jahre Röntgenstrahlen*, in Theuern

1996 – Posterbeitrag auf der Frühjahrstagung der Deutschen Physikalischen Gesellschaft (DPG) in Innsbruck, Österreich, zum Thema Quantenoptik
– Fachschaftstagung des Cusanuswerks am Fraunhofer-Institut für Solare Energiesysteme

1997 – Posterbeitrag auf der DPG-Frühjahrstagung in Münster
– Seminar *Stochastic Optimization* Summer Research Center, Telluride, Colorado
– Internationales Kolloquium *Finite Time Thermodynamics* in Berlin

1998 – Posterbeitrag auf der DPG-Frühjahrstagung in Konstanz
– Kurzvortrag beim Arbeitskreis Energie auf der DPG-Frühjahrstagung in Regensburg
– Vortrag auf dem Internationalen Arbeitskreis *Optimal Control Methods and their Application in Problems of Finite-Time Thermodynamics and Economics* am Program Systems Institute Pereslavl, Russland

1999 – Kurzvortrag auf der DPG-Frühjahrstagung in Heidelberg
– Gordon Research Conference *Modern Developments in Thermodynamics* in Il Ciocco, Barga, Italien

1999 – Kurs *High Performance Computing* am Edinburgh Parallel Computing Centre

Wissenschaftliche Veröffentlichungen

S. Hughes, J. M. Burzler, and B. S. Wherrett
Fast Fourier transform techniques for efficient simulation of Z-Scan Measurements, Journal of the Optical Society of America vol B 12, p. 1888 (1995).

J. M. Burzler, S. Hughes, and B. S. Wherrett
Split-step Fourier methods applied to model nonlinear refractive effects in optically thick media, Applied Physics B vol 62, pp. 389-397 (1996).

S. Hughes, G. Spruce, R. Rangel-Rojo, J. M. Burzler, B. S. Wherrett
Theoretical analysis of the picosecond, induced absorption, exhibited by chloro aluminium phthalocyanine (CAP), Journal of the Optical Society of America B, vol 14, no 2, pp. 400-404 (1997).

S. Hughes and J. M. Burzler
Theory of Z-scan measurements using Gaussian-Bessel, Rapid Communication in Physical Review A, vol 56, no 2, pp. R1103-R1106 (1997).

J. M. Burzler
Modellierung der Lichtausbreitung in und hinter optisch nichtlinearen Medien, Fachbuch erschienen beim Logos Verlag in Berlin, September 1997, 198 Seiten, ISBN 3-931216-57-8

S. Hughes, J. M. Burzler, and T. Kobayashi
Modeling of picosecond-pulse propagation for optical limiting applications in the Visible spectrum, Journal of the Optical Society of America B, vol 14, no. 11, pp. 2925-2929 (1997)

K. H. Hoffmann, J. M. Burzler, and S. Schubert
Endoreversible thermodynamics, Review Article, Journal of Non-Equilibrium-Thermodynamics, vol 22, no 4, pp. 311-355 (1997).

J. M. Burzler, P. Blaudeck, and K. H. Hoffmann
Optimal piston paths for Diesel engines, Kapitel 7 im Buch 'Thermodynamics of energy conversion and transport' herausgegeben von S. Sienuitycz and A. De Vos, erschienen bei Springer in New York, 2000, ISBN 0-387-98938-2

S. A Amelkin, J. M Burzler, K. H. Hoffmann, and A. M. Tsirlin
Optimal separation processes of binary mixtures, in Russisch, Journal of Theoretical foundations of chemical technology (Russland), no 3, (2001).

J. M Burzler, S. A Amelkin, and K. H. Hoffmann
Optimal endoreversible heat engines with polytropic branches, submitted to the International Journal of Applied Thermodynamics

S. Schubert, K. H. Hoffmann and J. M. Burzler
Inertial Effects on Gas Expansion with a Finite Driving Force, Preprint

S. A Amelkin, J. M Burzler, K. H. Hoffmann and A. M. Tsirlin
Minimal work for separation processes of binary mixtures, Preprint

J. M Burzler, S. A Amelkin, and K. H. Hoffmann
Optimal Distribution of Heat-Exchanger Costs in Thermodynamic Systems, Preprint